EMULSION POLYMERIZATION OF VINYL ACETATE: PARTICLE SIZE AND MOLECULAR WEIGHT DISTRIBUTIONS

EMULSION POLYMERIZATION OF VINYL ACETATE: PARTICLE SIZE AND MOLECULAR WEIGHT DISTRIBUTIONS

by

CHUE-KWOK JOHN KEUNG, B. Eng.

A Thesis

Submitted to the School of Graduate Studies

in Partial Fulfilment of the Requirements

for the Degree

Master of Engineering

McMaster University

April, 1974

MASTER OF ENGINEERING (1974) McMASTER UNIVERSITY
(Chemical Engineering) Hamilton, Canada

TITLE: Emulsion Polymerization of Vinyl Acetate:
Particle Size and Molecular Weight Distributions

AUTHOR: Chue-Kwok John Keung,
B. Eng. (McMaster University, Canada)

SUPERVISORS: Professors A. E. Hamielec and J. D. Wright

NUMBER OF PAGES: xi, 126

ABSTRACT

Emulsion polymerization of vinyl acetate was studied in a batch reactor system. The particle size distribution of the polyvinyl acetate particles was determined by electron microscopy. 'In Situ Polymerization' technique was used to harden the polymer particles before microscopic examination. A light transmission spectrophotometer was calibrated for particle size measurement with the data obtained from electron microscopy. A one-parameter exponential function was found to be a good approximation for the polyvinyl acetate particle size distribution. A convenient method which involves the measurement of turbidities at two wavelengths was proposed to determine the particle size distribution.

The second part of this thesis deals with the kinetics of vinyl acetate emulsion polymerization. It was found that a rate model similar to Case 1 of Smith-Ewart's theory was able

to predict the polymerization rate. A model previously developed in this laboratory was able to predict the molecular weight development in vinyl acetate emulsion polymerization. The logarithmic-normal distribution was a reasonably good approximation for the polyvinyl acetate molecular weight distribution.

ACKNOWLEDGEMENTS

The author wishes to express his gratitude to all institutions and persons who contributed to this work. He is particularly indebted to:

His research supervisors, Dr. A. E. Hamielec and Dr. J. D. Wright, for their enthusiasm, encouragement and guidance throughout the course of this research project.

Dr. T. Ishige for his valuable advice and assistance in gel permeation chromatography and electron microscopy.

Dr. N. Friis for much valuable discussion and advice in the theories of emulsion polymerization and for his work in light scattering.

Dr. J. Hodgins for his work in gamma-ray initiated polymerization.

His colleagues, S. Thomas and D. Goosney, for their valuable discussion.

The National Research Council of Canada for providing financial support in the form of a scholarship.

The Chemical Engineering Department, McMaster University, for a teaching assistantship.

His family for their moral and financial support throughout the course of his education.

TABLE OF CONTENTS

LIST OF FIGURES

LIST OF TABLES

1. INTRODUCTION

Emulsion polymerization is the most important commercial process for the production of polyvinyl acetate. Basically the monomer is polymerized in a mixture of water, emulsifier and a water-soluble free radical initiator. The end product is a dispersion of polymer particles in water and is called a 'latex'. The vinyl acetate homopolymer and copolymer latices are used as a base for latex paints, for adhesives, and for pigmented paper coatings.

Kinetically emulsion polymerization follows the normal steps of free radical polymerization. At the beginning, the system consists of emulsifier micelles, monomer droplets and initiator in the aqueous phase. Initiation takes place in the aqueous phase and free radicals diffuse into the micelles where solubilized monomer is polymerized and polymer particles are formed. More monomer diffuses into these polymer particles from the monomer droplets via the aqueous phase. Therefore propagation and termination take place in the polymer phase.

Emulsion polymerization has a number of advantages over other polymerization processes, solution or bulk. Due to the fact that radicals are separated from each other in particles

and therefore cannot terminate, radical concentration is high and therefore propagation rates are high. Polymerization rate is rapid and high molecular weight polymer can be produced. Heat transfer control is efficient since viscosity is low in the aqueous continuous phase. The end product in the form of a latex may be applied directly in many applications.

Investigations of vinyl acetate emulsion polymerization reported in the literature are in general disagreement. This is mainly due to the complexity of the surface phenomena in the heterogeneous system. However, several major conclusions can be drawn:

(1) Polymerization takes place in the particles.

(2) Number of free radicals per particle is very small.

(3) Number of particles has only a small effect on the rate of polymerization.

(4) Termination reactions are of little importance in molecular weight development.

(5) Molecular weight development is unaffected by initiator concentration and number of particles.

This thesis deals with the variables which affect polymer particle size and molecular weight development in vinyl acetate emulsion polymerization. A long term objective of the polymer and control groups is to develop a control

system for a latex reactor using a light transmission spectrophotometer as an on-line detector for particle size measurement interfaced with a dedicated minicomputer.

2. CLASSICAL THEORY OF EMULSION POLYMERIZATION

Emulsion polymerization is a process in which an aqueous suspension of a sparingly soluble monomer is converted into a stable dispersion of polymer particles in water. A typical emulsion polymerization recipe, as revealed in patents and trade literature, consists of:

Monomer	vinyl acetate	50-100 parts
Medium	water	100 parts
Emulsifier	sodium lauryl sulphate	2-6 parts
Initiator	potassium persulphate	0.5-1.5 parts

Water is the dispersion medium. Emulsifier is dispersed in the form of micelles. Monomer exists mainly as monomer droplets initially which have a size of approximately 1 to 10 microns. The remaining monomer is dissolved in the aqueous medium and solubilized in the micelles. The water soluble initiator decomposes to produce free radicals in the aqueous phase.

The emulsifier molecules are hydrophilic at one end and hydrophobic at the other. The hydrophobic ends aggregate to form micelles when the concentration of emulsifier exceeds a certain definite value called 'the critical micelle concentration'. A small amount of monomer is solubilized in

the interior of the micelles which have a size of approximately 50-100Å.

Harkins[1] was the first to propose a mechanism to explain the experimental observations in emulsion polymerization. His model is schematically represented in Figure 1.

Free radicals generated in the aqueous medium diffuse into the micelles and propagate. These 'stung' micelles are now referred to as monomer-swollen polymer particles. They are the chief loci of polymerization. The large monomer droplets act mainly as reservoirs supplying monomer to the reaction sites. As polymer particles grow, some of the micelles desorb to deliver the emulsifier necessary for stabilization of the polymer particles. Stage 1 ends when all the micelles are consumed and no new particles are formed. During this stage both the number of polymer particles and rate of polymerization increase with time. The percentage conversion of monomer is 5-15% at the end of stage 1, depending on emulsifier type and concentration and also of monomer type.

In stage 2 monomer continues to diffuse into the polymer particles at a rapid rate so that monomer concentration is maintained at an equilibrium level. Polymer particles grow with polymerization rate remaining constant as the number of polymer particles and monomer concentration within are constant.

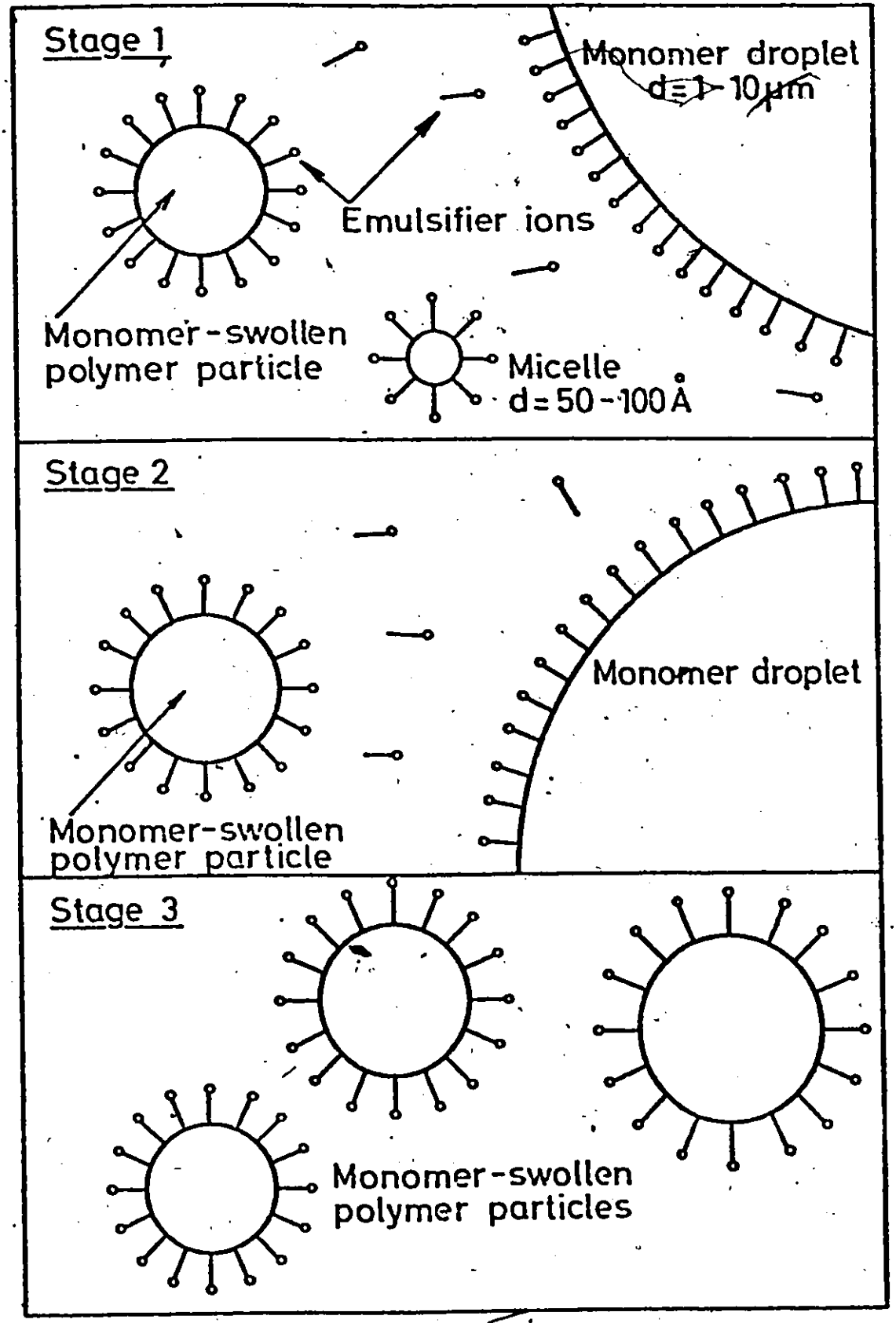

Fig. 1. Schematic representation of emulsion polymerization.

Stage 2 ends when all the residual monomer droplets have been consumed. In a typical styrene emulsion polymerization this occurs at a conversion of approximately 40-50%.

In stage 3 the system consists of only monomer-swollen polymer particles dispersed in water. Monomer concentration in the polymer particles falls as polymerization continues. The rate of polymerization decreases with a fall of monomer concentration and the number of polymer particles remains constant.

The first quantitative treatment of the kinetics of emulsion polymerization was given by Smith and Ewart[2]. These investigators studied the rate of many emulsion polymerization processes, the dependence of particle numbers on emulsifier and initiator concentrations, the diffusion rate of radicals and the formation of polymer particles. They were able to express the steady state kinetics of emulsion polymerization with a recursion formula. This formula was derived on the basis of the model proposed by Harkins. Smith and Ewart solved the recursion equations for three limiting cases. Later, a general solution was obtained by Stockmayer and O'Toole[4]. These solutions are valid only for monodisperse latices.

Smith and Ewart assumed that the kinetics were governed by three major processes:

(1) The rate of free radicals entering a single particle is given by ρ'/N, where

N = total number of particles,

ρ' = total rate of entrance into all N particles.

(2) The rate of radicals leaving a particle is given by $k_o a_p (n/v)$, where

k_o = desorption rate constant,

a_p = surface area of a polymer particle,

v = volume of a single polymer particle.

Therefore (n/v) is the concentration of free radicals in a particle.

(3) The rate of termination within a particle is given by $2k_{tp}n(n-1)/v$, where

k_{tp} = termination rate constant.

$(n-1)/v$ is the concentration of radicals with which any one of the n free radicals in the particle can react.

A steady state balance for number of particles containing n radicals, N_n, gives the recursion formula after Smith-Ewart.

$$N_{n-1}\left(\frac{\rho'}{N}\right) + N_{n+1}k_o a_p\left[\frac{(n+1)}{v}\right] + N_{n+2}k_{tp}(n+2)\left[\frac{(n+1)}{v}\right]$$

$$= N_n\left(\frac{\rho'}{N}\right) + N_n k_o a_p (n/v) + N_n k_{tp} n\left[\frac{(n-1)}{v}\right] \qquad (1)$$

This is the general expression for the distribution of free radicals in particles. Smith and Ewart then considered

three limiting cases.

Case 1. Number of free radicals per particle is small compared with unity.

In this case the rate of transfer of free radicals out of the particles is very fast. Therefore we need only consider particles with zero or one radical.

$$N_1 \frac{k_o a_p}{v} = \frac{N_o \rho'}{N} \qquad (2)$$

Since $N_o \cong N$,

$$\therefore \quad N_1 = \frac{\rho' v}{k_o a_p} \qquad (3)$$

In the steady state emulsion polymerization, the rate of termination is approximately equal to the rate of initiation. Therefore if termination takes place only in the polymer phase and occurs instantly when a free radical enters a particle already containing one radical, then

$$\rho = 2(\rho'/N) N_1 \qquad (4)$$

where ρ = rate of formation of radicals by decompostion of initiator.

From Equations 3 and 4 the rate of polymerization, R_p, is obtained as

$$R_p = k_p [M_p] N_1 = k_p [M_p] \left(\frac{V_p \rho}{2 k_o a_p}\right)^{\frac{1}{2}} \qquad (5)$$

where V_p is the total volume of the polymer phase.

This case applies to vinyl acetate emulsion polymerization where past investigations have shown that the concentration of free radicals per particle is much less than one[18, 24].

Case 2. The average number of free radicals per particle is equal to 0.5.

For this limiting case, the transfer of radicals out of polymer particles is negligible. The termination of a radical in a particle takes place immediately upon the entry of a second radical. Applying Equation 4 to this case where desorption is negligible gives

$$\rho = 2\,(\rho/N)\,N_1 \quad \text{where } \rho = \rho' \qquad (4a)$$

or in other words, $N_1/N = 1/2$ and since $N = N_0 + N_1$, N_0/N is also $\frac{1}{2}$. On the average, the number of free radicals per particle is equal to 0.5. Therefore, the overall rate of polymerization is given by

$$R_p = k_p[M_p]N/2 \qquad (6)$$

This equation has been found to hold for a number of emulsion polymerization systems, namely, styrene, isoprene and butadiene for conversions usually up to the end of stage 2.

Case 3. Number of free radicals per particle is large compared with unity.

In this case there are many radicals per polymer particle with each having the same number to within a very close approximation. We need treat only the 'statistical' polymer particle. From the recursion formula,

$$\frac{\rho}{N} = 2k_{tp}\left(\frac{n^2}{v}\right) \qquad (7)$$

The rate of polymerization can be described by the expression used for bulk polymerization:

$$R_p = k_p[M_p]Nn$$
$$= k_p[M_p]\left(\frac{V_p\rho}{2k_{tp}}\right)^{\frac{1}{2}} \qquad (8)$$

where n is the number of radicals per particle and is much greater than unity.

Stockmayer[3] was the first to obtain a general solution for the recursion formula proposed by Smith and Ewart. Later, Stockmayer's treatment was corrected and extended by O'Toole[4].

The recursion formula can be rearranged as:

$$(n+2)(n+1)N_{n+2} + m(n+1)N_{n+1} + \varepsilon N_{n-1}$$
$$= N_n[n(n-1) + mn + \varepsilon] \qquad (9)$$

where $$\varepsilon = \frac{v \rho'}{k_{tp} N} \qquad (10)$$

$$m = \frac{k_o a_o}{k_{tp}} \qquad (11)$$

The average number of radicals per particle, n, is

$$n = \frac{\zeta}{4} \frac{I_m(\zeta)}{I_{m-1}(\zeta)} \qquad (12)$$

where $\zeta^2 = 8\varepsilon$.

I_m denotes Bessel functions of the first kind. The rate of polymerization is then given by

$$R_p = k_p [M_p] N n \qquad (13)$$

Figure 2 is a plot of n as a function of ζ and m. It can be shown that the results are in agreement with the three limiting cases of Smith and Ewart.

The second problem in emulsion polymerization concerns the formation of polymer particles. A relationship between the number of particles formed and the initial concentration of emulsifier and initiator was also found by Smith and Ewart:

$$N = k(\rho/\mu)^{0.4}(Sa_s)^{0.6} \qquad (14)$$

where a_s = area occupied by one emulsifier molecule,

S = number of emulsifier molecules per unit volume of aqueous phase,

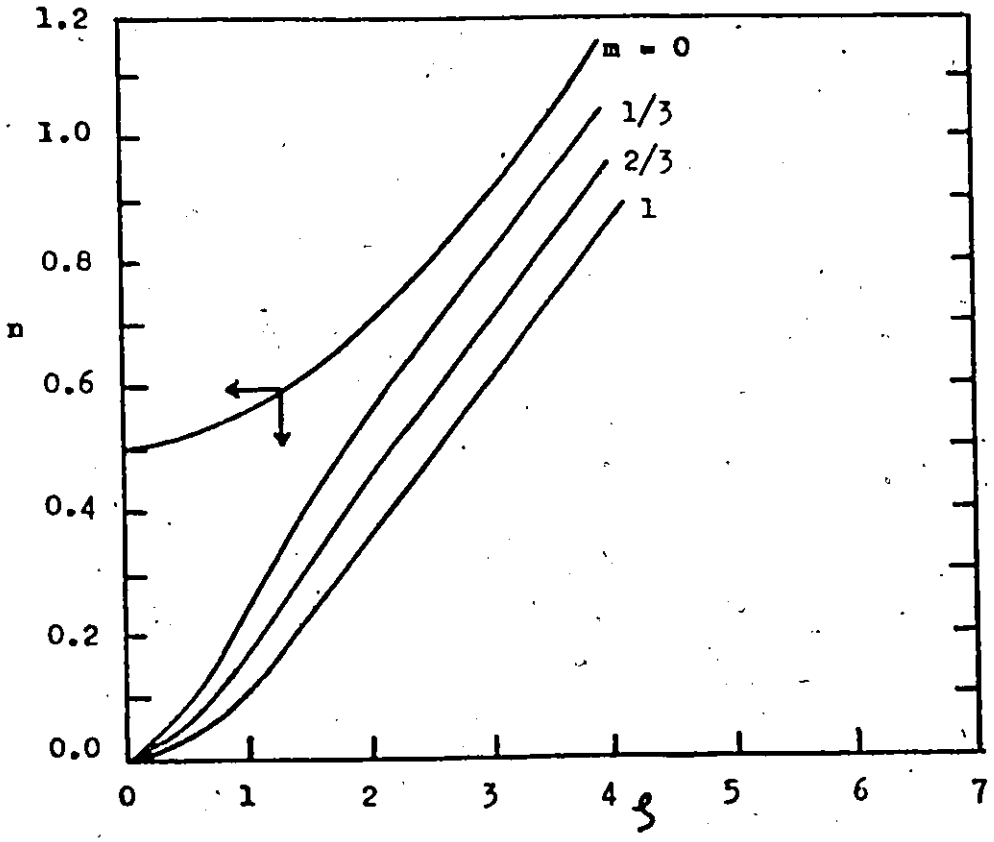

Fig. 2. n versus ζ and m (Stockmayer and O'Toole)

μ = rate of volume increase of a polymer particle,

k = constant.

In evaluating k, Smith and Ewart considered two idealized situations. First, all radicals were assumed to be captured by micelles as long as the micelles are present. In this case, k = 0.53. The number of particles predicted is too large owing to the neglect of radicals captured by polymer particles.

In the second situation, the rate of capture of radicals per unit area of the particle or micelle was assumed to be the same regardless of the size of the particle or micelle, then k = 0.37. The number of particles predicted is too small since the flux of radicals per unit area is inversely proportional to the radius of the particle involved.

Besides the theory of Smith and Ewart, Sheinker and Medvedev[5] proposed a different mechanism for isoprene polymerization. They considered polymerization to take place on the surface of the particles. For methyl methacrylate a mechanism, much like the one proposed by the Russian workers, was offered by Brodnyan et al.[6]. However, those theories have not been investigated to the same extent as the theory of Smith and Ewart. It is believed by most researchers that the polymerization takes place within the polymer particles.

3. PARTICLE SIZE MEASUREMENTS

3.1. INTRODUCTION

In the literature, electron microscopy and light scattering have been the standard methods for polymer particle size measurement. Electron microscopy can generate a lot of information, such as, size distribution, number-average and and weight-average particle diameters, but it is tedious. Light scattering provides an accurate measurement of weight-average particle diameter. It is a relatively tedious method and a very clean working environment for the instrument is required.

One of the major objectives of the present work is to develop the basis for an instrument to measure particle sizes, both number-average and weight-average diameters, on-line throughout the whole range of conversion in vinyl acetate emulsion polymerization.

3.2. LITERATURE SURVEY AND THEORETICAL BACKGROUND

3.2.1. ELECTRON MICROSCOPY

Electron microscopy is the standard experimental method for measuring particle size distribution from which the weight-average and number-average particle diameters can be calculated. In the literature micrographs of latices consisting of hard polymers, such as, polystyrene and polyvinyl chloride,

are of high quality. Though many investigators reported that particle size distribution of polyvinyl acetate latex was determined by electron microscopy the procedure was seldom described and the micrographs very seldom shown. Polyvinyl acetate is a film-forming polymer and is soft in nature. The polymer particles tend to flatten when treated for electron microscopic measurement. Drying stresses as well as heating from the electron beam collapse the normally spherical particles.

Bradford and Vanderhoff[27, 28] found that particles of soft polymers can be hardened by crosslinking with high-energy radiation. This method requires very large doses (20-30 megarads) and unfortunately it increases substantially the actual diameters of the particles.

The most effective method so far reported in the literature was developed by Vanzo[16]. This method is known as 'In Situ Polymerization'. A small amount of styrene is added to the polyvinyl acetate latex. It diffuses into the particles and when subjected to gamma-radiation of a dosage of 1 megarad, styrene polymerizes and a framework of polystyrene is built up within the particles and lends a great deal of resistance to deformation. Vanzo showed that the diameters of the polymer particles are not altered substantially by this method.

Furthermore his solubility study indicates that polyvinyl acetate particles may be swollen to over twice their volume with styrene before an external monomer phase forms. Therefore with the addition of a small amount of styrene to the latex no new particles consisting of pure polystyrene are generated.

The in situ polymerization hardening method developed by Vanzo has been adopted for particle size distribution study in the present work.

3.2.2. LIGHT TRANSMISSION TECHNIQUE

The use of light transmission is not common in polymer kinetics studies, particularly for polydisperse latices, such as, polyvinyl acetate. Heller et al.[29] has proven its validity in measurements with monodisperse polystyrene particles. Maron, Pierce and Ulevitch[30] used the method to measure polydisperse polybutadiene-styrene particles. Recently, Gulbekian[14] reported the use of light transmission method to determine particle diameters of polyvinyl acetate latex.

The basic principles of particle size measurement by light transmission is based on the Mie theory. It can be shown that the quantity, $\frac{A}{c}$, $\frac{\text{absorbance of sample}}{\text{concentration of sample}}$, at a fixed wavelength is only a function of the polymer particle diameter for monodisperse latices. Maron et al.[30] demonstrated experimentally that for a polydisperse latex, A/c is a function

of the weight-average particle diameter of the polymer, d_w, at a fixed λ .

$$\frac{A}{c} = \left(\frac{3\pi l}{4.606 d_p \lambda_m}\right) \frac{K^*}{\alpha} \qquad (15)$$

where l = path length of the transmission cell,

d_p = density of the polymer,

λ_m = wavelength of light in the medium,

$\alpha = \pi D/\lambda_m$, where D is the particle diameter for a monodisperse latex and corresponds to the weight-average particle diameter for a polydisperse latex,

K^* = light scattering coefficient.

Details of the derivation are shown in Appendix 9A.

Therefore, for a polymer latex with a fixed particle size distribution, A/c is a constant at a certain wavelength, λ_m, independent of the concentration, c.

If A/c for polyvinyl acetate latices with known particle size distribution (measured by electron microscopy and light scattering) is measured at a fixed wavelength, a calibration curve of A/c versus particle diameter can be established for measurement at that wavelength. This method was used to calibrate a Beckman DU spectrophotometer.

Pierce[31] evaluated various commercial light transmission detectors for particle size measurement. He

calibrated the instruments with the Mie Theory tabulations of Heller, Pangonis and Jacobson[32]. Pierce found good agreement between turbidity and light scattering measurements. However, this method gives calibration curves for weight-average particle diameters only. Details of this calibration method are given in Pierce's report[31] and will not be discussed further.

3.3. EXPERIMENTAL PROCEDURE

3.3.1. MATERIALS AND POLYMERIZATION PROCEDURE

Vinyl acetate, obtained from Glidden Company, was distilled twice and kept in a refrigerator before use. The emulsifier, purified grade sodium lauryl sulphate (Quolac ON-WD) was obtained from Alcolac Chemical Corporation. Laboratory grade potassium persulphate of 99.7% purity was obtained from Fisher Scientific Co. and was used as initiator. These chemicals were used without further purification. Distilled water with an electrical conductivity of less than 3×10^{-6} mhos was used as the dispersion medium and solvent for the initiator. Nitrogen, used for purging the reaction mixture, was obtained from a standard gas cylinder. Traces of oxygen were removed by bubbling the nitrogen gas through a 5% pyrogallol solution in 2N NaOH.

The polymerization apparatus is shown in Figure 3. It consisted of a 3- litre reaction vessel immersed in a water

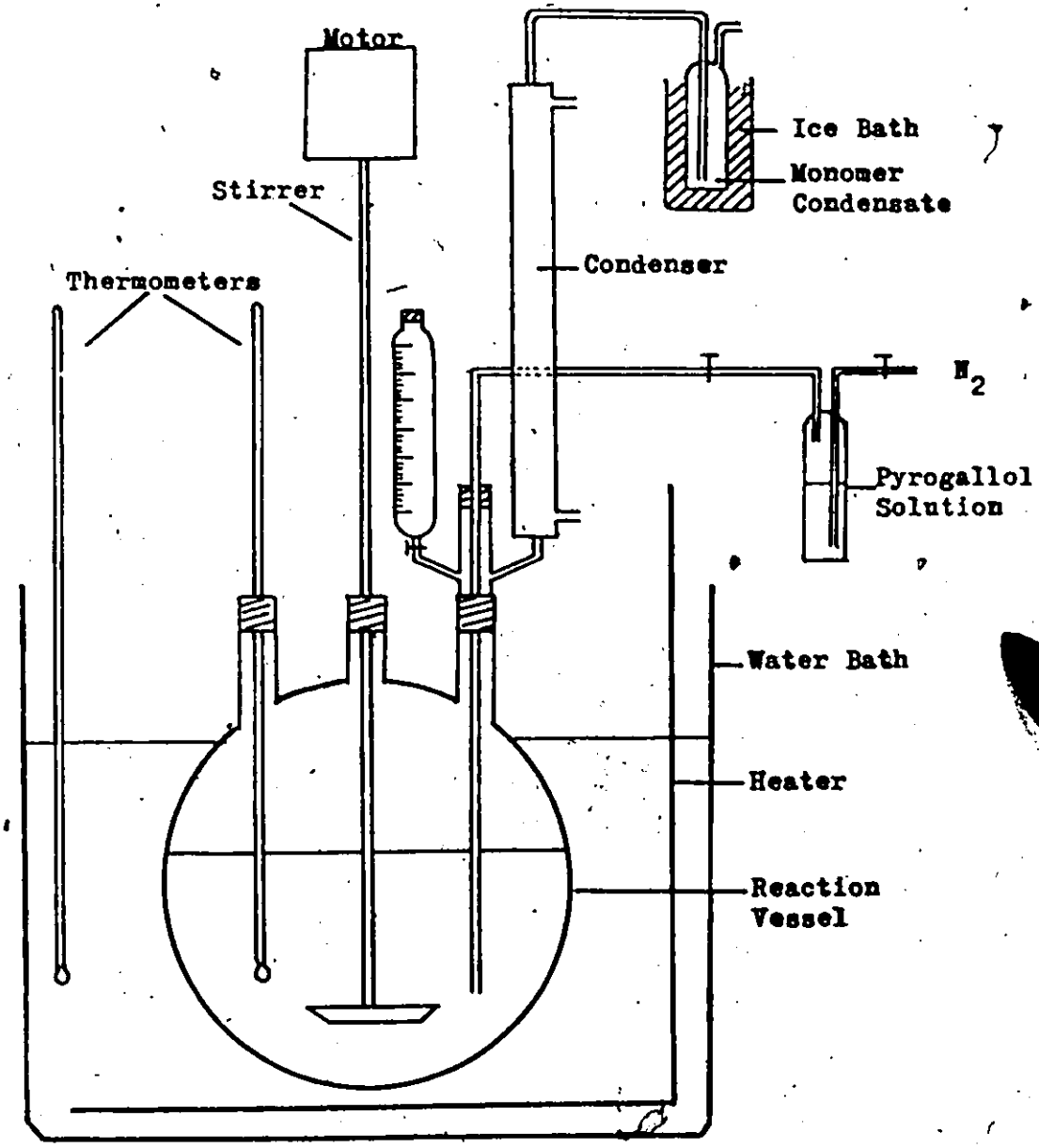

Fig. 3. Polymerization Apparatus

bath. A heating filament with temperature control was used to maintain the temperature of water in the bath. The reaction vessels had inlets for a thermometer, a nitrogen-gas inlet, a reflux condenser and a stirrer with speed control.

Before polymerization was initiated, the mixture of vinyl acetate monomer, water and emulsifier was purged with nitrogen for an hour. For all experiments, the emulsion comprised of 1750 ml H_2O and 1.2 gm initiator. The initiator was predissolved and was purged with nitrogen before reaction started. Various amounts of monomer and emulsifier were used to control the particle size. The temperature of the reactor was maintained at 50 $\pm$ 1°C. The emulsion was stirred at 150 r.p.m.

Conversion was determined by freezing the samples in liquid nitrogen to break the emulsion. The precipitated polymer was washed and dried to constant weight in a vacuum oven at 25°C. Samples of latex were withdrawn from the reactor for hardening by gamma-ray initiation of absorbed styrene and for light scattering and light transmission measurements.

3.3.2. PARTICLE SIZE DETERMINATION

3.3.2.1. ELECTRON MICROSCOPY

The following experimental procedure was adopted to treat polyvinyl acetate samples for particle size distribution study:

(1) The polyvinyl acetate latex at essentially complete conversion was diluted to 5% solid content.

(2) An amount of styrene equivalent to 10% of the weight of polyvinyl acetate was added to the polymer. It was shaken well to allow the styrene to diffuse into the polymer particles.

(3) The sample was irradiated with a Cobalt 60 gamma-radiation source with a total dose of 2 megarad.

(4) Copper grids were covered with formvar film. Then they were covered with carbon in a vacuum evaporator and mounted in a microscopic slide.

(5) The latex sample was divided into portions and diluted 100 times, 200 times and 400 times respectively. A small drop of Dow monodisperse polystyrene latex of diameter 2640 Å was added as an internal standard. Then one droplet of each portion was put on a grid surface.

(6) After drying, the grids on a slide were shadowed in a vacuum evaporator with gold-palladium alloy. The shadowing angle was measured.

(7) The grids were examined with a Philips Model 300 electron microscope. Micrographs were taken at a magnification x22,000.

(8) The micrographs were printed. About 1000 particles were

counted to determine the particle size distribution.

3.3.2.2. LIGHT TRANSMISSION AND LIGHT SCATTERING

A latex sample from the reactor was diluted from 100 to 200 times. The diluted samples were transferred to the optical cells for absorbance measurement. Detailed instructions for the operation of the Beckman DU spectrophotometer are given in the Beckman manual. The values of absorbance, A, at wavelength 5890Å, 5000Å and 4000Å for the diluted latex samples were measured and the quantity, A/c, calculated at each wavelength.

The weight average particle diameter of the sample was also determined by light scattering. The values obtained from light scattering were compared with those from electron microscopic measurement. Details of the light scattering technique are given in Appendix 9D.

3.4. RESULTS

3.4.1. ELECTRON MICROGRAPHS

Figures 4 and 5 show micrographs of polyvinyl acetate latices which were treated with the in situ polymerization hardening technique. It was found that the ratio of the shadow length to the diameter of the particle was almost the same as that of the spherical standard indicating that the polyvinyl acetate particles were spherical. The radii

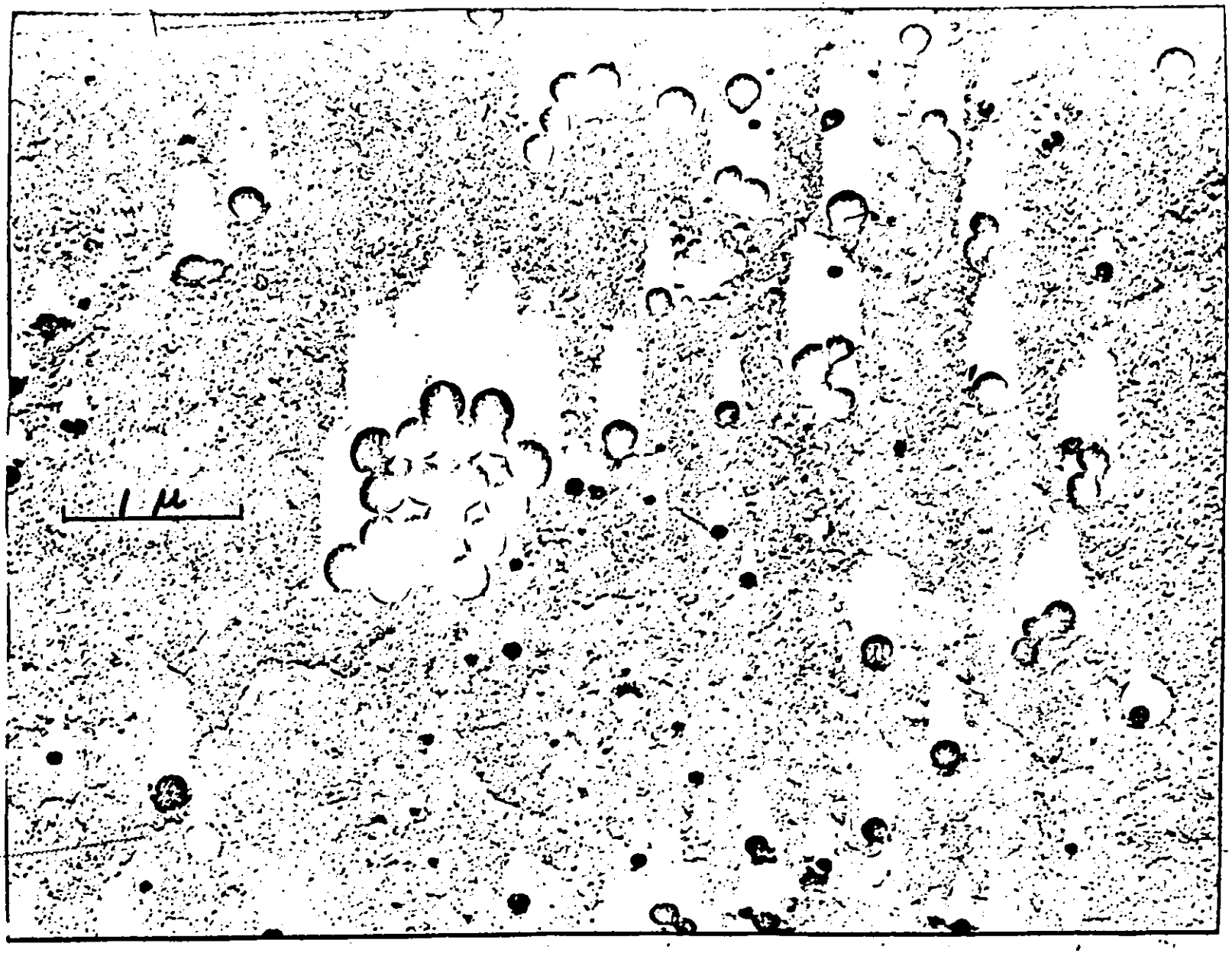

Figure 4. Micrograph of hardened polyvinyl acetate particles

Figure 5. Micrograph of hardened polyvinyl acetate particles

of particles were calculated from the shadow length and the shadowing angle and these were almost the same as the radii measured directly from the prints.

Figure 6 shows a micrograph of polyvinyl acetate latex obtained without hardening of the particles. It can be seen that the particles are not spherical.

3.4.2. PARTICLE SIZE DISTRIBUTION

Table 1 is a list of experiments that were performed in the particle size distribution study. Both Experiment No. A5

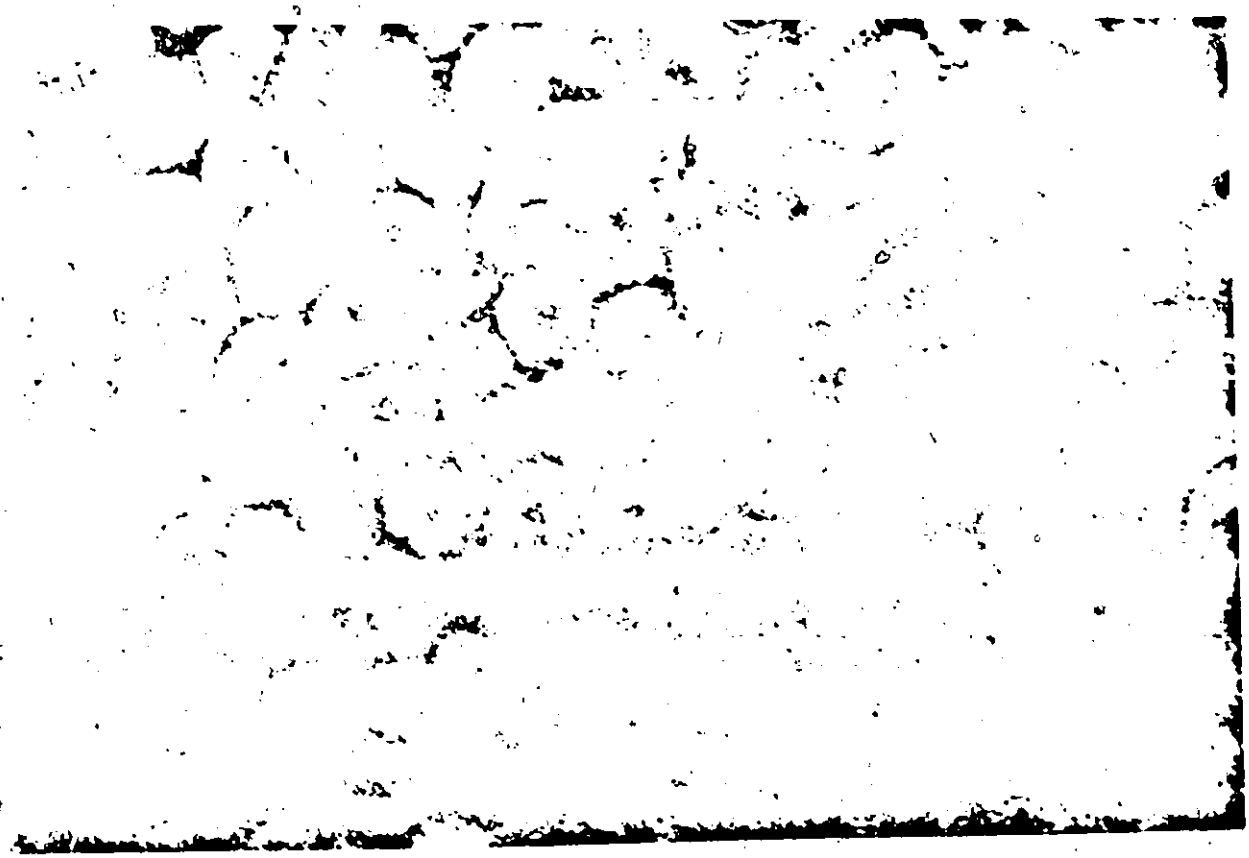

Fig. 6. Micrograph of an untreated polyvinyl acetate

and A7 were seeded from the PVAc latices of Experiment No. A4 and A6. The frequency data for Experiment No. A1 to A7 are listed in Appendix 9E.

TABLE 1

Experiments for Particle Size Distribution

Expt. No.	VAc(ml)	Water(ml)	$K_2S_2O_8$(gm)	SLS(gm)
A1	800	1750	1.2	5.0
A2	800	1750	1.2	15.0
A3	400	1750	1.2	30.0
A4	400	1750	1.2	8.0
A5	400	(+ PVAc latex from Expt. A4)		
A6	400	1750	1.2	12.5
A7	400	(+ PVAc latex from Expt. A6)		

Figure 7 shows the particle size distribution of a sample from Experiment A6 and Figure 8 shows the distribution of a sample from Experiment A7. The histograms indicate that particle size distributionsare skewed. This appears to be in agreement with the experimental results obtained by Vanzo[16].

From the micrographs it is possible to calculate the weight-average particle volume, $\bar{v}_w$, and number-average particle

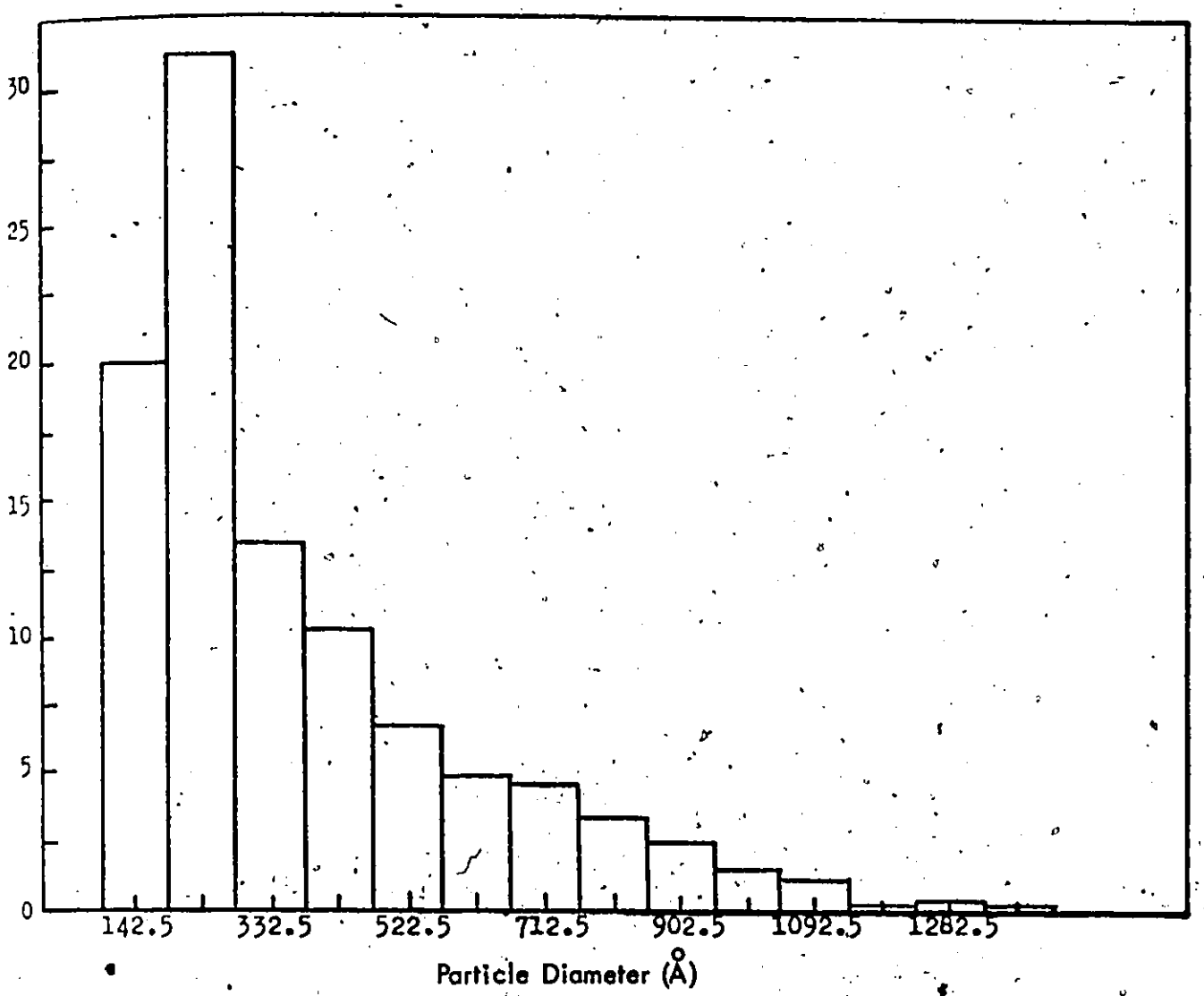

Fig. 7. Particle size distribution, Expt. A6.

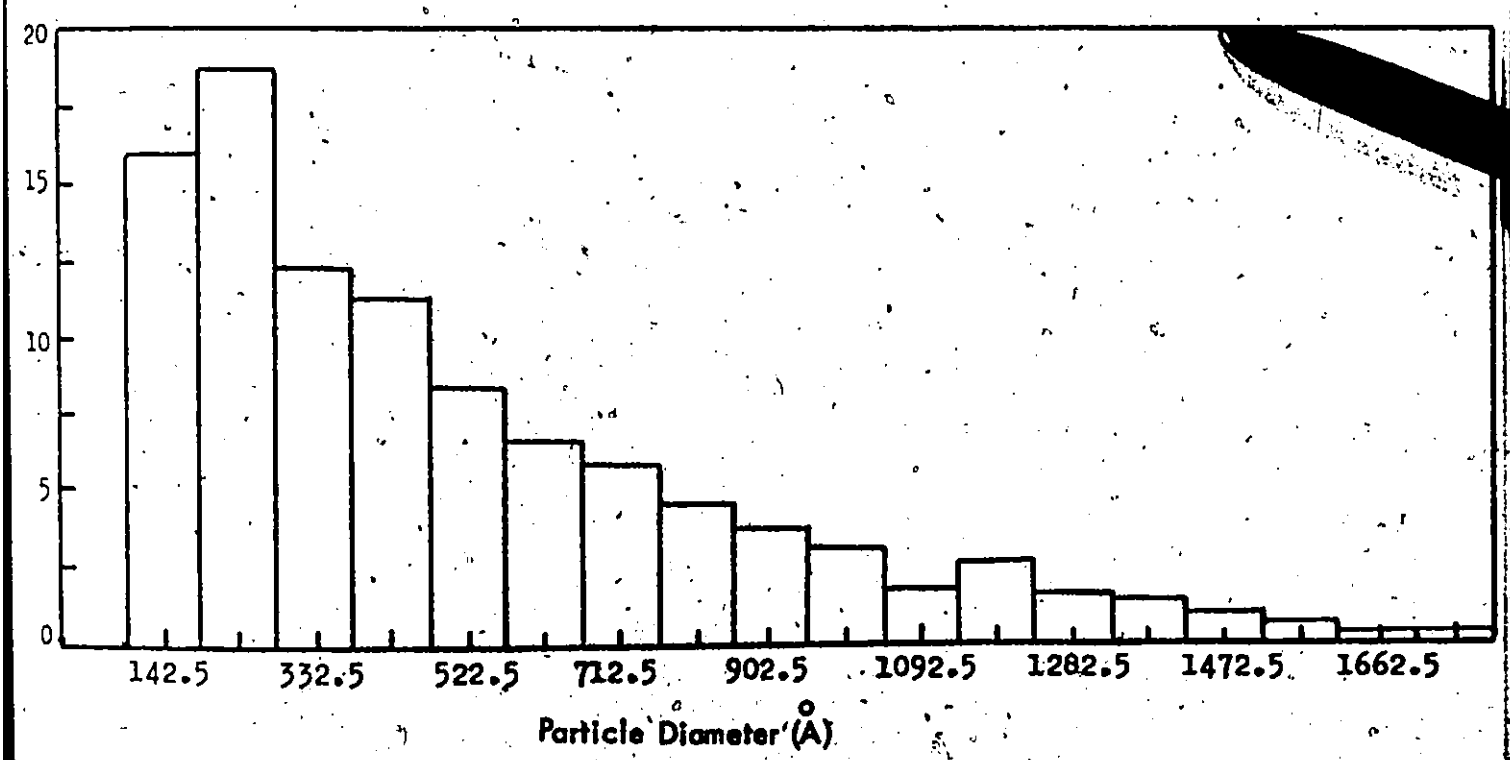

Fig. 8. Particle Size distribution, Expt. A7.

volume, $\bar{v}_n$, defined as

$$\bar{v}_w = \frac{\pi}{6} \frac{\Sigma n_i d_i^6}{\Sigma n_i d_i^3} \qquad (16)$$

$$\bar{v}_n = \frac{\pi}{6} \frac{\Sigma n_i d_i^3}{\Sigma n_i} \qquad (17)$$

where n_i denotes number of particles with a diameter, d_i.

The weight-average particle diameters of 7 polyvinyl acetate latices were calculated from particle size distributions and are compared with values obtained from light scattering in Table 2. The values obtained with these two independent methods are in good agreement. They differ by less than 10% which is well within experimental error.

Experiments A3, A4 and A6 were prepared with the same concentration of monomer and initiator. Only the emulsifier concentration was varied. It is of interest to know the effect of emulsifier concentration on the number of polymer particles in this case. Figure 9 is a plot of number of particles per c.c. versus emulsifier concentration. It was found that number of polymer particles was proportional to the 0.5 power of the emulsifier concentration, i.e.,

$$N \propto [E]^{0.5} \qquad (18)$$

TABLE 2

Comparison of d_w's from Electron Microscopy and from Light Scattering

Expt. No.	d_w(E.M.)(Å)	d_w(L.S.)(Å)
A1	1650	1565
A2	1230	1120
A3	770	700
A4	910	1100
A5	1360	1430
A6	850	936
A7	1160	1250

This is in agreement with the recent work of Nomura[18] and Friis[24] who also used sodium lauryl sulphate as the emulsifier.

In the work of Vanzo[16] and Friis[24] one particle size distribution was measured by electron microscopy and the ratio, $\bar{v}_w / \bar{v}_n$, was found to be 2.6. This value was assumed to be valid for all polyvinyl acetate latex particle size distributions obtained over a range of reaction conditions. Number-average particle diameters could then be computed from weight-average particle diameters obtained from light scattering data.

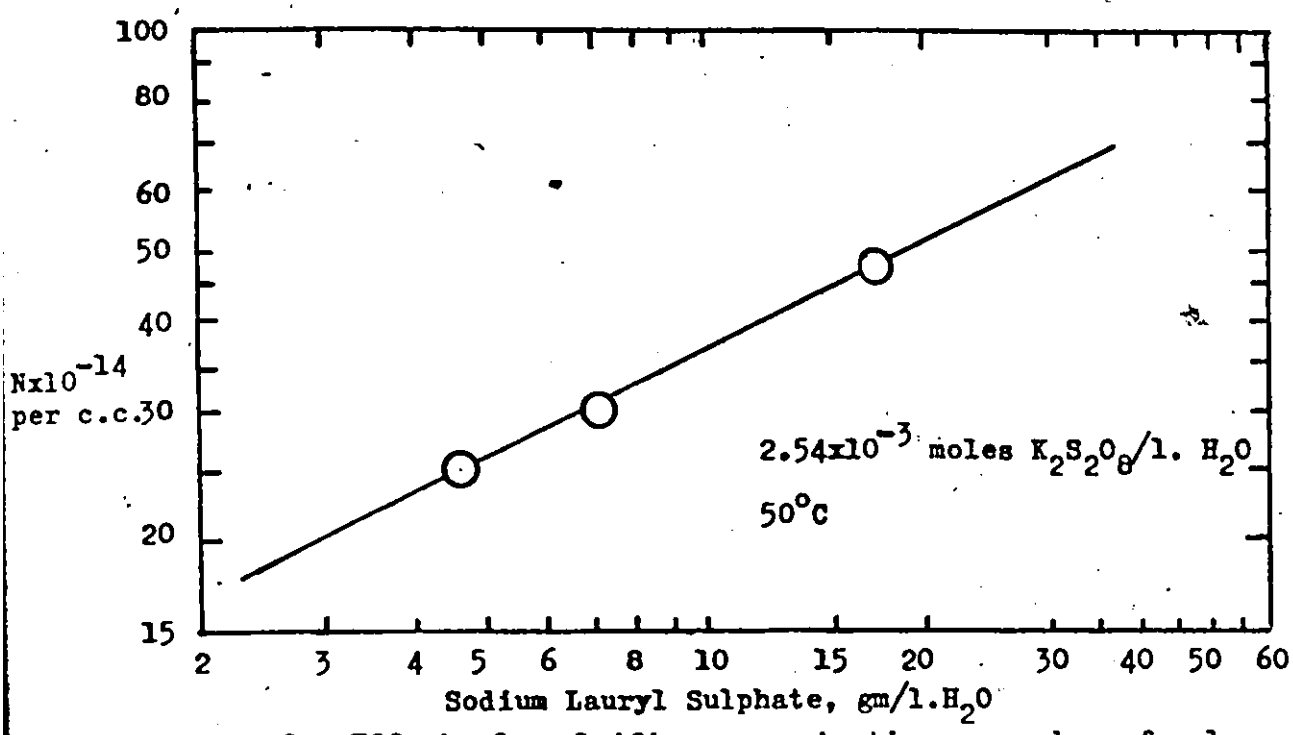

Fig. 9. Effect of emulsifier concentration on number of polymer particles at complete conversion.

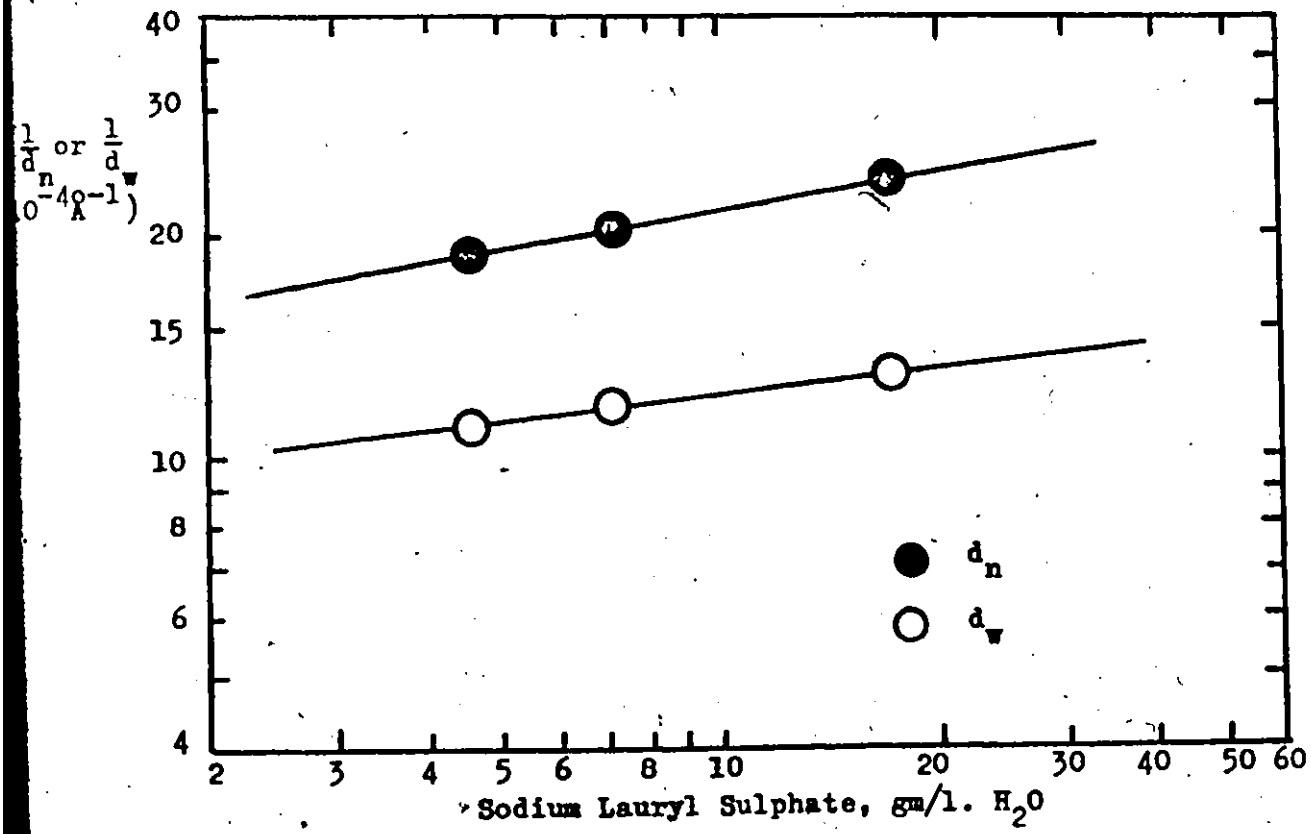

Fig. 10. Effect of emulsifier concentration on number-average and weight-average particle diameters at complete conversion.

In the present work, seven particle size distributions were measured and the ratio, $\bar{v}_w / \bar{v}_n$, was found to vary from 3.47 to 6.18 (Table 3). Therefore a fixed distribution cannot be assumed for vinyl acetate emulsion polymerization. Patsiga[15] did not apply the hardening technique and obtained a value of 2 for $\bar{v}_w / \bar{v}_n$. Undoubtedly, the techniques of hardening and shadowing have facilitated the counting of small particles which would otherwise have been missed.

Figure 10 shows the relationship between d_n, d_w and emulsifier concentration at complete conversion and at fixed initial initiator concentration. It can be established from the experimental data that

$$1/d_n \propto [E]^{0.167} \qquad (19)$$

$$1/d_w \propto [E]^{0.122} \qquad (20)$$

Therefore at complete conversion,

$$d_n = 0.0485\ d_w^{1.365} \qquad (21)$$

3.4.3. CALIBRATION CURVES FOR LIGHT TRANSMISSION SPECTROPHOTOMETER

To meet the Mie theory requirements of no secondary scattering and no particle interactions, the quantity, A/c, in Equation 15 has to be extrapolated to c = 0. Fortunately it was found experimentally that A/c is a constant for the range of

concentrations under consideration(<2 gm/l.). A/c is therefore a function of particle diameter and wavelength only.

For the seven particle size distributions determined by electron microscopy, their A/c values for wavelengths 5890Å, 5000Å and 4000Å were also measured (Table 3). Therefore calibration curves, A/c versus d_w or d_n, can be established. Figure 11 shows a typical calibration curve determined in this manner. A calibration curve calculated using the Mie theory light scattering coefficients tabulated by Heller et al.[32] is compared to that determined with electron microscopic data (Figure 11). They are in good agreement, particularly, for particle diameters less than 1200Å.

TABLE 3

Data of Light Transmission and Electron Microscopy Measurements

Expt.No.	$\frac{A}{c}(\lambda=4000Å)$	$\frac{A}{c}(\lambda=5000Å)$	$\frac{A}{c}(\lambda=5890Å)$	d_w(Å)	d_n(Å)	$\bar{v}_w/\bar{v}_n$
A1	0.9820	0.5450	0.3425	1650	1090	3.47
A2	0.6780	0.3500	0.2080	1230	685	5.80
A3	0.1710	0.0732	0.0406	770	420	6.18
A4	0.4350	0.2075	0.1188	910	520	5.38
A5	0.7040	0.3630	0.2160	1360	840	4.25
A6	0.3185	0.1440	0.0800	850	490	5.23
A7	0.5490	0.2690	0.1555	1160	650	5.70

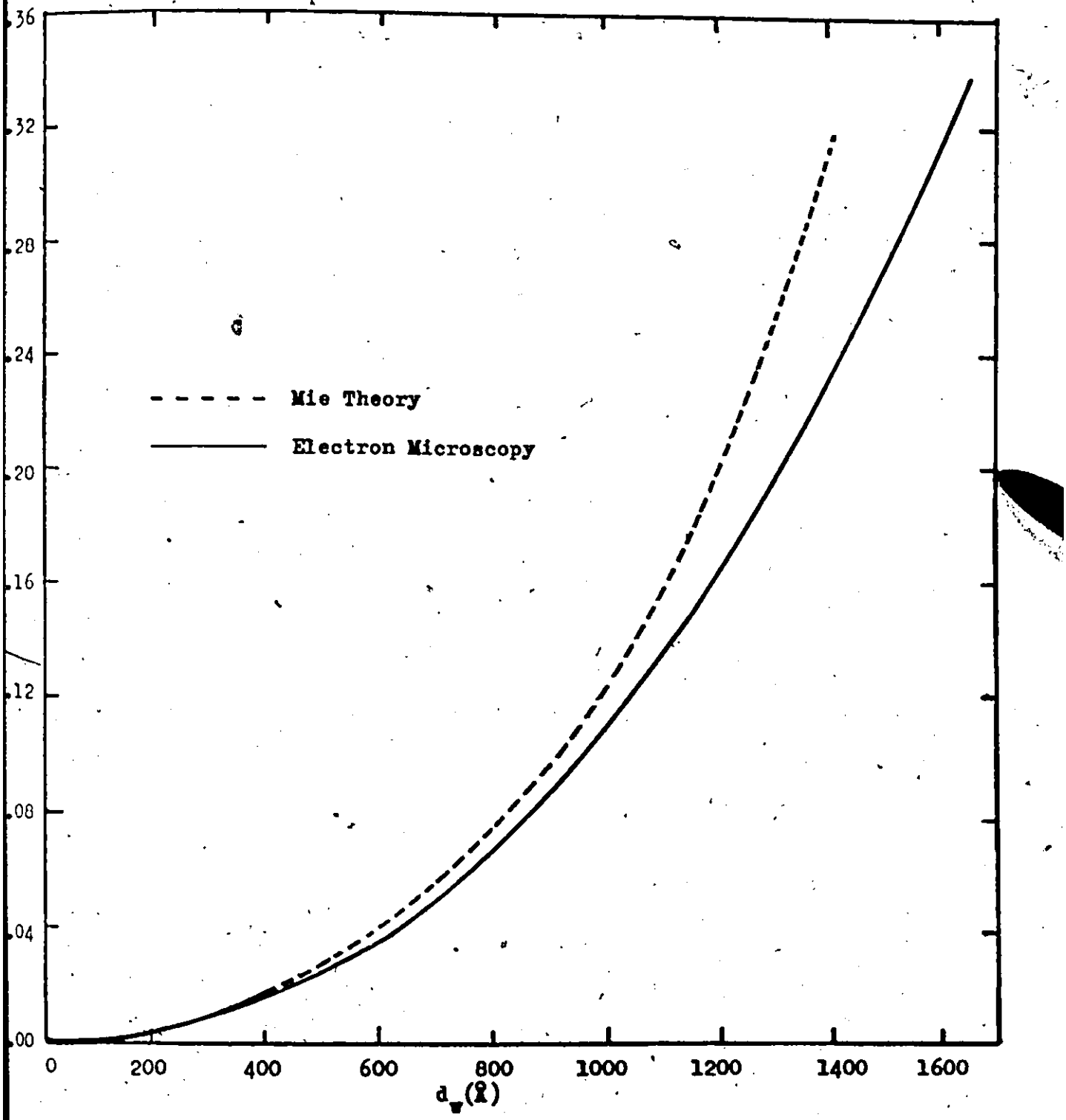

Fig. 11. Calibration curve, A/c versus d_w at λ = 5890Å.

4. EMULSION POLYMERIZATION OF VINYL ACETATE

4.1. INTRODUCTION

Smith and Ewart's theory finds good agreement with styrene emulsion polymerization but it cannot explain the experimental observations with vinyl acetate. A number of investigators have ascribed this non-conformity to the moderate solubility of vinyl acetate in water (2.1 wt% at 50°C for VAc and 0.037 wt% for styrene at 50°C)[7] and to the susceptibility of vinyl acetate radicals to chain transfer reactions during polymerization.

Though a fair amount of research has been done in vinyl acetate emulsion polymerization the results so far are contradictory. The detailed kinetics of the process is still unknown. One reason is that a uniform recipe and uniform experimental conditions have not been employed.

References 8 to 25 comprise the majority of research on vinyl acetate emulsion polymerization conducted during the past two decades. The following is a brief account of these reports.

4.2. LITERATURE SURVEY AND THEORETICAL BACKGROUND

4.2.1. POLYMERIZATION MECHANISMS

The relatively high solubility of vinyl acetate in water led several investigators to propose that polymerization actually takes place in the water phase, namely, Patsiga[9],

Gershberg[11], Gulbekian[14]. In this model, the monomer is supplied first by the monomer droplets and then by the monomer-swollen particles. The growing polymer molecules are stabilized by adsorption of ionic soap on their surface. The reaction medium will then have a constant composition and this will imply a constant rate of reaction.

The water phase polymerization mechanism fails to explain the high rate of polymerization and the large molecular weights generally obtained in an emulsion system. Polymerization in water phase would generally give linear polymer whereas polyvinyl acetate is highly branched. Friis et al.[22] calculated that the average number of branched points per monomer molecule of a polyvinyl acetate molecule at high conversion is more than 10.0. Furthermore, there are other evidences that do not support this model. In a study of the polymerization of vinyl acetate in aqueous media Napper et al.[13] observed a marked increase in the polymerization rate as soon as the initially formed polymer precipitated from the solution as polymer particles. This suggests that the major locus of polymerization is the polymer particles. Dunn and Taylor[20] showed that the concentration of monomer in the water phase dropped by a factor of 2 in going from 30 to 85% conversion. Therefore, the reaction medium is not constant as suggested.

In 1970, Litt, Patsiga and Stannett[10] presented a model to explain the almost zero-order dependence of rate on $[M_p]$. Their hypothesis is that polymerization proceeds mainly in the particles while termination occurs mainly in the aqueous phase. Polymerization is initiated in the aqueous phase. As the polymer grows it picks up soap and becomes a polyelectrolyte. After many collisions, the polymer is swept up by a particle. This implies a non-diffusion-controlled process with an activation energy necessary for breaking through the ionic double layers of the polymer and the particle. Growth of the now nonsolvated radical continues in the particle until chain transfer to monomer occurs. The major termination occurs when the neutral butyrolactonyl radical with perhaps several vinyl acetate residues added reacts with a growing aqueous radical. A secondary termination step is sweep-up of a growing radical into a particle containing a radical.

However Litt et al. also found that $[M_{aq}]$ was proportional to $[M_p]^{\frac{1}{2}}$. When this is substituted into their model it appears that rate of polymerization should decrease with the 0.25-0.5 power of $[M_p]$ over most of the polymerization range. This is inconsistent with experimental data.

In 1971, Harriott[21] presented a rate model for vinyl acetate emulsion polymerization. He hypothesized that

growth and termination take place primarily inside the swollen polymer particles. During polymerization an equilibrium distribution of radicals is established by a high rate of interchange of radicals between polymer particles. The rapid escape of radicals from particles is possible because of the relatively high rate of chain transfer to monomer and the moderate water solubility of monomeric and oligomeric radicals.

Friis[24] pointed out that data from previous research did not support this model. The model would predict a concave curve for conversion versus time plot in the range, 20-80% conversion and this is never observed in the literature.

The low concentration of free radicals per particle suggests that vinyl acetate emulsion polymerization can be described by Case 1 of the Smith-Ewart's theory. In fact, a number of models[24, 18] have been presented based on a mechanism involving the rapid escape and reabsorption of radicals in the polymer particles. Goosney[23] was able to predict molecular weight development up to 70% conversion based on this mechanism.

Friis[24] suggested that the mechanism of vinyl acetate emulsion polymerization is similar to that of vinyl chloride. He derived a rate model which was based on the vinyl chloride emulsion polymerization model developed by Ugelstad[36]. The data and conclusions based on this model compare favourably

with that of Nomura. Thus, it has been possible to obtain concurrent results from different laboratories.

4.2.2. EFFECTS OF VARIABLES

Vinyl acetate emulsion polymerization is a complex heterogeneous process with at least three phases (monomer phase, polymer phase and aqueous phase) and five components (polymer, monomer, initiator, emulsifier and water). In the past, a fair amount of research has been done to elucidate the effect of these variables on the rate of polymerization. Again, the experimental results are contradictory.

The effect of initiator concentration on rate of polymerization has received much attention. Gershberg[19] reported that the order of reaction with respect to initiator concentration is 0.6. Litt et al.[10] found an order of 1.0. Dunn and Taylor[20] found 0.64 and Dunn and Chong[26], 1.0 for low concentration and 0.6 for $[I] > 2 \times 10^{-4}$. O'Donnell[11] also found a shift from about 1 at low concentration to 0.7. Harriott[21] pointed out that exponents greater than 0.5 may be caused by impurities which have more effect at low persulphate levels, or by changes in the rate constant for decomposition of persulphate. Recently Nomura[18] and Friis[25] reported a value of 0.5.

Friis[24] reported the intrinsic viscosity of PVAc

to be independent of initiator concentration. In fact it is generally concluded that the initiator concentration does not appreciably affect the number of polymer particles in the system.

Litt et al.[10] found that the emulsifier concentration has no effect on the rate of polymerization. Gershberg[19] found that the rate of polymerization is proportional to the 0.25 power of emulsifier concentration. Nomura[18] found that emulsifier concentration had less effect on the rate of polymerization than in the emulsion polymerization of water-insoluble monomer such as, styrene. Friis[24] found the value of the exponent to be approximately 0.12.

Emulsifier concentration has a significant effect on the number of polymer particles. Gershberg[19] reported that the number of particles increases with 0.2 power of emulsifier concentration. French[8] found that the value of the exponent should be 3. From Nomura's data[18], it could be calculated that number of particles is proportional to the square root of the emulsifier concentration. The same value was reported by Friis.

The water-to-monomer ratio should not affect the kinetics of emulsion polymerization. This is true only if relatively high ratios are being used. Litt et al.[10] found experimentally that the rate of polymerization is almost

independent of monomer concentration in the particles until 85-90% conversion.

A number of investigators[8, 13, 24] concluded that the number of particles is independent of conversion beyond a conversion of about 10%. Priest[12] reported a decrease in number of particles from a certain critical conversion. Priest explained this as being due to an increased rate of particle coalescence as the particles become larger.

Stannett et al.[10] found the rate of polymerization to be independent of the number of particles. Friis found that $R_p \propto N^{0.25}$.

Motoyama[17] found that the effect of stirring on the particle number is more important in the emulsion polymerization of vinyl acetate than in that of styrene. Usually violent stirring causes a decrease in the rate of emulsion polymerization. Lindemann[7] discussed the effect of agitation on the rate of emulsion polymerization of vinyl acetate. In some of the early literature reference was made to the fact that agitation decreased the rate of polymerization. It was found later that oxygen, which was still present in traces, was responsible for this effect.

Temperature changes the rate of polymerization due to its significant effect on the rate constants.

In order to establish the point at which the separate monomer phase disappears some investigators have followed the diffusion of monomer into the polymer particles during polymerization. French[8] found the separate monomer phase vanished at 13.5%. Vanzo[16] found it to be 32%. Nomura[18] found a value of 23%. Friis[24] found the monomer phase disappeared at a conversion of 20%.

4.2.3. MOLECULAR WEIGHT DEVELOPMENT

For the past two decades all the research efforts in vinyl acetate emulsion polymerization have been devoted to the development of kinetic models which can predict the rate of polymerization. Goosney's[23] experimental and theoretical work in this laboratory is a first attempt to derive a model which can account for the molecular weight development in the process. His investigation was extended and a model[22] which is based on the equations developed by Graessley[37] and Stein[38] for predicting molecular weight development in vinyl acetate bulk polymerization was established. The following is a brief account of the model developed in this laboratory and the details are described in Reference 22.

Consider a single statistical particle in the emulsion system. It represents the whole population of particles and therefore the moments of distribution in this particle is the

value of the moments in all particles when mixed together.

In free radical polymerization a growing radical, $P_r^\bullet$, may enter any one of the following reactions:

Propagation	$P_r^\bullet + M \xrightarrow{k_p} P_{r+1}^\bullet$	(22)
Monomer transfer	$P_r^\bullet + M \xrightarrow{k_{fm}} P_r + P_1^\bullet$	(23)
Polymer transfer	$P_r^\bullet + P_s \xrightarrow{k_{fp}} P_r + P_s^\bullet$	(24)
Terminal double-bond polymerization	$P_r^\bullet + P_s \xrightarrow{k_p^*} P_{r+s}^\bullet$	(25)
Termination by disproportionation	$P_r^\bullet + P_s^\bullet \xrightarrow{k_{td}} P_r + P_s$	(26)
Termination by combination	$P_r^\bullet + P_s^\bullet \xrightarrow{k_{tc}} P_{r+s}$	(27)

In vinyl acetate emulsion polymerization it has been shown that termination reactions are not important[22]. Therefore, their contribution to molecular weight development can be neglected.

There are two stages in the process. In stage 1 the reaction mixture consists of three phases, namely, the monomer phase, monomer-swollen polymer particles and aqueous phase. In stage 2, monomer phase disappears and there are only 2 phases, namely, monomer-swollen polymer particles and water phases.

During stage 1, monomer-polymer ratio remains constant while the particle grows. The system can be described by the

following equations:

$$\frac{Q_o}{V_p}\frac{dV_p}{dt} = (k_{fm}[M_p] - k_p^* Q_o)Y_o \qquad (28)$$

$$\frac{Q_1}{V_p}\frac{dV_p}{dt} = (k_p[M_p] + k_{fm}[M_p])Y_o \qquad (29)$$

$$\frac{Q_2}{V_p}\frac{dV_p}{dt} = 2Y_o(k_p[M_p] + k_p^* Q_1)\left(\frac{k_p[M_p]+k_{fm}[M_p]+k_{fp}Q_2+k_p^*Q_1}{k_{fm}[M_p]+k_{fp}Q_1}\right) + k_p[M_p]Y_o \qquad (30)$$

where $Q_o = \sum_{r=1}^{\infty} P_r$

$Q_1 = \sum_{r=1}^{\infty} rP_r$

$Q_2 = \sum_{r=1}^{\infty} r^2 P_r$

$Y_o = \sum_{r=1}^{\infty} (P_r^\bullet)$

P_r = concentration of molecules with r repeating units,

$P_r^\bullet$ = concentration of radicals with r repeating units.

From Equations 28, 29 and 30 the number-average and weight-average molecular weights in stage 1 can be expressed as:

$$M_n = m_o Q_1/Q_o = \frac{m_o(k_p[M_p]+k_{fm}[M_p]+k_p^*Q_1)}{k_{fm}[M_p]} \qquad (31)$$

$$M_w = m_o Q_2/Q_1 = m_o \frac{2(k_p[M_p]+k_p^*Q_1)^2+k_p[M_p](k_{fm}[M_p]+k_{fp}Q_1)}{k_p[M_p](k_{fm}[M_p]+k_{fp}Q_1)-2k_{fp}Q_1(k_p[M_p]+k_p^*Q_1)} \qquad (32)$$

The equations can be solved with the following rate constants:

$k_p = 1.89 \times 10^7 \exp(-5650/RT)$ lit./mole-sec.

$k_{fp} = 1.43 \times 10^6 \exp(-9020/RT)$ lit./mole-sec.

$k_{fm} = 3.55 \times 10^6 \exp(-9950/RT)$ lit./mole-sec.

$k_p^* = 1.07 \times 10^7 \exp(-5650/RT)$ lit./mole-sec.

During stage 2 a single particle can be regarded as a locus of bulk polymerization with very slow initiation and termination reactions. Therefore equations derived by Graessley[37] and Stein[38] for bulk polymerization are directly applicable.

$$\frac{dQ_o}{dX} = c_m M_o - \frac{KQ_o M_o}{[M_p]} \tag{33}$$

$$\frac{dQ_1}{dX} = M_o \tag{34}$$

$$\frac{dQ_2}{dX} = M_o + 2\left(M_o + \frac{KQ_1 M_o}{[M_p]}\right)\left(\frac{[M_p] + c_p Q_2 + KQ_1}{c_m [M_p] + c_p Q_1}\right) \tag{35}$$

where $c_m = k_{fm}/k_p$

$c_p = k_{fp}/k_p$

$K = k_p^*/k_p$

$[M_p] = M_o(1 - X)$

Equations 33, 34 and 35 can be solved numerically with the initial values of Q_o, Q_1 and Q_2 calculated from Equations 28, 29 and 30.

During stage 2, the rate constant k_p^* decreases with

conversion since terminal double bond polymerization is diffusion-controlled. k_p^* is expressed as

$$k_p^* = A_o + A_1X + A_2X^2 + A_3X^3 \quad (36)$$

where $A_o = 1.07 \times 10^7 \exp(-5650/RT)$

$A_1 = -169.59$

$A_2 = -479.92$

$A_3 = -1014.3$

The experimental results of Goosney were found to fit the model from 0 to 100% conversion.

4.3. EXPERIMENTAL PROCEDURE

4.3.1. MATERIALS AND POLYMERIZATION PROCEDURE

The chemicals and equipment were the same as those described in Section 3.3.1.

The general experimental procedure was the same. Emulsion samples were drawn from the reactor in ten to twenty minutes intervals. Their percentage conversion was determined.

In all experiments, the recipe consists of 1000 ml distilled water and 400 ml vinyl acetate and varying amounts of initiator and emulsifier.

4.3.2. PARTICLE SIZE AND MOLECULAR WEIGHT DETERMINATION

The emulsion samples were diluted from 100 to 200

times. Their absorbance was measured with Beckman DU spectrophotometer. After calculating their ratios, A/c, their number-average and weight-average diameters could be obtained from the calibration curves established from previous electron microscopic work.

Molecular weight distribution of the polymer samples was determined using a Waters Associates Chromatograph Model No. ALC-201. Polyvinyl acetate samples were dissolved in tetrahydrofuran (THF) to form a solution of 0.25 wt%. The chromatograph was operating at room temperature (25°C) and at carrier solvent flow rate of 2.5 ml/min. The GPC was previously calibrated (calibration procedure described in Appendix 9B).

The chromatograms were interpreted for molecular weights using a digital program developed in this laboratory.

4.4. RESULTS

4.4.1. CONVERSION VERSUS TIME CURVES

Figure 12 shows the conversion versus time curves at different initiator concentrations. Qualitatively it can be observed that there was an accelerating period from 0 to about 20% conversion. Then the rate of polymerization was constant from 20% to almost 90%. Afterwards the rate decreased.

In literature, many investigators reported an induction period when polymerization starts. In the present

work this was not observed. The reaction started as soon as initiator was added to the emulsion system. This could be due to two reasons. The monomer used in the present work had been distilled twice with a vacuum distillation system. Practically all traces of inhibitors in the vinyl acetate were removed. Before polymerization the mixture of emulsifier, water, and monomer was purged with nitrogen for approximately one hour to remove traces of oxygen. Dissolved oxygen can be a major factor that inhibits the reaction. The emulsion system was also continuously purged with nitrogen during the reaction.

The effect of initiator concentration on the rate of polymerization can be determined from Figure 13. The rate was calculated from the linear portions of the conversion versus time curves. Figure 13 shows the log-log plot of polymerization rate versus initiator concentration.

The rate of polymerization was found to be proportional to 0.525 power of the initiator concentration. This is in good agreement with a number of findings in the literature[18,24,20,19]. Thus, it can be concluded that the rate of polymerization is approximately proportional to the square root of the initiator concentration.

Figure 14 shows that the rate of polymerization increased when a quantity of initiator was added to the emulsion

system during the reaction. It has often been a practice in industry to add more initiator to the reactor at the final stage of polymerization. This pushes the polymerization process to higher conversion in a far shorter time.

The rate of polymerization is given by

$$R_p = \frac{k_p [M_p]}{N_A} Nn$$

Since R_p can be determined from the slope of the conversion versus time curve and N, the number of polymer particles per litre, can be calculated from the particle diameter

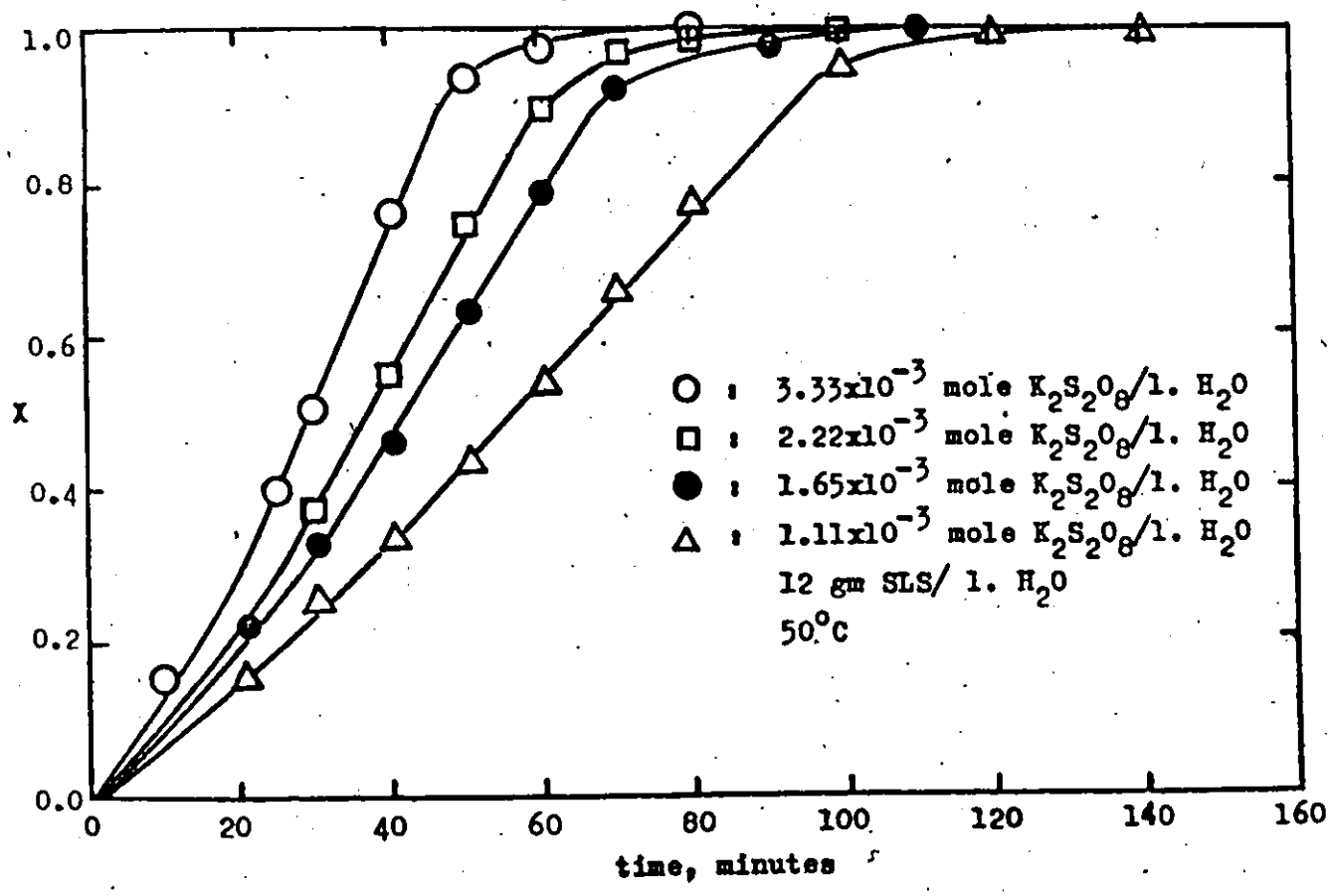

Fig. 12. Conversion versus time at different initiator levels.

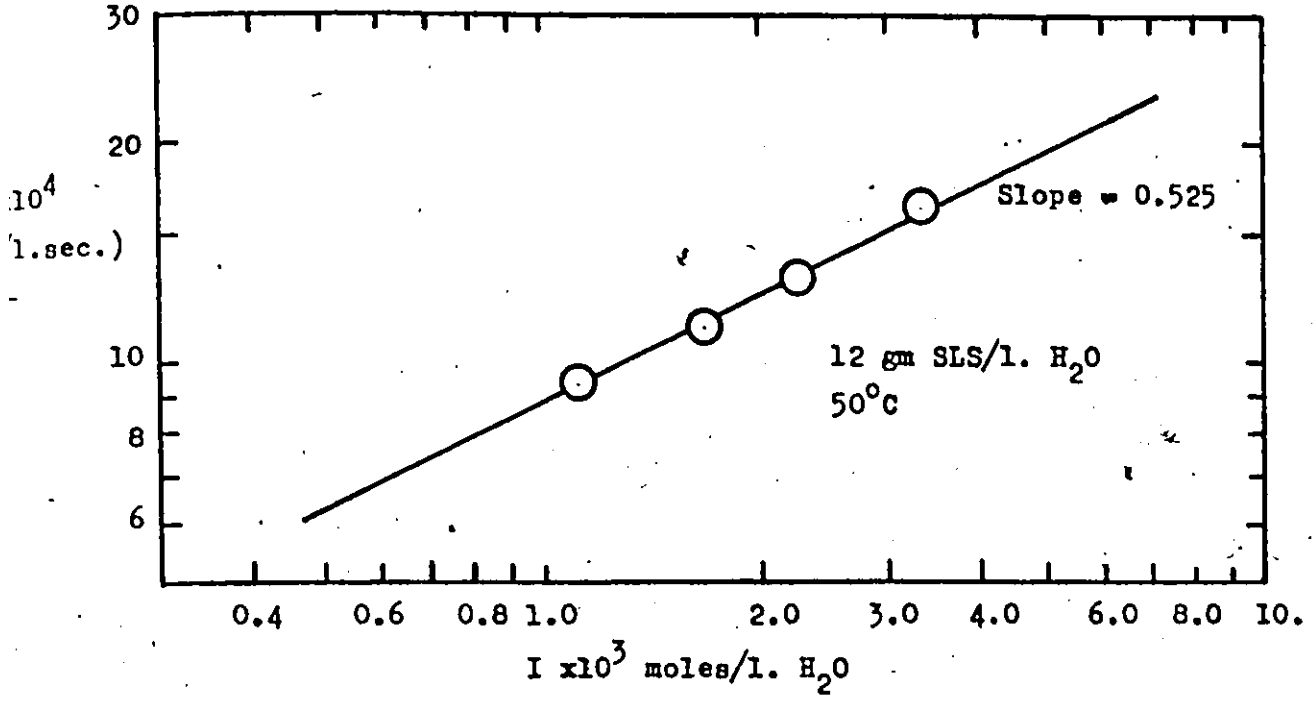

Fig. 13. Rate of polymerization versus initiator concentrations.

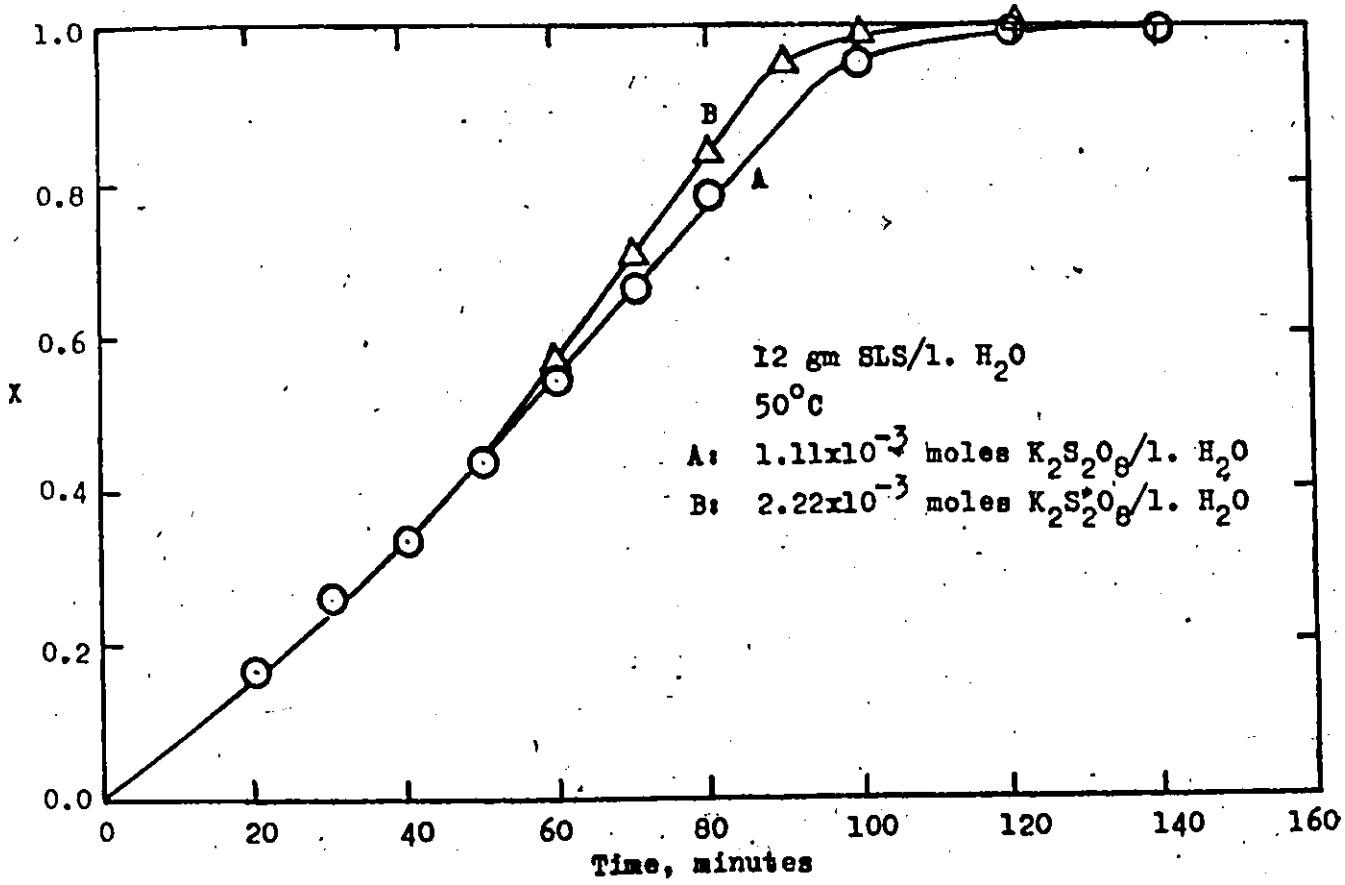

Fig. 14. Effect of adding initiator during polymerization.

(Section 4.4.2.), n, the average number of radicals per particle, can be calculated.

Figure 15 shows the average number of radicals per particle, n, versus conversion for a typical polymerization process. n was found to be small throughout the whole conversion range though it increased rapidly from low to high conversion.

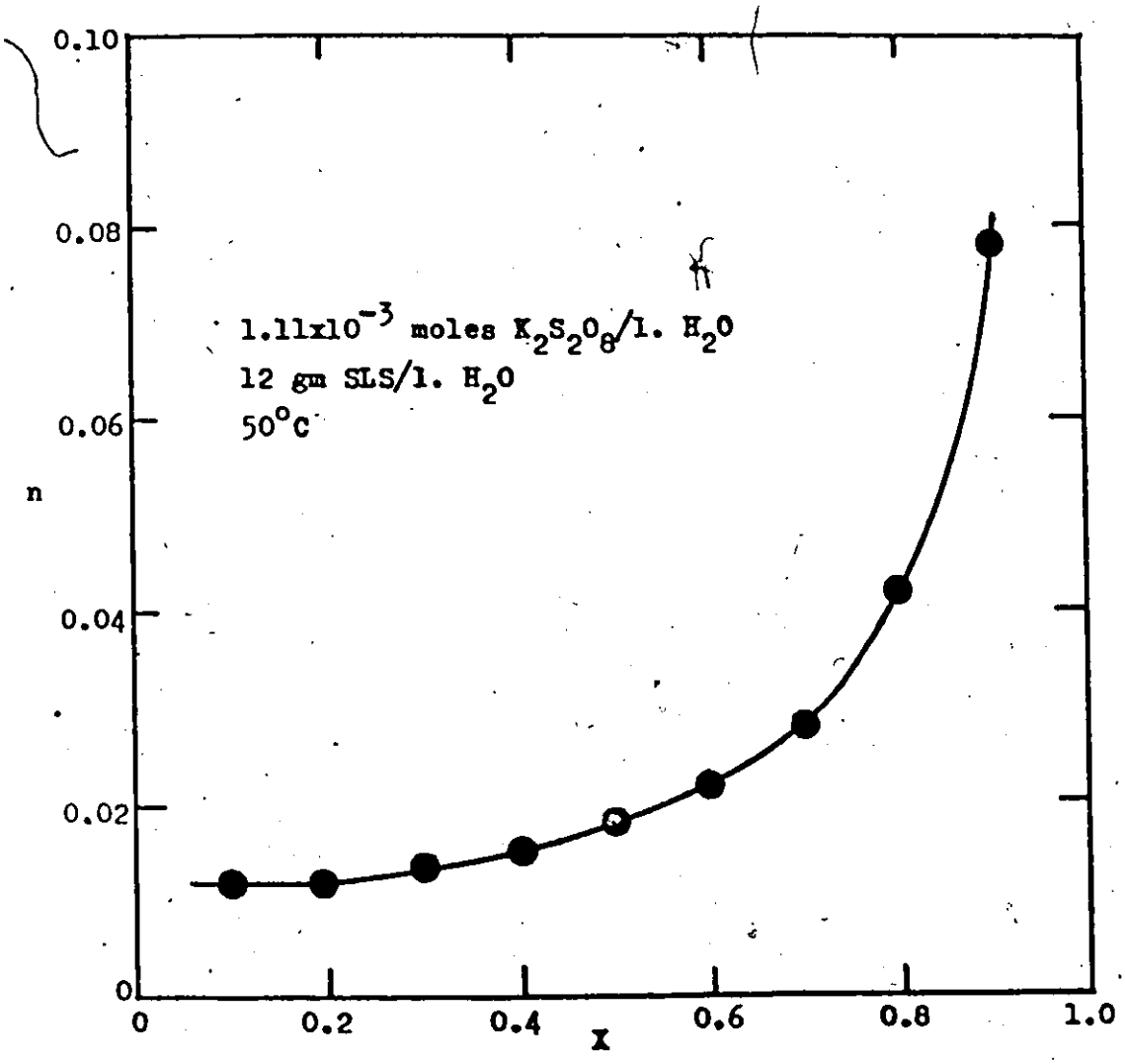

Fig. 15. Average number of radicals per particle versus conversion.

Figure 16 shows the conversion versus time curves at different emulsifier concentrations. It can be seen that the slopes of these curves are not very different from each other. it appears that emulsifier concentration has a negligible effect on the rate of polymerization in the range of concentrations considered in this report. This is not in disagreement with recent investigations reported in the literature. Patsiga[10] reported a zero effect. Friis[24] reported that rate of polymerization was proportional to the 0.12 power of emulsifier concentration. In the report of Nomura[18], a small effect due to emulsifier concentration can be seen only when the difference in emulsifier concentration is more than 10 times.

The experiments were repeated with laboratory grade sodium lauryl sulphate as emulsifier supplied by Fisher Scientific Co. and with the same initiator concentration as the previous experiments. Figure 17 indicates that the rate of polymerization was not affected by different emulsifier concentration.

It is of interest to notice from Figures 16 and 17 that the rates of polymerization were very different when two types of sodium lauryl sulphate supplied by different manufacturers were used. This strongly indicates that impurities in the emulsifier have a significant effect on the rate of polymerization.

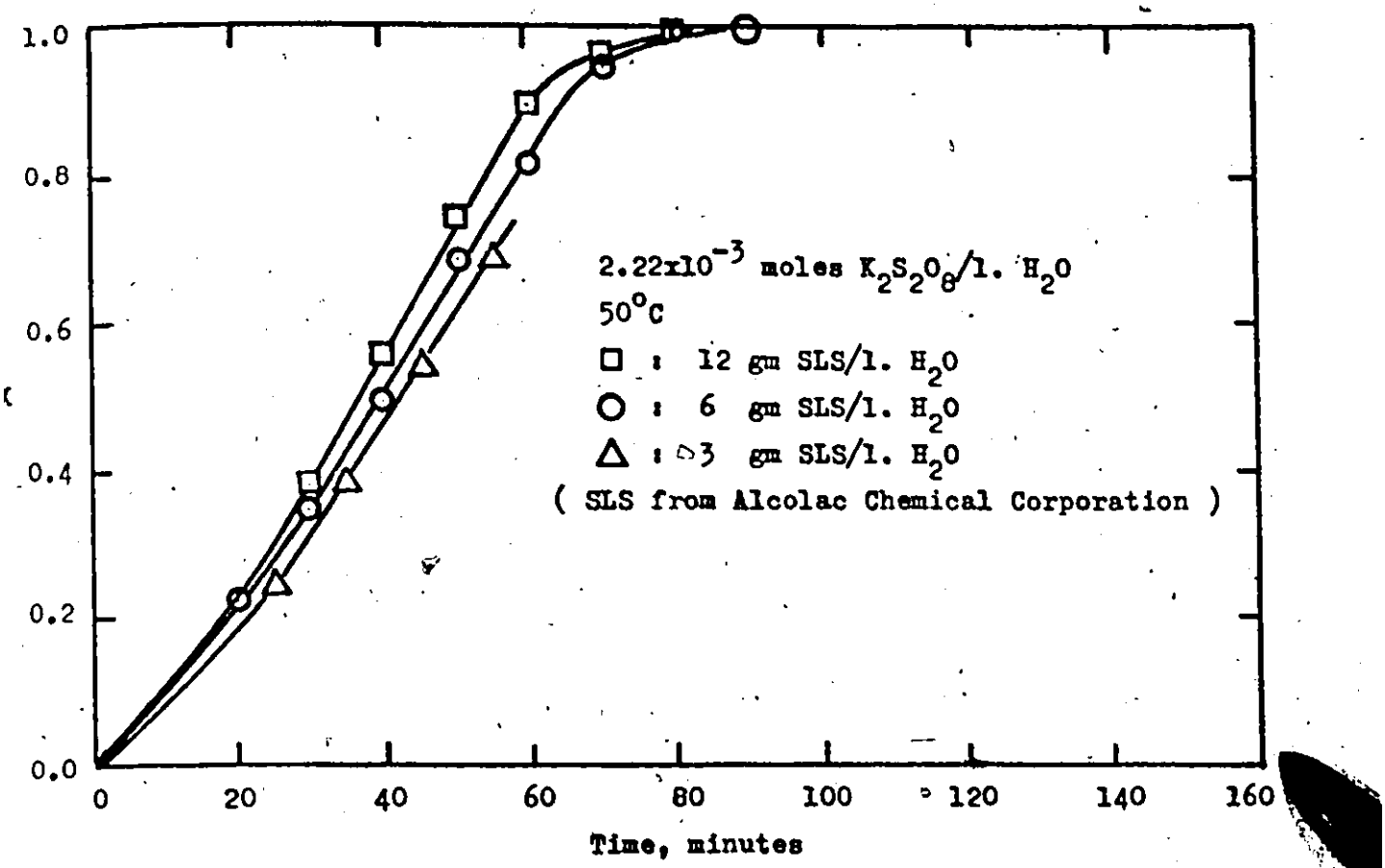

Fig. 16. Conversion versus time at different emulsifier concentrations.

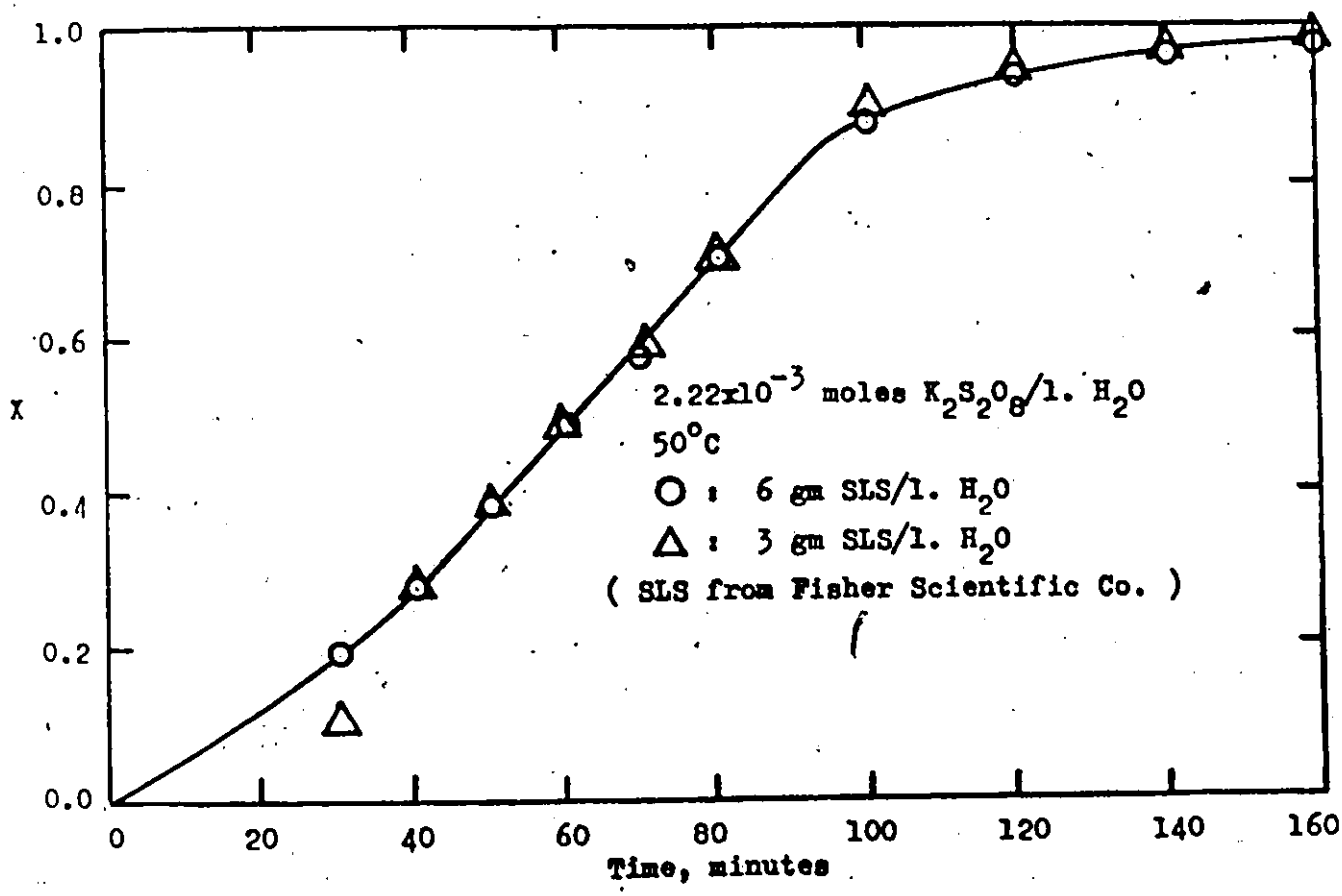

Fig. 17. Conversion versus time at different emulsifier concentrations.

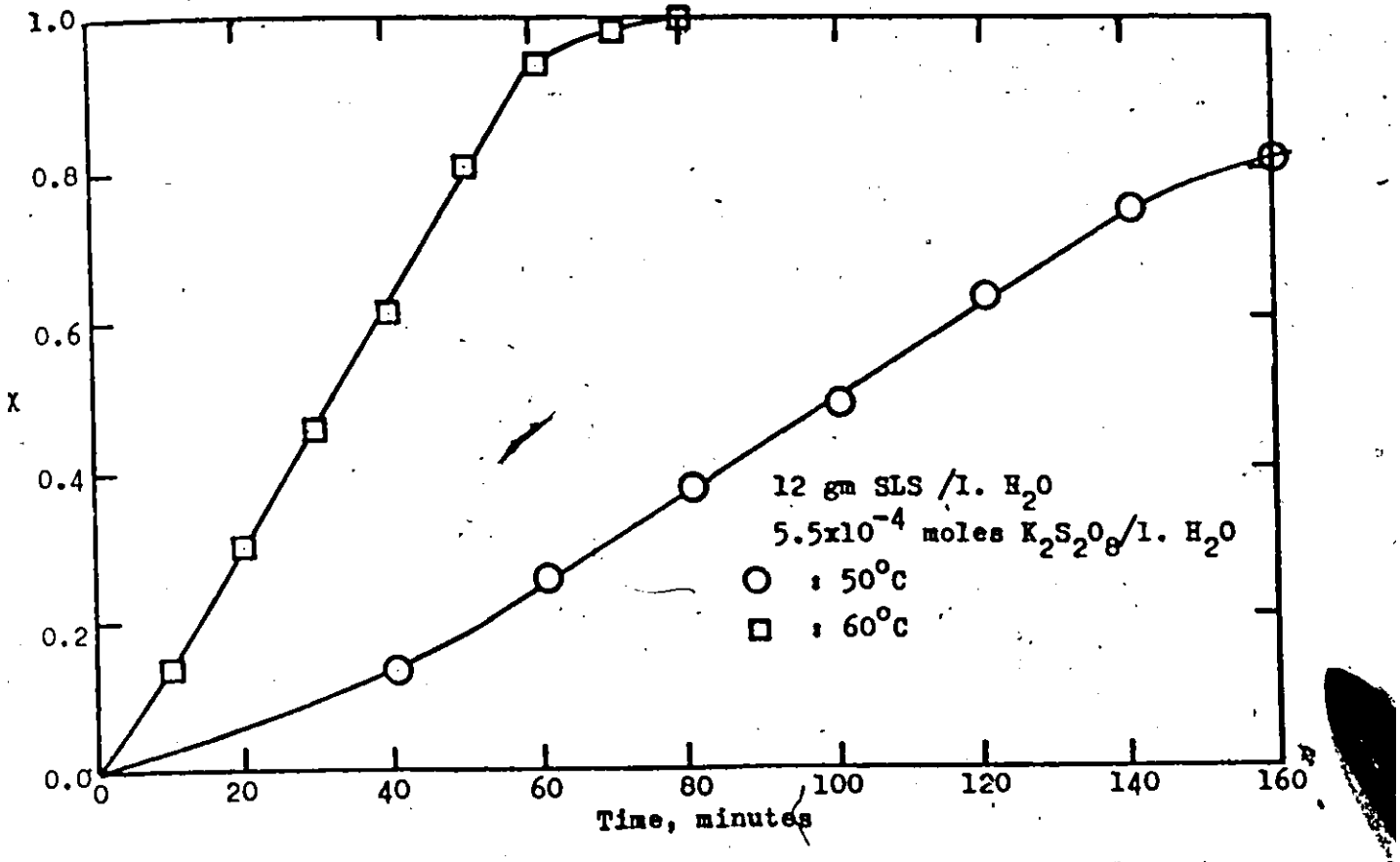

Fig. 18. Conversion versus time at different temperatures.

The results also help to explain why it has been impossible to obtain comparable experimental data in different laboratories.

Figure 18 shows the polymerization curves at two different temperatures. It indicates that temperature has an appreciable effect on the rate of polymerization. At the higher temperature the value of the rate constant for initiator decomposition is much larger.

4.4.2. NUMBER-AVERAGE AND WEIGHT-AVERAGE PARTICLE DIAMETERS

Figure 19 and Figure 20 show the number-average and

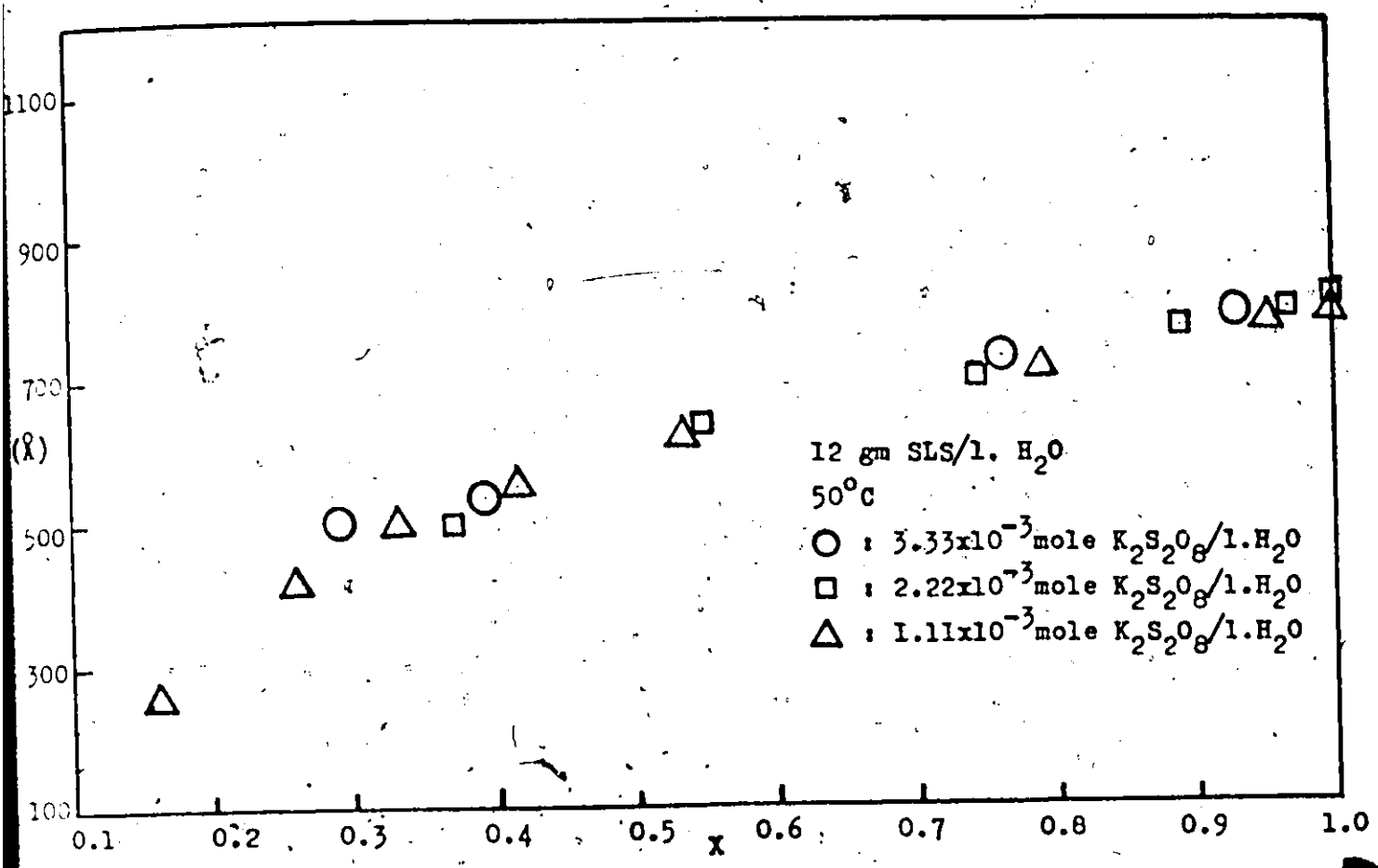

Fig. 19. Number-average particle diameter versus conversion at different initiator levels.

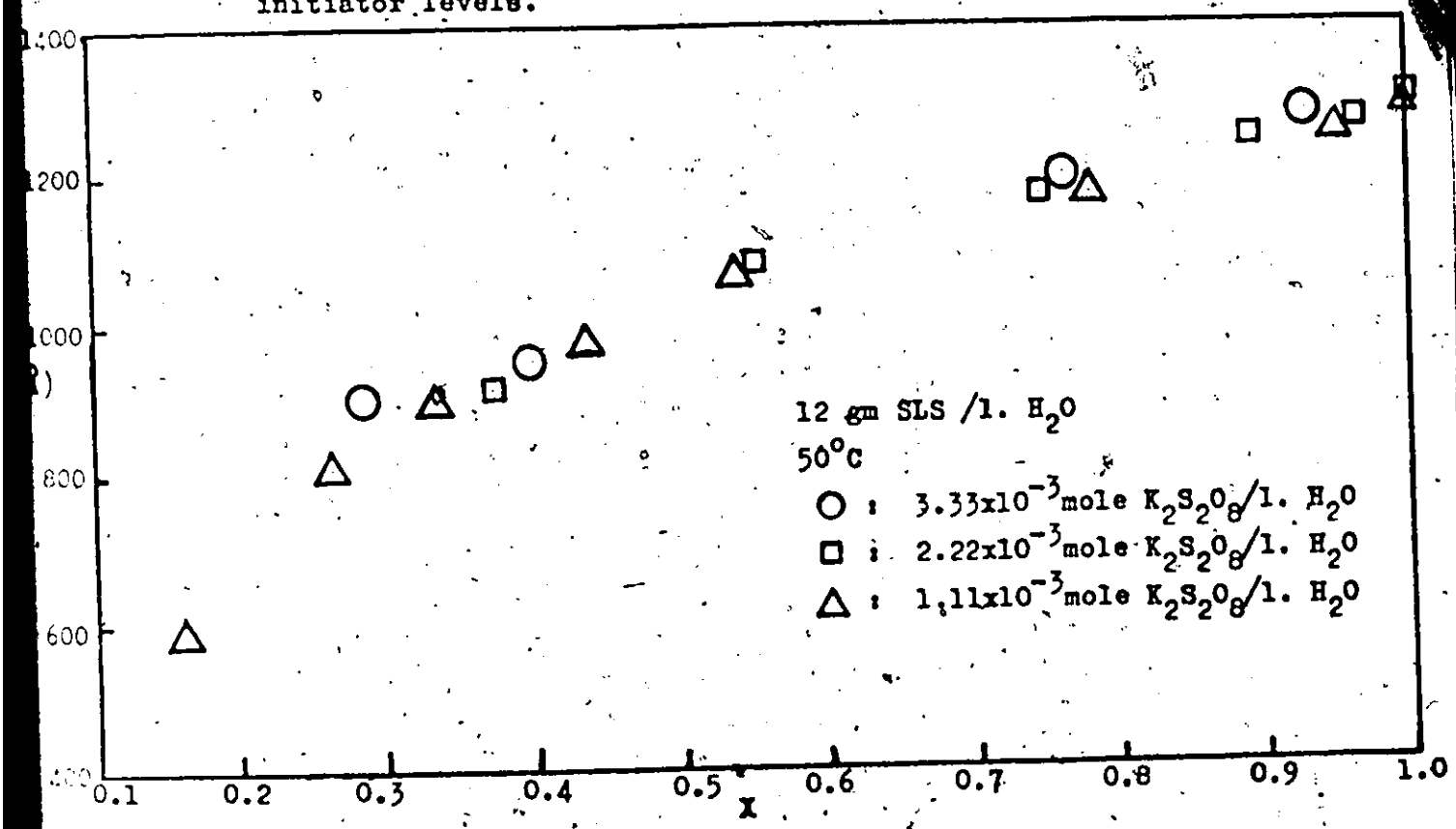

Fig. 20. Weight-average particle diameter versus conversion at different initiator levels.

weight-average particle diameters versus conversion for the polymerization processes at different initiator concentration. The data indicate that initiator concentration does not have any influence on the particle size.

There have been few attempts in the literature to estimate particle diameters during polymerization but there are data [24] which indicate that the total number of polymer particles is not influenced by initiator concentration. Thus, the present data agree with investigations reported in the literature.

Figure 21 is a plot of the total number of particles versus conversion at different initiator concentration. The total number of particles was estimated from the values of d_n in Figure 20. The data seem to scatter from 12×10^{17} to 18×10^{17} particles/litre but they can be considered constant within these limits. Several investigators using light scattering and electron microscopy [8, 24] have concluded that the number of particles remains constant from 10 to 100% conversion. The same conclusion was drawn for vinyl chloride emulsion polymerization [24].

Figure 22 and Figure 23 show the number-average and weight-average diameters versus conversion for the polymerization curves in Figure 16. It indicates that emulsifier concentration

has a great influence on particle size development. The total number of particles shown in Figure 24 strongly indicates that the total number of particles remain constant within the range of conversion considered.

The number of polymer particles was calculated to be approximately proportional to the 0.7 power of the emulsifier concentration. Figure 25 shows the total number of polymer particles versus conversion for the polymerization curves shown in Figure 17. In this case, the total number of particles is approximately proportional to the 0.4 power of the emulsifier

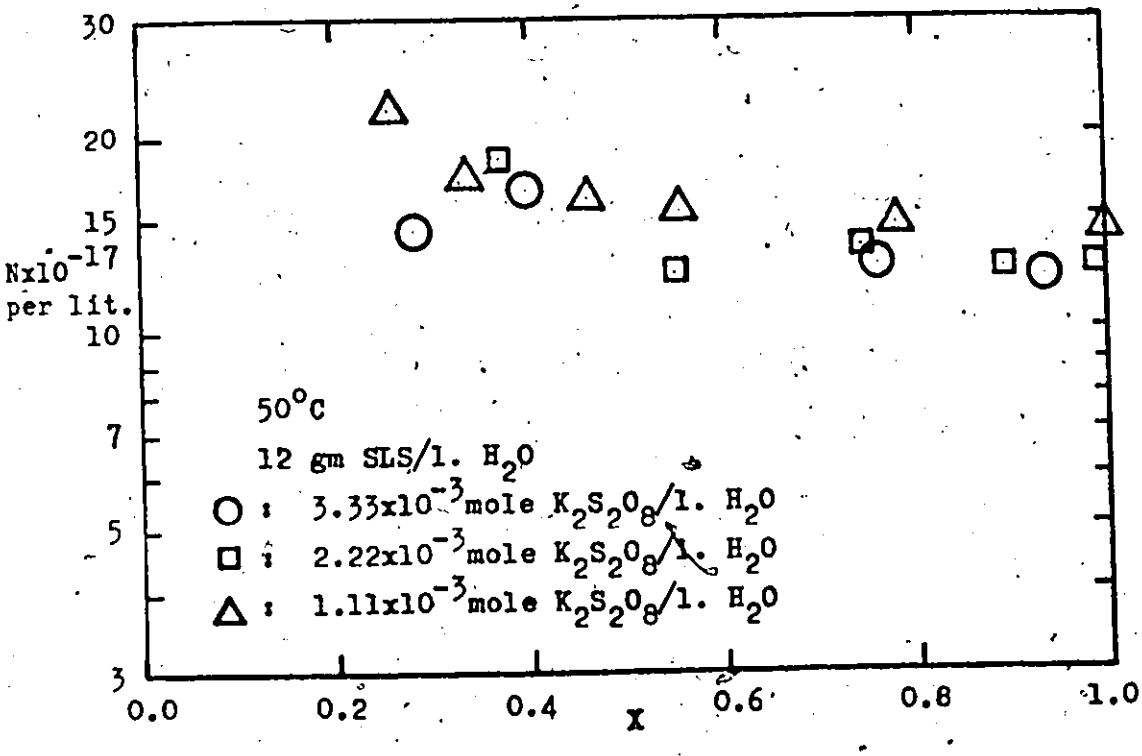

Fig. 21. Number of particles versus conversion at different initiator concentrations.

concentration. Considering that these values were estimated from absorbance measurements, they are not in disagreement with the value, 0.5, computed directly from electron microscopic data in Section 3.4.

Figure 26 and Figure 27 show the number-average and weight-average particle diameters versus conversion for polymerization processes at 50°C and 60°C and at the same emulsifier concentration. It appears that temperature has a slight influence on particle size development.

4.4.3. MOLECULAR WEIGHTS

Figure 28 to Figure 33 show the effect of initiator, emulsifier and temperature on number-average, M_n, and weight-average, M_w, molecular weights during polymerization. The findings agreed with the experimental work of Goosney[23] that:

(1) M_n and M_w are independent of initiator concentration.
(2) M_n and M_w are independent of emulsifier concentration.
(3) Temperature and conversion are the major variables in molecular weight development.

The solid lines in the figures represent the theoretical model developed in this laboratory[22]. The data agree with the predictions of the model within the limits of experimental errors. Thus, this model is effective in predicting molecular weight averages for a batch latex reactor under a variety of operating conditions.

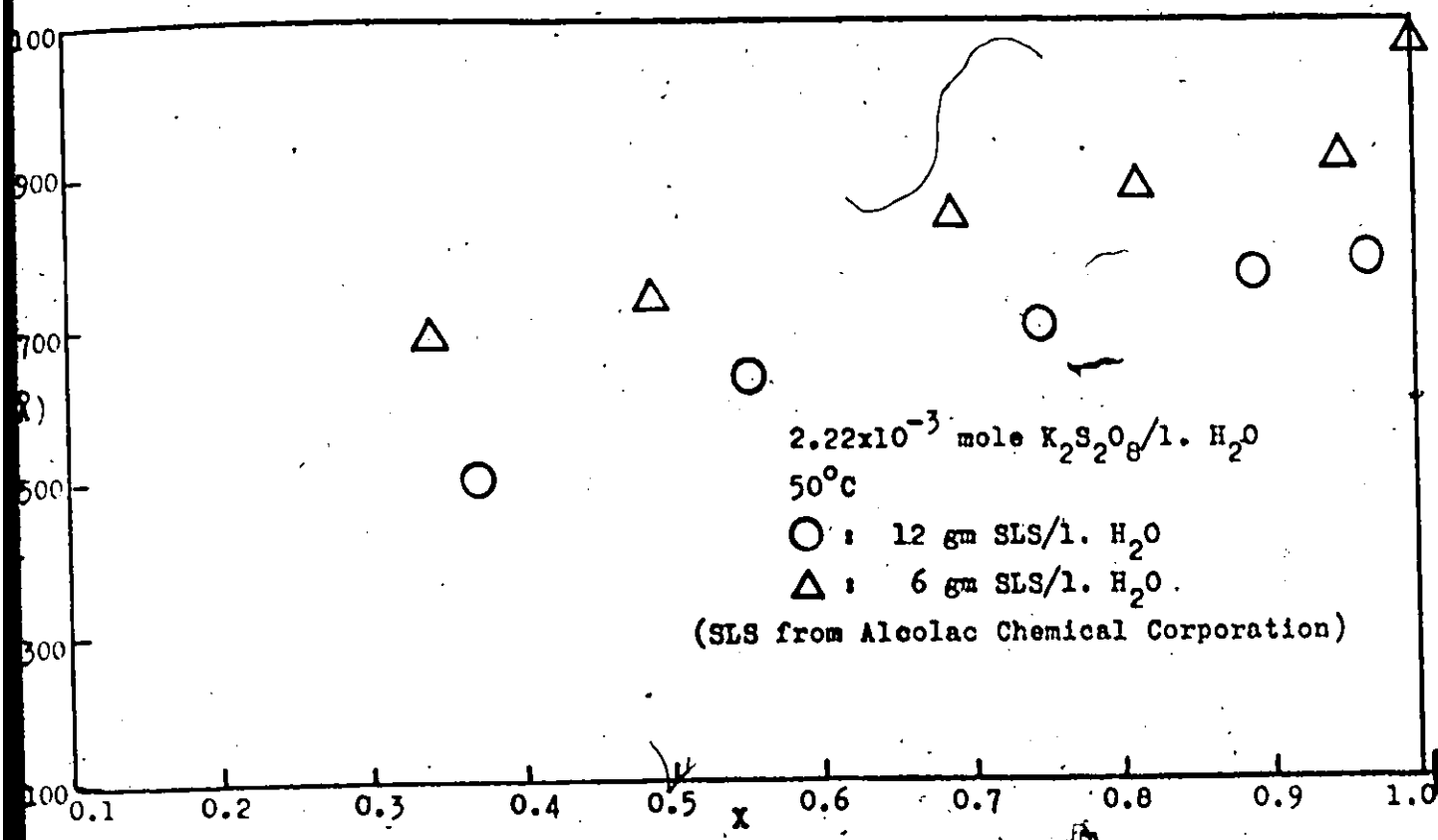

Fig. 22. Number-average particle diameter versus conversion at different emulsifier concentrations.

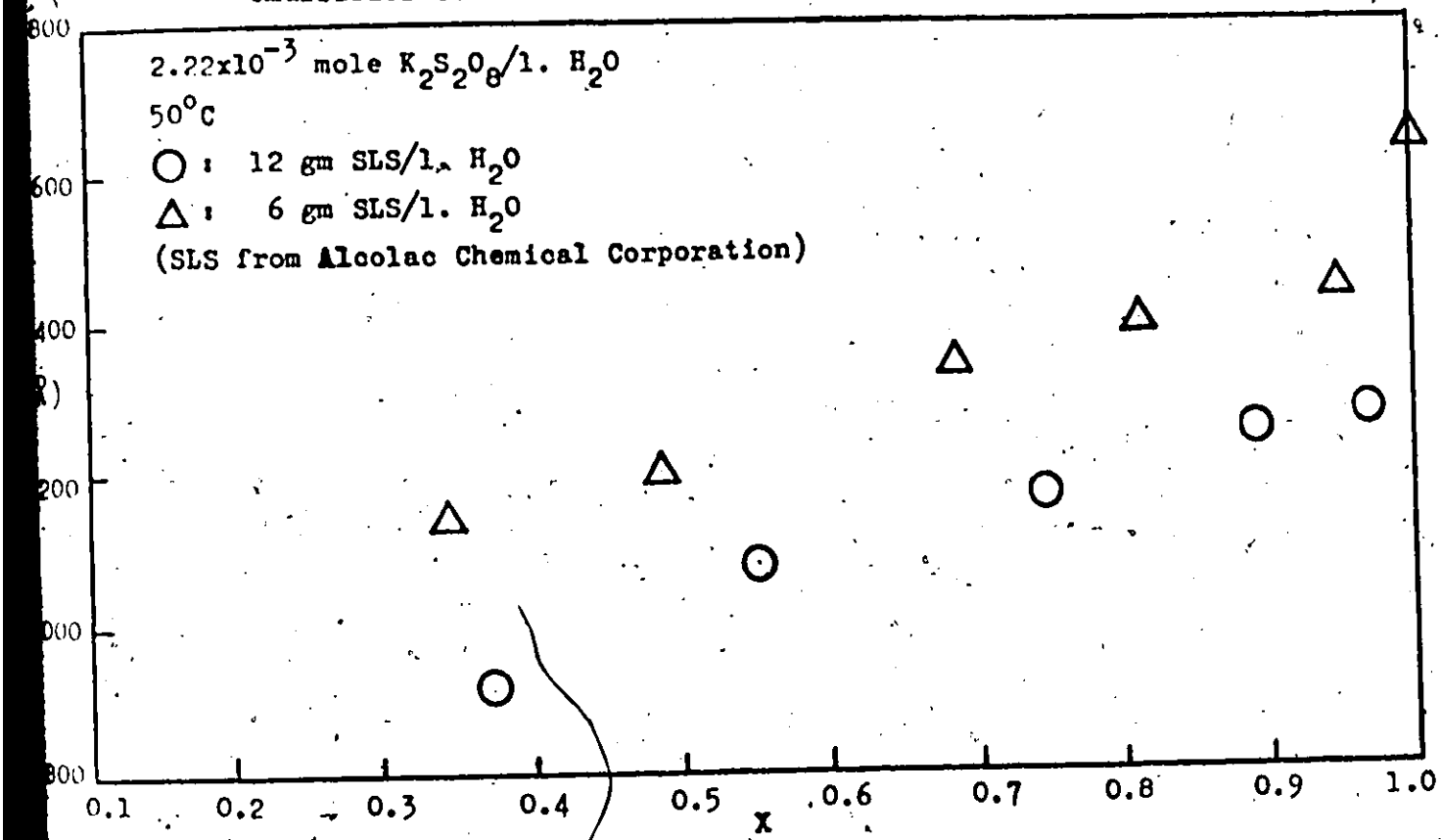

Fig. 23. Weight-average particle diameter versus conversion at different emulsifier concentrations.

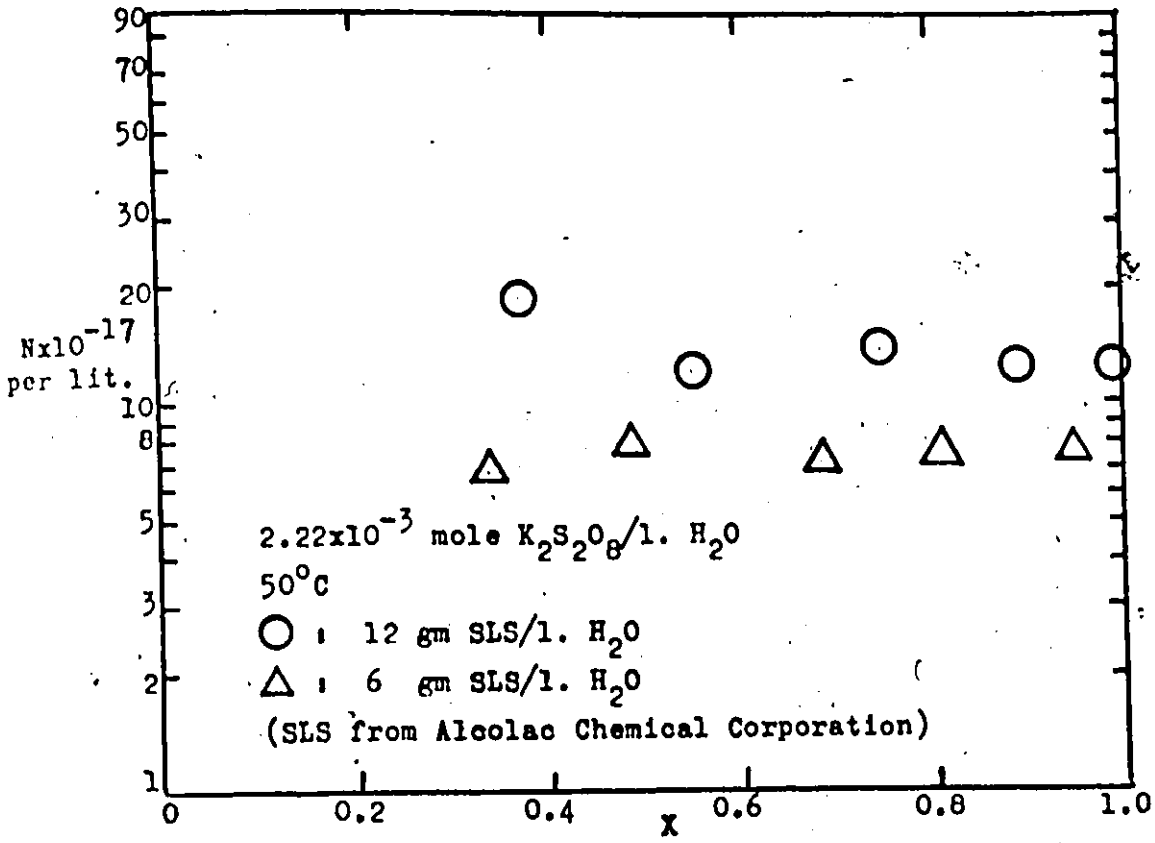

Fig. 24. Number of polymer particles versus conversion at different emulsifier levels.

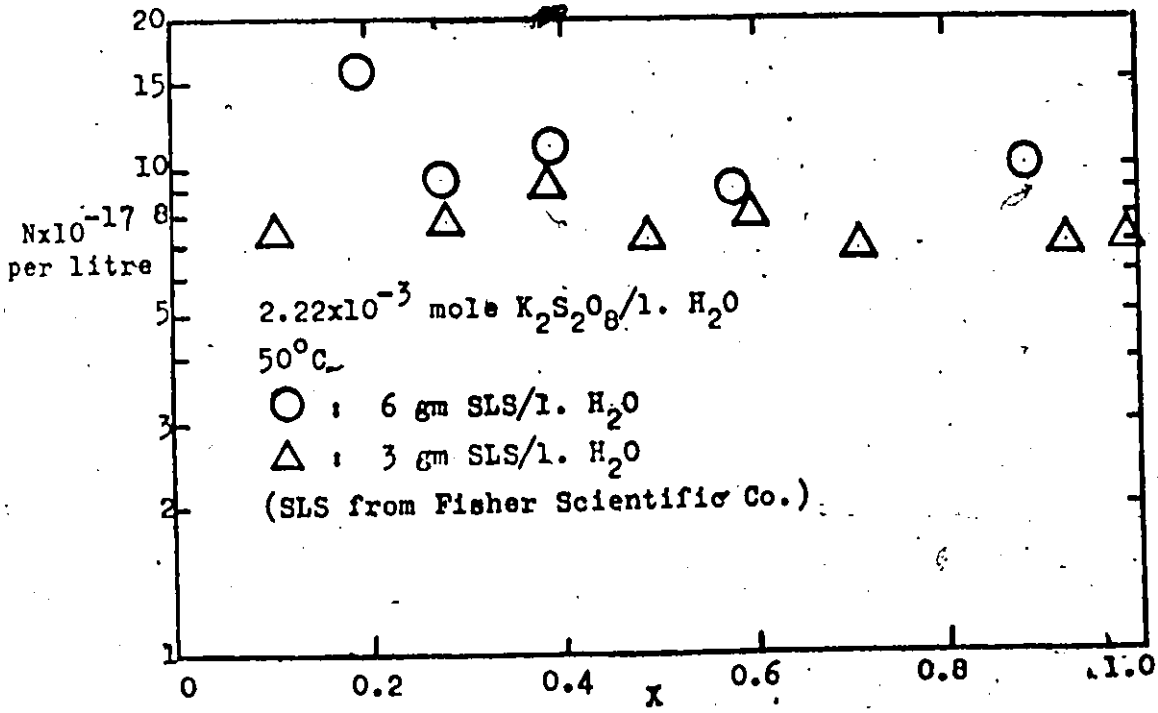

Fig. 25. Number of polymer particles versus conversion at different emulsifier levels.

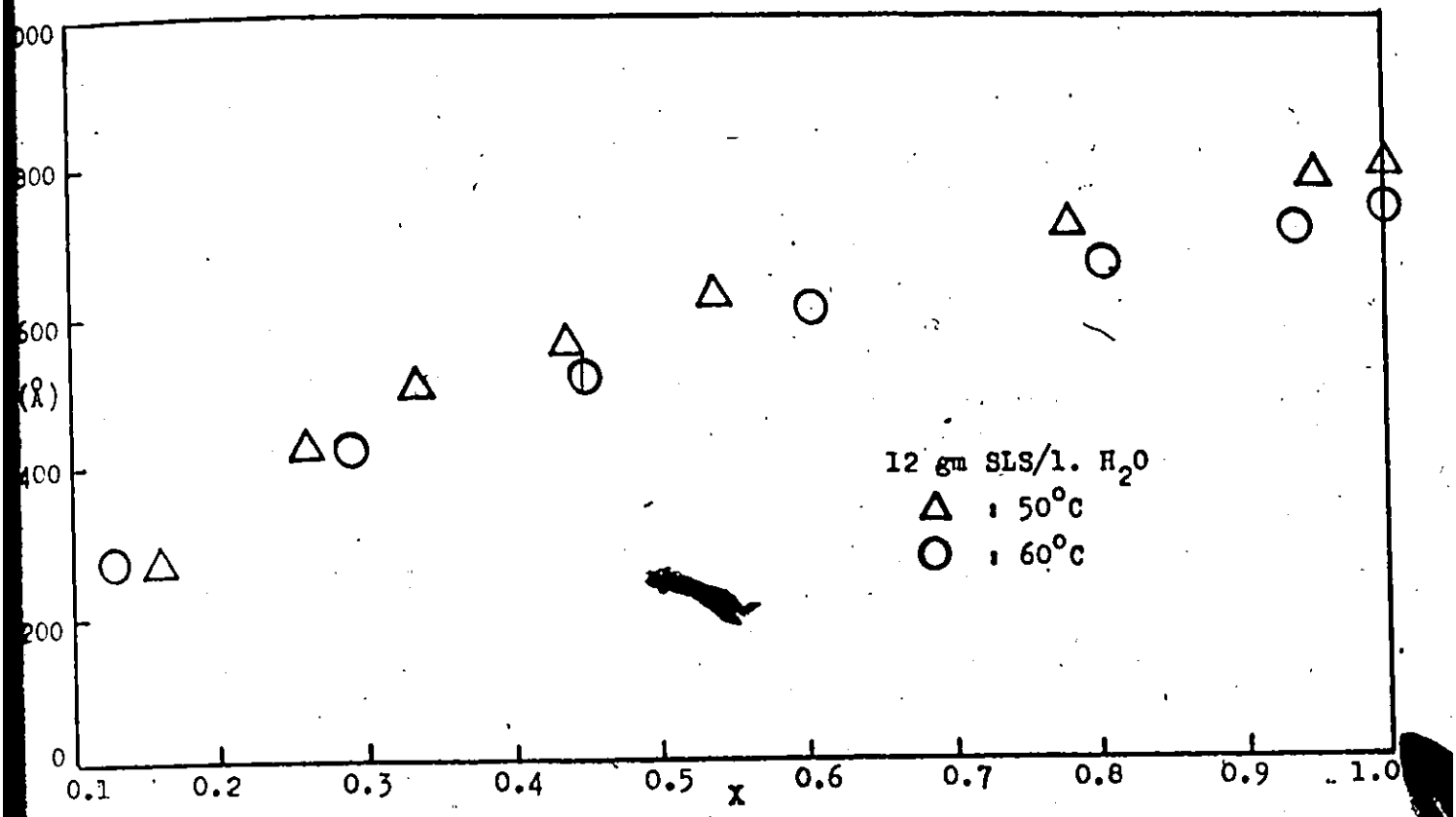

Fig. 26. Number-average particle diameter versus conversion at different temperatures.

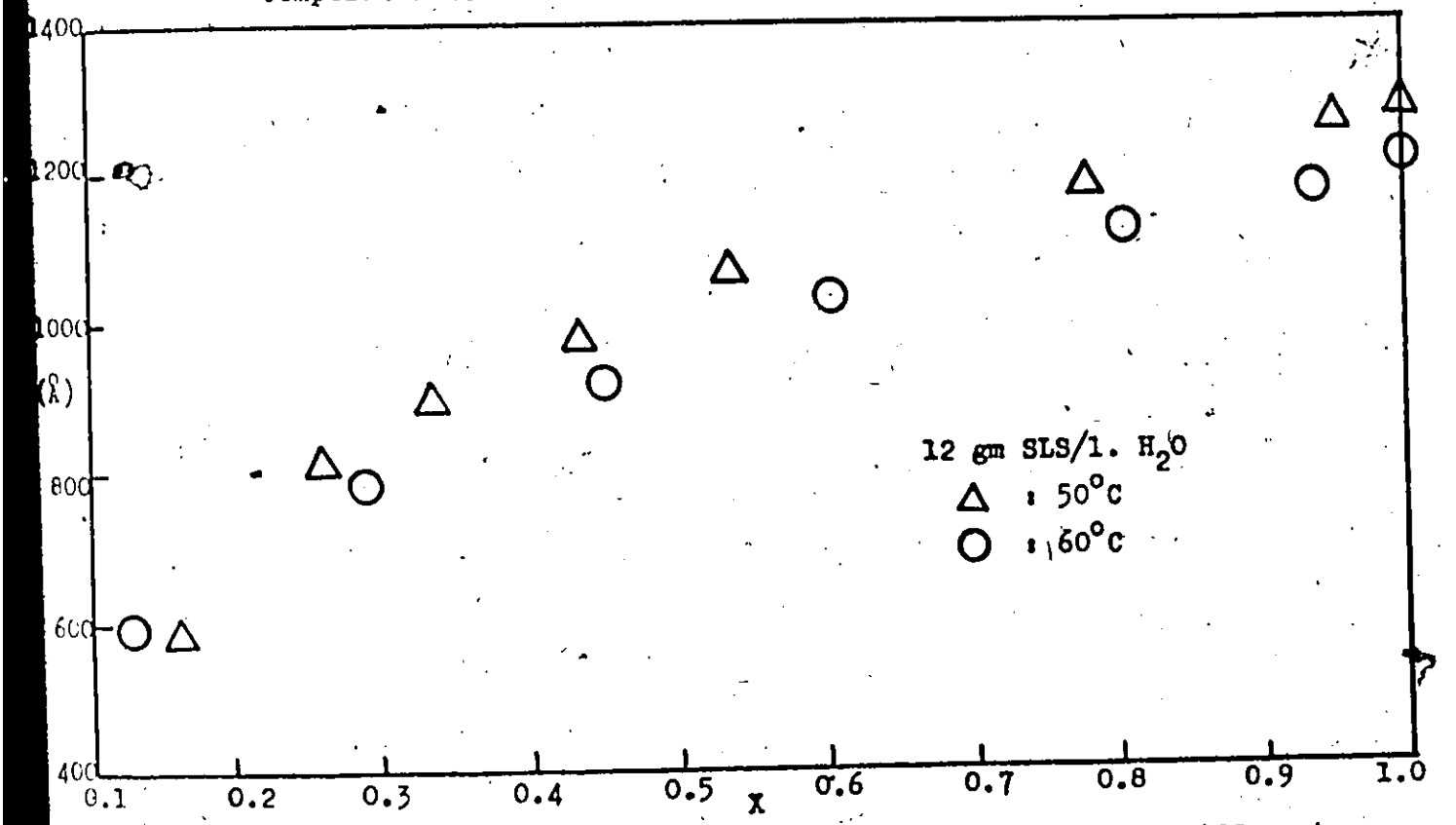

Fig. 27. Weight-average particle diameter versus conversion at different temperatures.

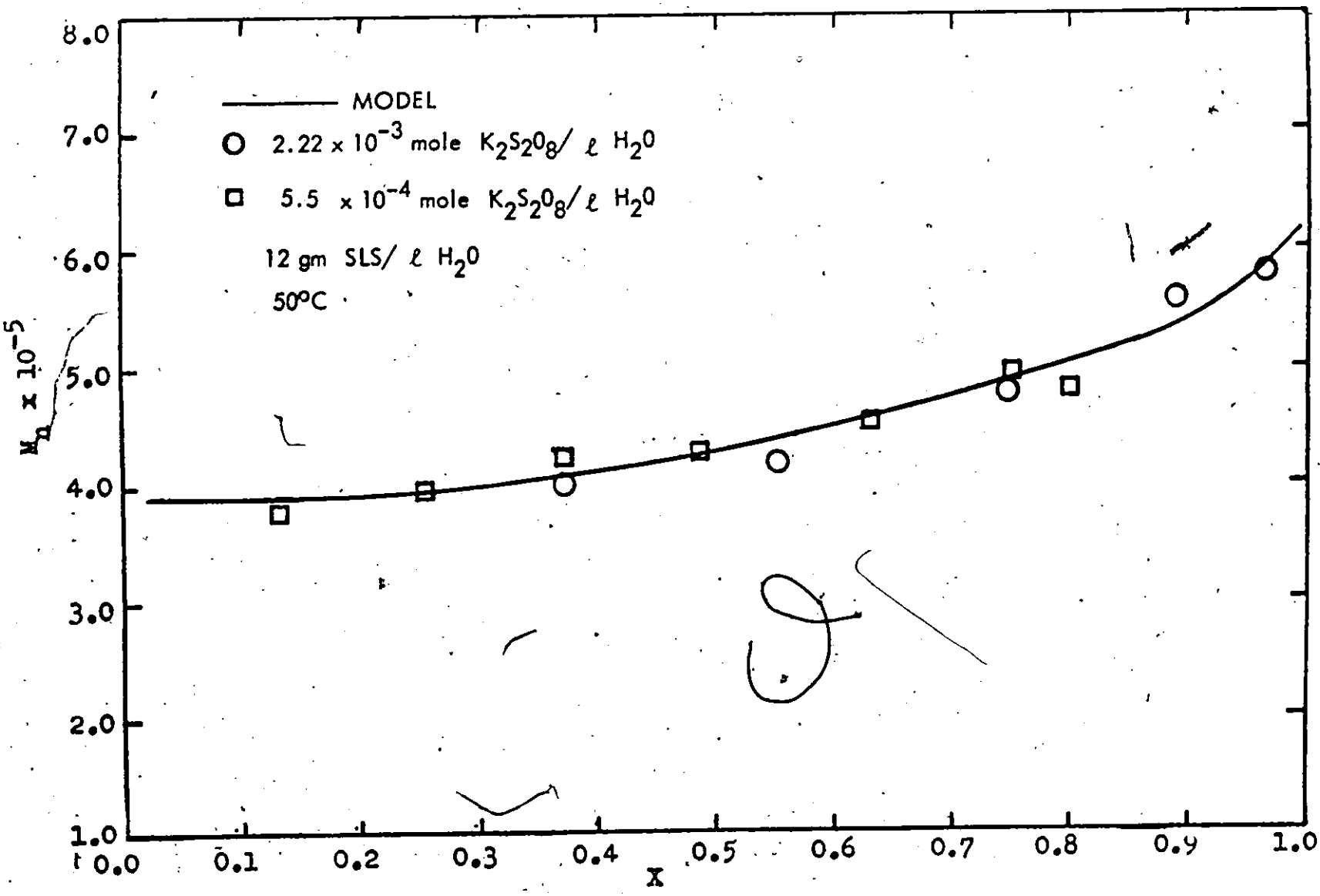

Fig. 28. Effect or initiator concentration on M_n during the course of polymerization

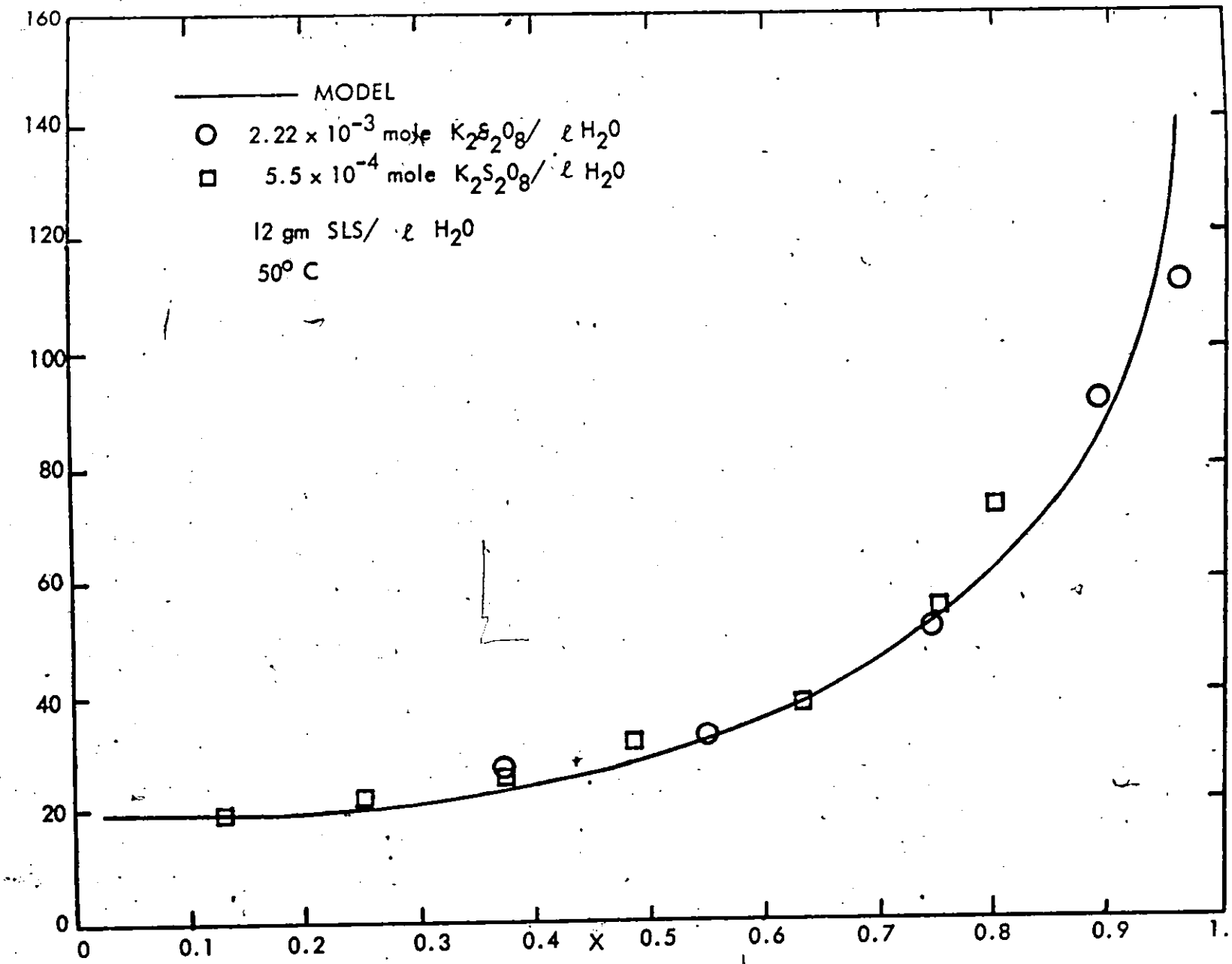

Figure 29. Effect of initiator concentration on M_w during the coutse of Polymerization.

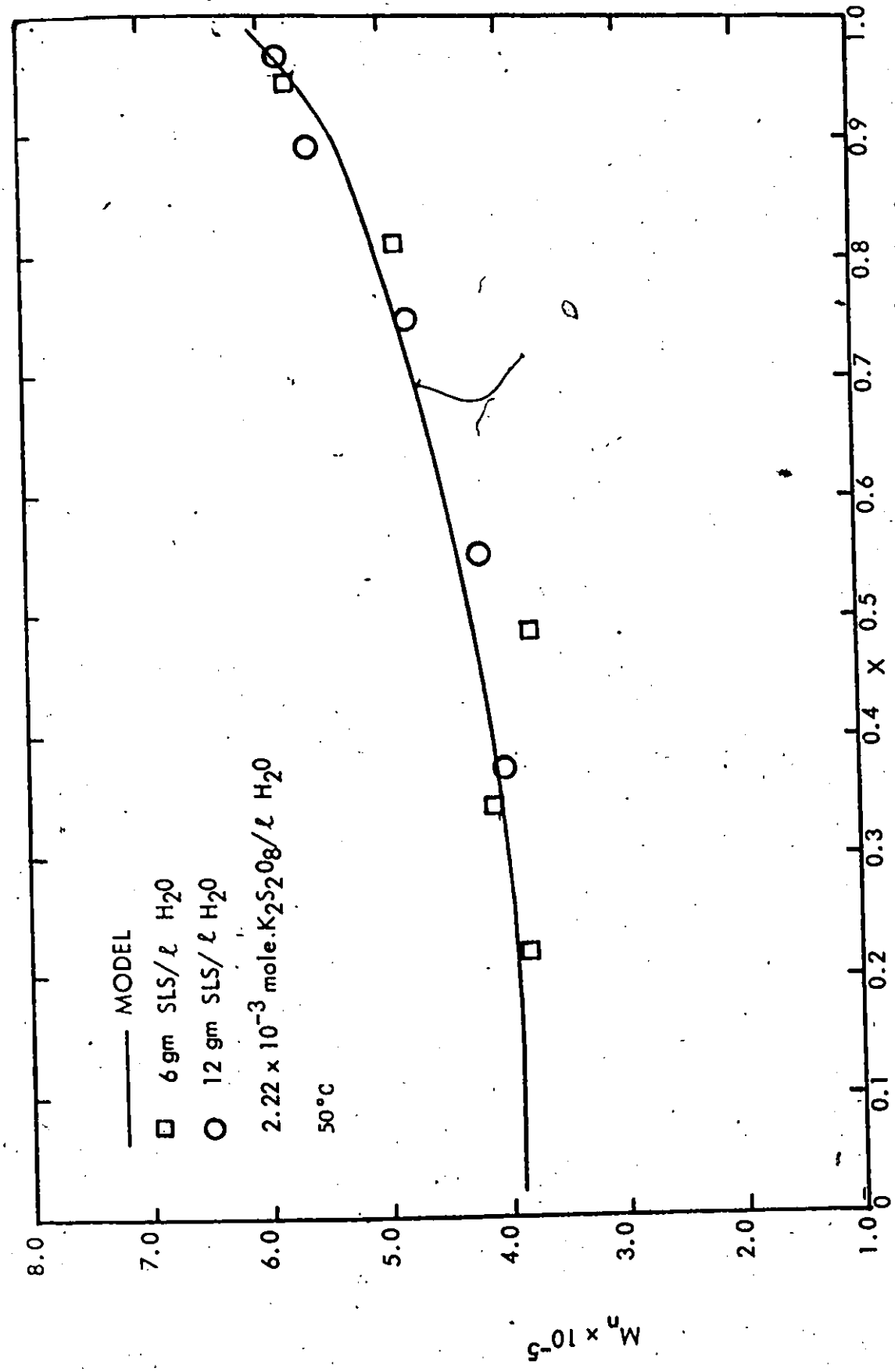

Figure 30. Effect of Emulsifier Concentration on M_n during the course of Polymerization.

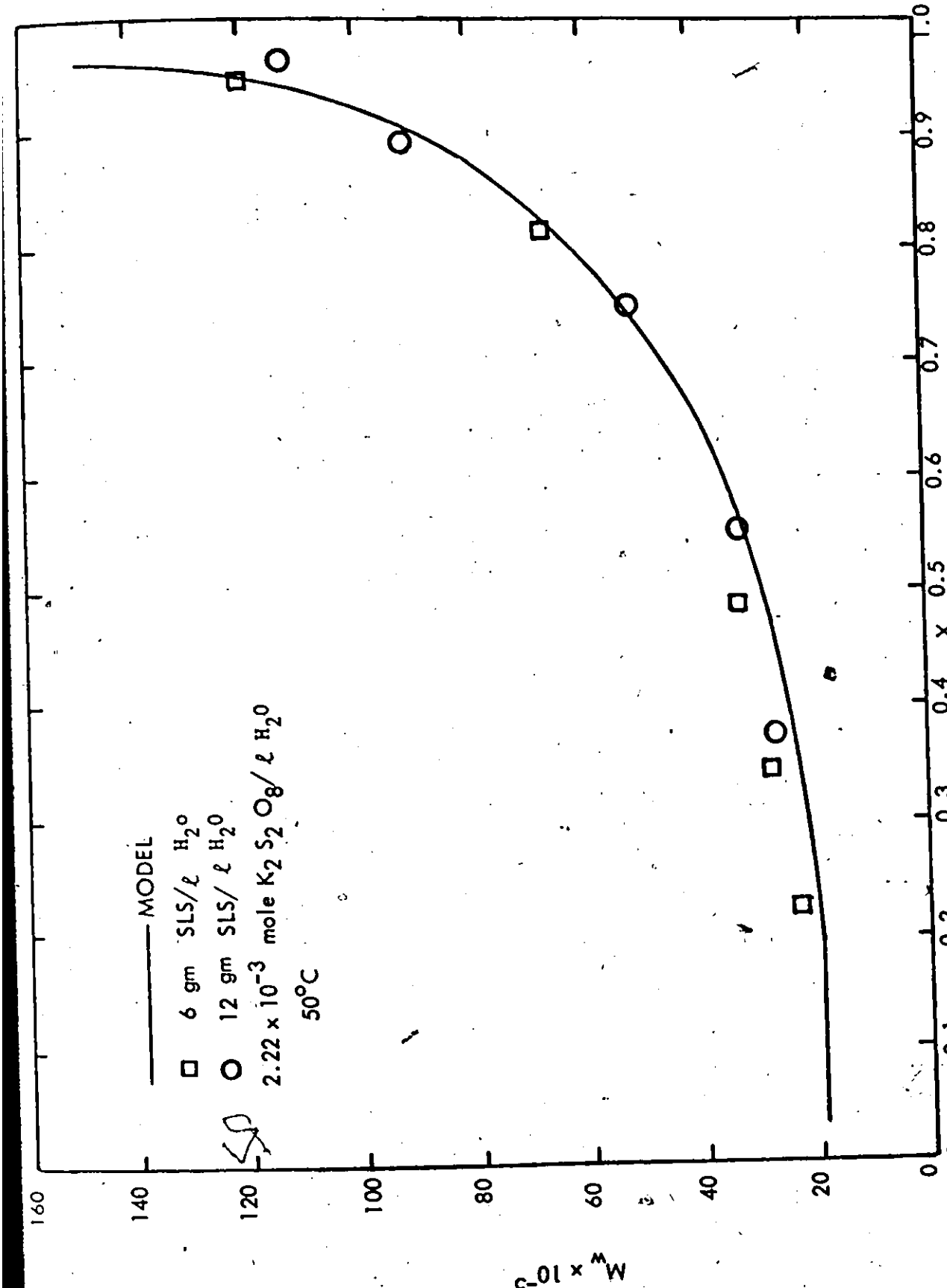

Figure 31. Effect of Emusifier Concentration on M_w during the course of Polymerization.

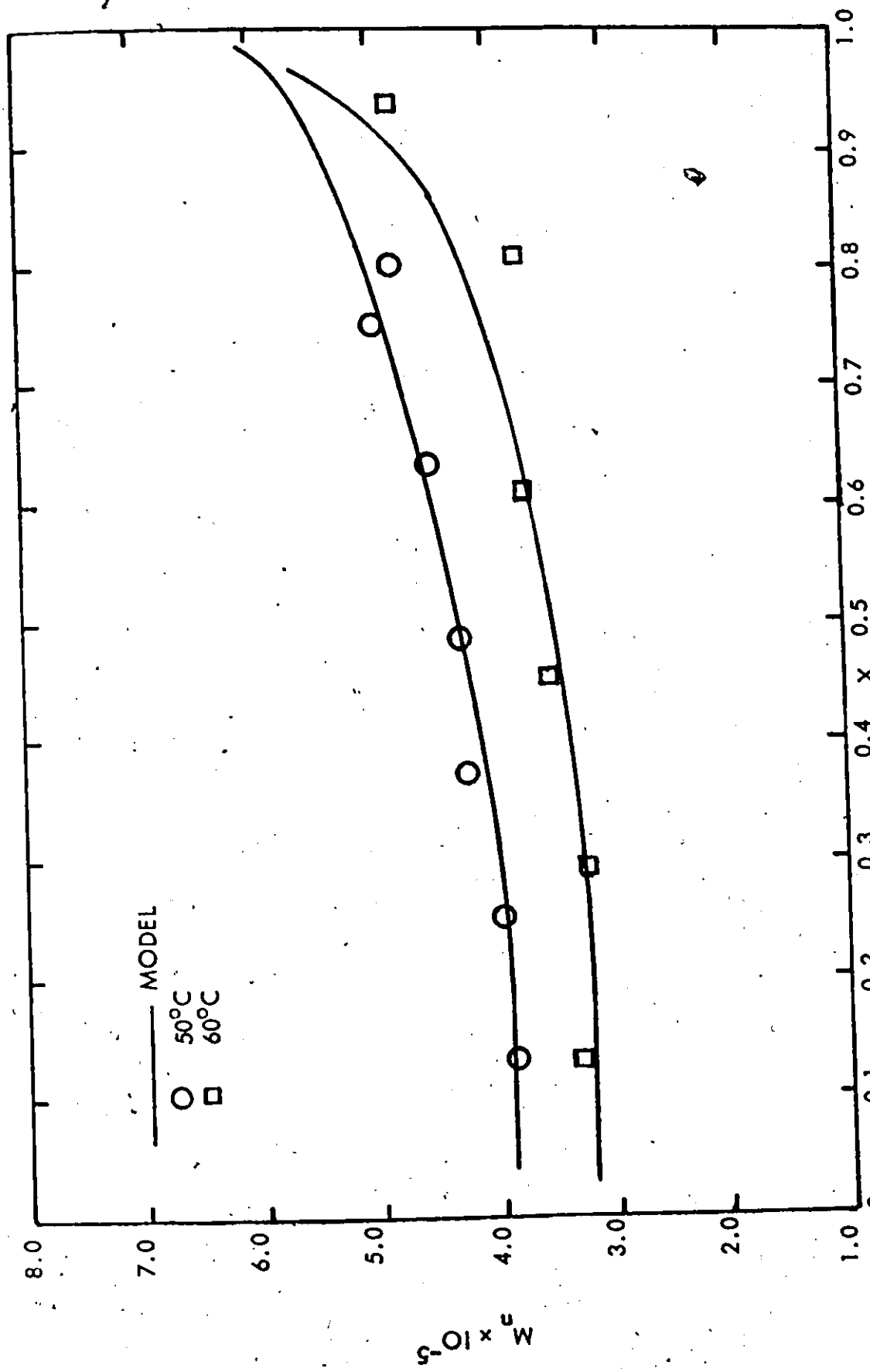

Figure 32. Effect of Temperature on M_n during the course of Polymerization.

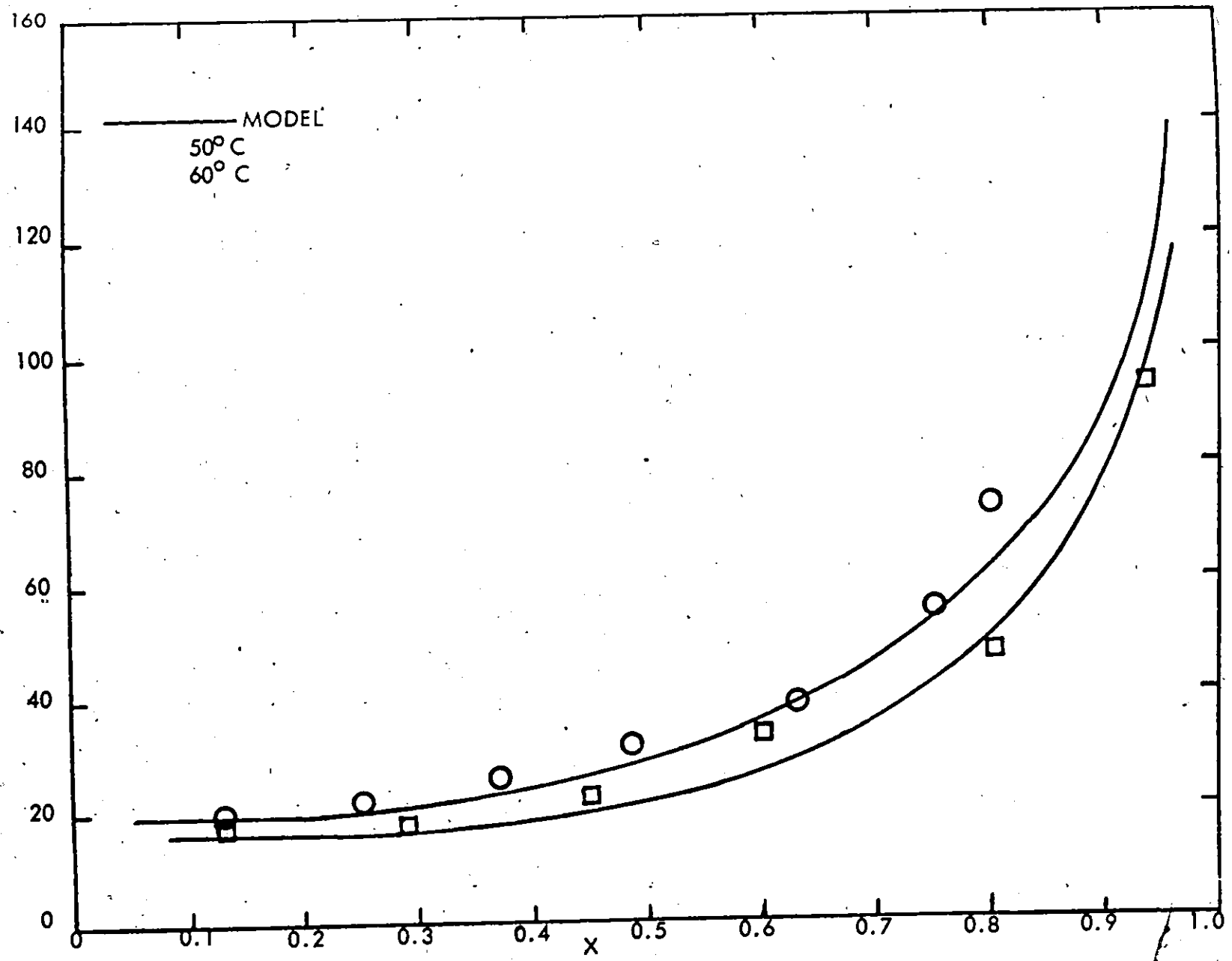

FIG. 33 Effect of Temperature on M_w during the Course of Polymerization.

4.4.4. MOLECULAR WEIGHT DISTRIBUTIONS

Consider a chromatogram of a polyvinyl acetate sample. The chromatogram height at a retention volume, V, represents the weight fraction of polymer at a molecular weight, M, which corresponds to V. Therefore,

$$W(M)dM = W(\ln M)d\ln M = -W(V)dV \qquad (37)$$

where $W(V)dV$ = weight fraction of polymer in retention volume range V to V + dV,

$W(M)dM$ = weight fraction of polymer in molecular weight range M to M + dM, corresponding to V to V + dV.

The calibration curve is expressed as

$$M = D_1 \exp(-D_2 V) \qquad (38)$$

where D_1 and D_2 are constants.

$$\ln M = -D_2 V + \ln D_1 \qquad (39)$$

From Equation 38, $\frac{dM}{dV} = -D_1 D_2 \exp(-D_2 V) = -D_2 M$ (40)

$$\therefore \quad \frac{dV}{dM} = \frac{-W(M)}{W(V)} = -\frac{1}{D_2 M} \qquad (41)$$

$$\therefore \quad W(M) = \frac{W(V)}{D_2 M} \qquad (42)$$

From Equation 39, $\frac{d \ln M}{d V} = -D_2$ (43)

From Equation 37,

$$W(M) = \frac{W(V)}{D_2} \cdot d(\ln M) = W(\ln M) d(\ln M)$$

therefore, $W(\ln M) = W(V)/D_2$ (44)

Since W(V) can be measured from the chromatogram, W(lnM) can be evaluated.

Figures 34 and 35 show the plots of W(ln M) as a function of molecular weight, M and conversion, X, in a semi-logarithmic scale for polyvinyl acetate samples polymerized at 50°C and 60°C respectively. At higher conversion, transfer to polymer and terminal double bond polymerization become important and the high degree of branching greatly increases the high molecular weight fractions.

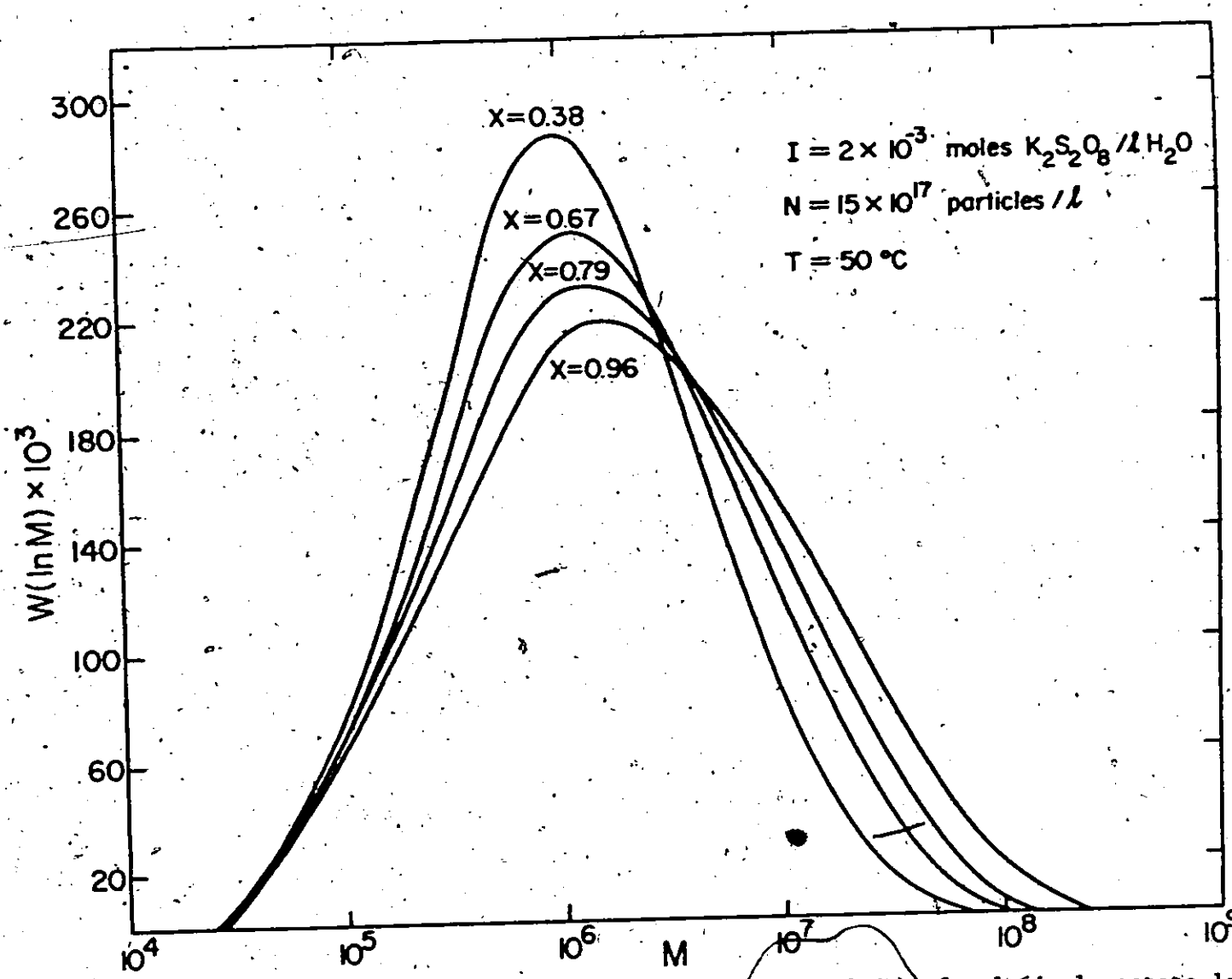

Figure 34. Molecular weight distribution (MWD) of polyvinyl acetate latex.

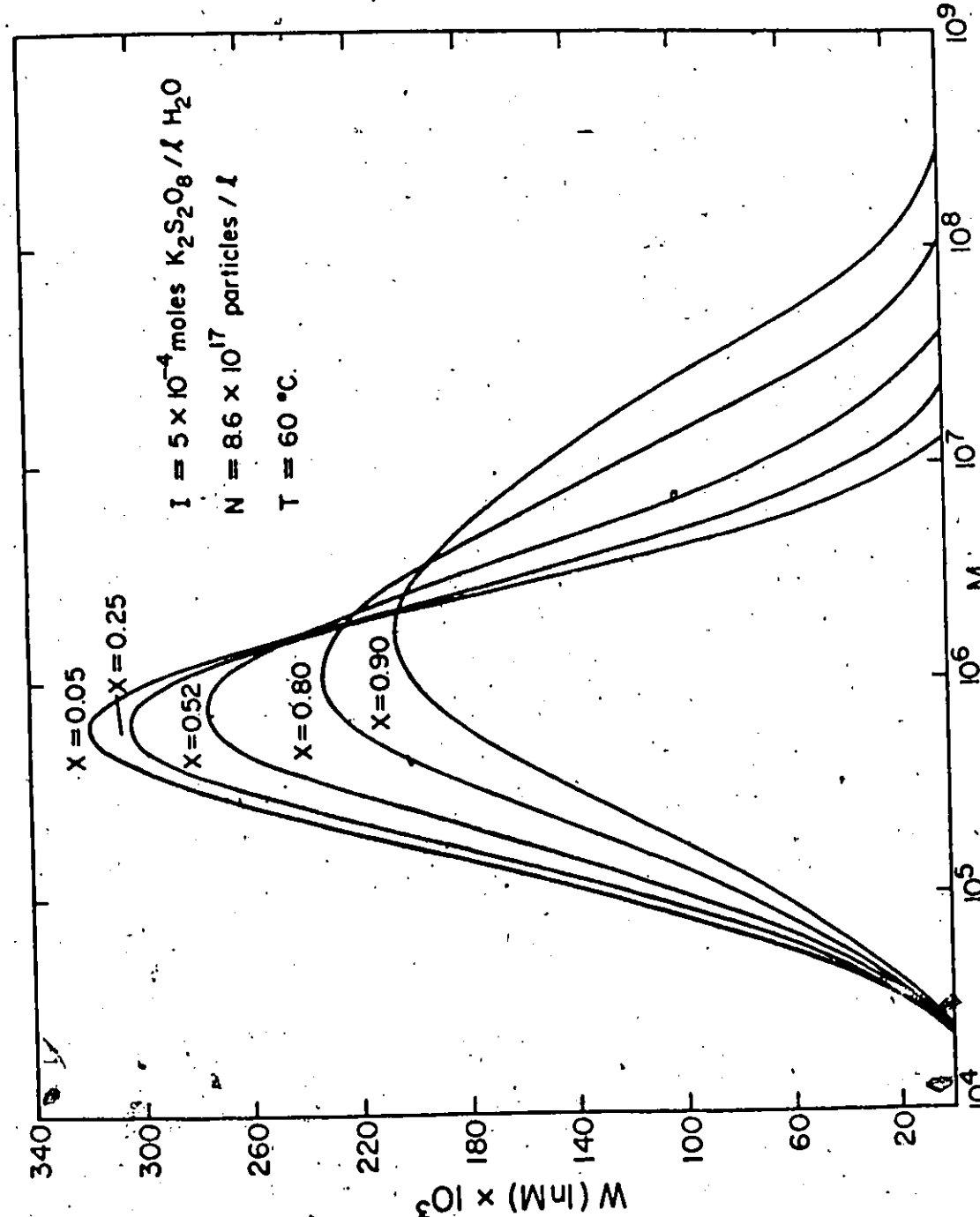

Figure 35. Molecular weight distribution (MWD) of polyvinyl acetate latex.

4.4.5. EFFECTS OF STIRRING

The influence of stirring on the rate of polymerization was briefly studied. Experiments of the same recipe were run at stirring rates from 100 r.p.m. to 500 r.p.m. It was found that stirring did not change the rate of polymerization from 100 to 300 r.p.m. However, vigorous stirring at 500 r.p.m. caused a decrease in the rate of polymerization and foaming appeared on the surface of the emulsion indicating that the emulsion was unstable.

It is felt that the rate of polymerization can depend, to a certain extent, on the rate of stirring, shape of the stirrer and the shape of the reactor. As long as the agitation is sufficient to keep the chemical species well mixed, the rate of stirring should not affect the rate of polymerization. Too vigorous stirring exerts an excessive shear rate on the emulsion which then becomes unstable.

5. DISCUSSION

5.1. INTRODUCTION

The experimental results in Sections 3 and 4 show good agreement with recent investigations[16, 18, 24] in vinyl acetate emulsion polymerization. The in situ polymerization hardening technique has proved to be effective in the microscopic studies of soft polymer particles, such as, polyvinyl acetate. The conversion versus time curves indicate that the rate of polymerization is constant over most of the conversion range. The average number of radicals per polymer particle is small compared with unity. This leads to the possibility that Case 1 of Smith-Ewart's theory may be able to predict the rate of polymerization. The measurements of particle diameters using light transmission measurements indicate that emulsifier concentration is the major controlling factor in particle size development. Though the results seem to show that there is influence in particle size due to temperature difference they are too close to allow a definite conclusion. From the point that temperature affects molecular weight development there should be an influence in particle growth since this must be directly related to polymer formation in the particles. Accounting for the decrease in terminal double bond polymerization the model developed by Graessley[37] and Stein[38]

for vinyl acetate bulk polymerization is able to predict the molecular weight development in vinyl acetate emulsion polymerization.

The points mentioned have been discussed in details in Sections 3 and 4. Several major points, such as, particle size distribution and its implications, rate models for vinyl acetate emulsion polymerization and molecular weight distribution will be discussed below.

5.2. PARTICLE SIZE DISTRIBUTION

One peculiar feature of the present experimental work on particle size distributions of polyvinyl acetate latices was that more small particles, in the range 100Å to 300Å, were observed than those reported in the literature[24, 16, 14, 8]. It is felt that during electron microscopic observations, small particles can easily be neglected in a large population.

A number of researchers reported that the particle size distribution of polyvinyl acetate latex should fit a logarithmic-normal distribution[16, 8, 4], though few have shown a quantitative demonstration. It is found that the present experimental data do not conform with a logarithmic normal distribution but as shown in Figure 36, they can be approximated by a one-parameter exponential distribution of the form:

$$F(D) = a \exp(-bD) \quad \text{for } D_o \leq D \leq D_N \qquad (45)$$

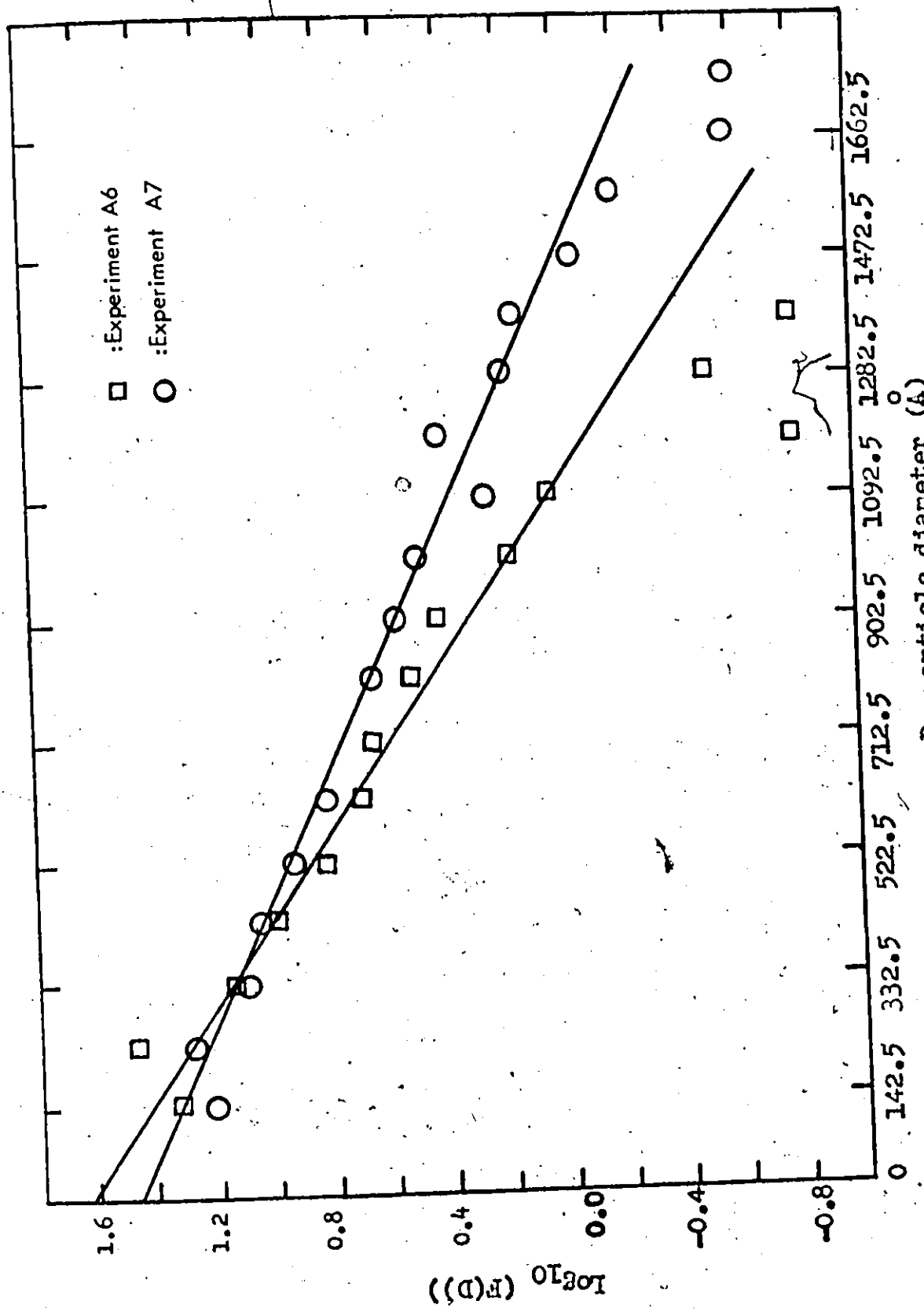

Fig. 36. Log_{10}(frequency) versus particle diameter, Expt. A6 and Expt. A7.

where D_o = diameter of the smallest particle,

D_N = diameter of the largest particle in the system,

and $$a = \frac{1}{\int_{D_o}^{D_N} \exp(-bD)dD}$$ using normalization.

From the figure, the particles in the range 0 Å - 100 Å which were missed in the microscopic observations due to the resolution limit of the electron microscope can be estimated by extrapolation. The bulk of particles in the intermediate size range fit the exponential model excellently. A number of particles in the large size range does not lie on the model. This could mainly be due to experimental error, simply because the population of large particles might not be well represented in the micrographs.

Assuming the exponential relationship of Equation 45, d_n and d_w were evaluated and compared with the data from electron microscopy. Table 4 indicates that d_n and d_w are not very far away from those previously determined from electron microscopy.

That a one-parameter exponential distribution model fits the particle size distribution also leads to a convenient method of determining particle size distribution without the use of calibration curves. Consider the turbidity, τ_1^*, of a latex at wavelength λ_{m1}.

TABLE 4

d_n's and d_w's from Electron Microscopy (EM) and from Exponential Distribution, in Å

Expt. No.	d_n(EM)	d_n(Model)	d_w(EM)	d_w(Model)
A1	1090	1070	1650	1600
A2	685	610	1230	1160
A3	420	390	770	800
A4	520	540	910	1050
A5	840	790	1360	1240
A6	490	485	850	970
A7	650	670	1160	1280

$$\tau_1^* = \int_{D_o}^{D_N} K^*(D, \lambda_{ml}) \frac{\pi}{4} D^2 n_p F(D) dD \qquad (46)$$

where n_p = total number of particles per unit volume in a polydisperse sample.

$n_p F(D)dD$ is, then, the number of particles per unit volume of disperse system which have radii between D and (D+dD).

Therefore F(D) is a normalized function such that

$$\int_{D_o}^{D_N} F(D)dD = 1 \qquad (47)$$

$$a = 1/\int_{D_o}^{D_N} \exp(-bD)dD \qquad (48)$$

From Equation 46, $$\tau_1^* = \frac{\pi}{4} n_p a \int_{D_o}^{D_N} K^*(D, \lambda_{ml}) D^2 \exp(-bD)\, dD \qquad (49)$$

The concentration of polymer particles is given by

$$c = \int_{D_o}^{D_N} \frac{\pi}{6} D^3 d_p n_p F(D)\, dD$$

$$= \frac{\pi}{6} n_p a d_p \int_{D_o}^{D_N} D^3 \exp(-bD)\, dD \qquad (50)$$

Dividing Equation 49 by Equation 50,

$$\frac{\tau_1^*}{c} = \frac{1.5 \int_{D_o}^{D_N} K^*(D, \lambda_{ml}) D^2 \exp(-bD)\, dD}{d_p \int_{D_o}^{D_N} D^3 \exp(-bD)\, dD} \qquad (51)$$

The light scattering coefficients, $K^*(D, \lambda_{ml})$ are tabulated in Heller et al.[32] τ_1^* and c are experimentally measured. Therefore, Equation 51 can be solved for b using a single variable search. Substituting into Equation 48, a can be found and thus the whole distribution function is determined. Furthermore, n_p can be evaluated from Equation 50 since a and b are known. In summary, by measuring the turbidity of a polymer sample at a fixed wavelength λ_{ml} and its concentration, c, the following information concerning particle size and polymerization can be generated:

(a) the distribution function, $F(D)=ae^{-bD}$ for $D_o \leq D \leq D_N$ and therefore weight-average and number-average particle diameters,

(b) the total number of polymer particles, n_p, per unit volume of emulsion,

(c) the turbidities of the polymer sample at other wavelengths can be predicted.

Table 5 shows the comparison of experimental and predicted values for turbidities, weight-average and number-average particle diameters.

Another method which appears more promising is to measure turbidities at two wavelengths, λ_{m1} and λ_{m2}.

$$\tau_1^* = \int_{D_o}^{D_N} K^*(D, \lambda_{m1}) \frac{\pi}{4} D^2 n_p a \exp(-bD) dD \qquad (46)$$

$$\tau_2^* = \int_{D_o}^{D_N} K^*(D, \lambda_{m2}) \frac{\pi}{4} D^2 n_p a \exp(-bD) dD \qquad (46a)$$

Therefore a single variable search for b can be performed from

$$\frac{\tau_1^*}{\tau_2^*} = \frac{\int_{D_o}^{D_N} K^*(D, \lambda_{m1}) D^2 \exp(-bD) dD}{\int_{D_o}^{D_N} K^*(D, \lambda_{m2}) D^2 \exp(-bD) dD} \qquad (52)$$

Then the distribution and n_p are determined. Furthermore, this method allows the prediction of concentration, c, from Equation 50 since n_p, a and b are known.

Table 6 shows the comparison of experimental and predicted values for turbidities, concentration, weight-average and number-average particle diameters. A comparison of Tables 5 and 6 indicates that the two methods agree. The turbidities and weight-average particle diameters are very accurately predicted. The number-average particle diameters are small compared with experimental values. This can be explained as follows. The model predicts that the majority of polymer particles are small (< 200 Å in diameter). The numerical values of K^* for small particles at this small size range have not yet been evaluated and therefore the values used in the present calculation were obtained by extrapolation. This is probably the major source of errors. Therefore, it is recommended that in future an accurate value of K^* at small diameter range can be calculated from the basic Mie theory equations.

How the latex particles grow remains a mystery. No mechanism has yet been proposed to account for polyvinyl acetate particle growth. From the recent reports[18, 24] and the findings in the present work of particle size distribution

a qualitative explanation is proposed as follows. When particles are first formed at the initial stage, the distribution is probably normal. The free radicals formed in the aqueous phase diffuse into the particles and the majority of them escape into water again. Chances are that, on the average, a particle with a large volume gets more radicals than a small one since $N > N_1$. Therefore, a large particle will propagate at a faster rate to form an even larger particle. During stage 1, micelles continue to be stung and more polymer particles are formed. This even adds to the population of small particles while large particles receive more radicals and propagate at a rapid rate. This is an explanation as to why there is a very large number of very small particles in the emulsion and why the particle size distribution is so broad.

TABLE 5

Comparison of Experimental and Predicted Values Using One Turbidity Measurement (at λ = 4000 Å) and known Concentration

No.	A1		A2		A3		A4		A5		A6		A7	
	Experimental	Predicted	Experimental	Predicted	Experimental	Predicted	Experimental	Predicted	Experimental	Predicted	Experimental	Predicted	Experimental	Predicted
τ^* (λ=5890Å)	1.197	1.084	0.723	0.717	0.166	0.164	0.468	0.435	0.765	0.761	0.320	0.313	0.548	0.544
τ^* (λ=5000Å)	1.905	1.735	1.211	1.205	0.299	0.301	0.818	0.781	1.285	1.269	0.576	0.566	0.950	0.951
d_n (Å)	1090	680	685	570	420	320	520	480	840	570	490	410	650	520
d_w (Å)	1650	1460	1230	1210	770	650	910	940	1360	1240	850	830	1160	1070

TABLE 6

Comparison of Experimental and Predicted Values Using 2 Turbidity Measurements

(at λ = 4000 Å and λ = 5890 Å)

No.	A1		A2		A3		A4		A5		A6		A7	
	Experimental	Predicted	Experimental	Predicted	Experimental	Predicted	Experimental	Predicted	Experimental	Predicted	Experimental	Predicted	Experimental	Predicted
τ^* (λ=5000Å)	1.905	1.891	1.211	1.214	0.299	0.303	0.818	0.819	1.285	1.282	0.576	0.575	0.948	0.948
Conc., c (gm/lit.)	1.518	1.394	1.504	1.526	1.774	2.474	1.712	1.273	1.537	1.680	1.736	1.931	1.532	1.603
d_n (Å)	1090	780	685	570	420	290	520	620	840	550	490	390	650	510
d_w (Å)	1650	1590	1230	1220	770	580	910	1070	1360	1210	850	800	1160	1060

5.3. RATE OF POLYMERIZATION

Since 1970, four major models have been proposed for vinyl acetate emulsion polymerization. The models of Harriott[21] and Stannett[10] were discussed in Section 4.2.1. and were found to be inconsistent with experimental data. The models of Friis[24] and Nomura[18] are both based on a mechanism involving rapid escape and reabsorption of radicals in the polymer particles. This reasonably explains the low value of radicals per polymer particle in vinyl acetate emulsion polymerization.

The model of Friis[24] is represented by the following rate equations:

$$R_p = \frac{k_p[M_p]}{N_A}(2k_i f[I])^{\frac{1}{2}}\left(\frac{N_A^2 V_p}{2k_{tp}} + \frac{N}{2k_d}\right)^{\frac{1}{2}} \qquad (53)$$

where k_p = propagation rate constant,

k_i = initiation rate constant,

$[I]$ = concentration of initiator,

f = initiator efficiency factor,

k_{tp} = termination rate constant,

k_d = desorption rate constant.

The model of Nomura[18] is represented by the following rate equation:

$$R_p = \frac{k_p[M_p]}{N_A}\left(\frac{k_i f[I]\delta_m k_p}{3D_w k_{tr}\varphi}\right)^{\frac{1}{2}}\left(\frac{3}{4q(1-\psi_c)}\right)^{1/3}[M_o]^{1/3}N^{1/6}x_c^{1/3} \qquad (54)$$

where D_w = diffusion coefficient of monomeric radicals in aqueous phase,

q = density of monomer-swollen polymer particles,

$[M_o]$ = initial monomer concentration,

δ_m = partition coefficient of monomeric radicals between aqueous and polymer phases,

$$\varphi = \left(1 + \frac{D_w}{\delta_m D_p}\right)^{-1}$$

$$\psi_c = 1 - x_c$$

In spite of its complicated form, Equation 54 could be reduced to a simple form[24]

$$R_p = \frac{k_p[M_p]}{N_A}(2k_i f[I])^{\frac{1}{2}}\left(\frac{N}{2k_d}\right)^{\frac{1}{2}} \qquad (55)$$

since Nomura defined the desorption rate constant as

$$k_d = \left(\frac{3D_w\varphi}{\delta_m r^2}\right)\frac{k_{tr}}{k_p} \qquad (56)$$

and since

$$\left(\frac{3}{4\pi q(1-\psi_c)}\right)^{1/3}[M_o]^{1/3}x_c^{1/3} = \left(\frac{3[M_o]}{4\pi q}\right)^{1/3} = \left(\frac{3V_p}{4\pi}\right)^{1/3} = rN^{1/3} \qquad (57)$$

Comparing Equation 54 and Equation 55, the only difference is that the term, $\frac{N_A^2 V_p}{2k_{tp}}$, is missing in Nomura's model. In a typical vinyl acetate emulsion polymerization, there are about 10^{18} particles/litre in the system. Friis showed that at this particle concentration, the term, $N/2k_d$, is the dominant term and $N_A^2 V_p/2k_{tp}$ is less than 10% of the former term. Thus it can be concluded that the two models are actually very close to each other. Moreover, their experimental findings agree with each other.

It has been shown in Figure 15 that the average number of radicals per particle in the present work is much less than one. In Case 1 of Smith-Ewart's theory the rate of polymerization is given by Equation 5,

$$R_p = \frac{k_p[M_p]}{N_A}\left(\frac{V_p \rho}{2k_o a_p}\right)^{1/2} \qquad (5)$$

ρ is $2k_i f[I]$ and V_p is proportional to N, the total number of polymer particles.

$$\therefore R_p \propto \frac{k_p[M_p]}{N_A}(2k_i f[I])^{\frac{1}{2}}\left(\frac{N}{2k_o a_p}\right)^{\frac{1}{2}} \qquad (58)$$

This has the same form as the model of Friis or Nomura. The only difference among these two models and the Case 1 of Smith-Ewart's theory lies in the definition of the desorption rate constant.

Equation 53 was calculated with the following values for the rate constants:

$k_{tp} = 2\exp(17.662-0.4407X-6.753X^2-0.3495X^3)$ l./mole-sec.

$k_p = 3500$ l./mole-sec.

$2k_i f = 2.5 \times 10^{-6}$/sec.

$d_p = 1150$ gm./l.

$d_m = 933.8$gm./l.

$$k_d = \Phi k_{tr}[M_p]/N_A \qquad (59)$$

where

$$\Phi = \frac{2D_p}{r^2}\left(\frac{2D_p}{r^2} + k_p[M_p]\right)^{-1} \qquad (60)$$

$$D_p = D_p^o \exp\left(\frac{-\beta X d_m(1-\alpha_1)}{(1-X)d_p + \alpha_1 X d_m}\right) \quad \text{for } X > x_c \qquad (61)$$

$$D_p = D_p^o \exp\left(\frac{-\beta x_c d_m(1-\alpha_1)}{(1-x_c)d_p + \alpha_1 x_c d_m}\right) \quad \text{for } X \leq x_c \qquad (62)$$

r = radius of a polymer particle

$D_p^o = 10^{-8}$ dm^2/sec

$\beta = 3.2$

$\alpha_1 = 0.3$

$k_{tr} = 0.75$ l./mole-sec.

$$[M_p] = \frac{(1-X)\, d_m}{86(1-X+Xd_m/d_p)} \quad \text{moles/l. for } X > x_c \qquad (63)$$

$$[M_p] = \frac{(1-x_c)\, d_m}{86(1-x_c+x_c d_m/d_p)} \quad \text{moles/l. for } X \leq x_c \qquad (64)$$

Figure 37 shows that the model predicts the conversion rate accurately from 20% to almost complete conversion after adjusting for the dead time delay.

5.4. MOLECULAR WEIGHT DISTRIBUTION

The molecular weight distribution curves in Figures 34 and 35 appear to fit a logarithmic-normal distribution of the form:

$$W(\ln M) = \frac{1}{(2\pi)^{\frac{1}{2}}\sigma} \exp\left\{-(\ln M - \ln\bar{M})^2/2\sigma^2\right\} \qquad (65)$$

Figure 38 shows a plot of $\log_{10}W(\ln M)$ vs. $(\ln M - \ln\bar{M})^2$. The linear relationship proves that the logarithmic normal distribution is a reasonably good approximation for the polyvinyl acetate molecular weight distribution.

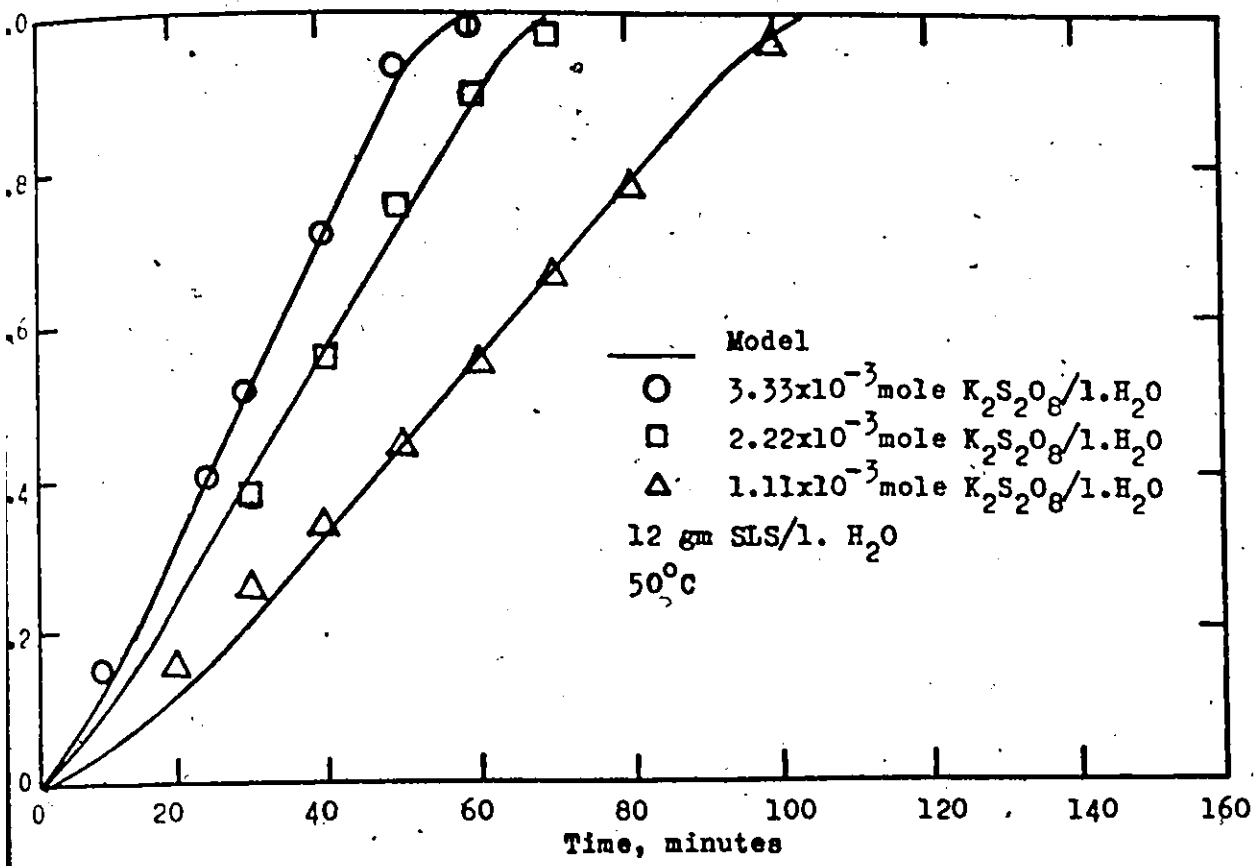

Fig. 37. Conversion versus time curves.

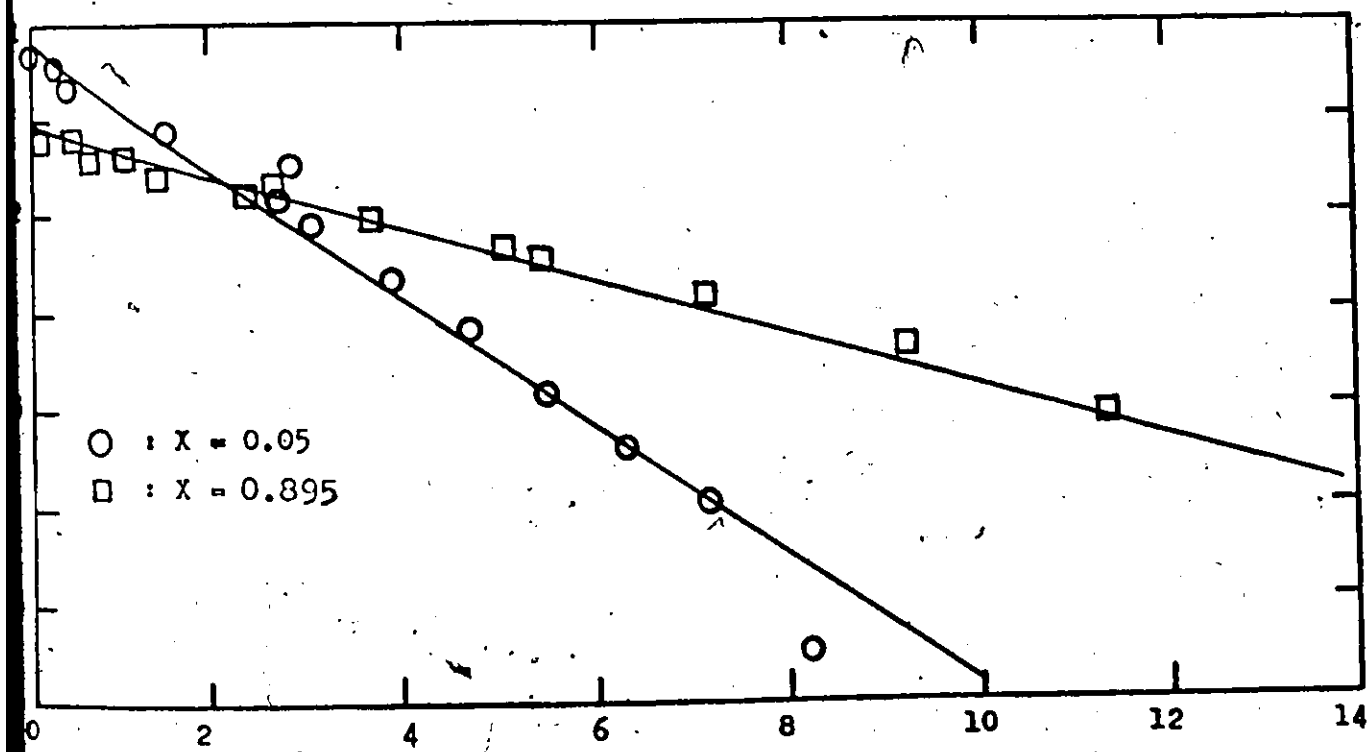

Fig. 38. Log_{10} W(lnM) versus $(lnM - \overline{lnM})^2$ at 60°C.

6. CONCLUSIONS

The following conclusions can be drawn from the experimental investigations in the present study.

(1) Light transmission spectrophotometry is an efficient technique for the measurement of number or weight average diameters of polymer particles in vinyl acetate emulsion polymerization. The frequency distribution of a polyvinyl acetate latex can be approximated by the function

$$F(D) = a \exp(-bD)$$

By measuring turbidities at 2 wavelengths, the particle size distribution, the number of particles in the system and concentration of polymer can be computed by solving the following integral equations:

$$\int_{D_o}^{D_N} F(D)dD = 1$$

$$\tau_1^* = \int_{D_o}^{D_N} K^*(D, \lambda_{m1}) \frac{\pi}{4} D^2 n_p F(D)dD$$

$$\tau_2^* = \int_{D_o}^{D_N} K^*(D, \lambda_{m2}) \frac{\pi}{4} D^2 n_p F(D)dD$$

$$c = \int_{D_o}^{D_N} \frac{\pi}{6} D^3 d_p n_p F(D)dD$$

(2) The total number of particles in vinyl acetate emulsion polymerization is approximately proportional to the square root of the emulsifier concentration.

(3) The rate of polymerization is approximately proportional to the square root of the initiator concentration.

(4) The effect of emulsifier concentration on the rate of polymerization is negligibly small compared with the effect due to temperature and initiator concentration.

(5) The total number of polymer particles in vinyl acetate emulsion polymerization is constant in the conversion range, 20 to 100%.

(6) The weight-average and number-average particle diameters are independent of initiator concentration. They are influenced by emulsifier concentration and to a small extent, by temperature changes.

(7) The weight-average and number-average molecular weights are independent of initiator and emulsifier concentrations. Conversion and temperature are the major variables in molecular weight development.

(8) The kinetic model developed in this laboratory[22] can predict the molecular weight development in a batch latex reactor system up to high conversion under a variety of operating conditions.

(9) The molecular weight distribution (MWD) of polyvinyl acetate for the whole conversion range is logarithmic-normal when W(lnM) is plotted versus M. Polydispersity increase with conversion as a consequence of chain branching reactions, transfer to polymer and terminal double bond polymerization which become more important as the polymer concentretion increases.

(10) The rate models of Friis[24] and Nomura[18] were shown to be similar to Case 1 of Smith-Ewart's theory. Only the definition of the desorption rate constant is different in these three models. Using the desorption rate constant developed by Friis, the rate data measured in the present study fit his model.

7. NOMENCLATURE

a = constant in Equation 45

a_p = surface area of a polymer particle

a_s = surface area occupied by 1 emulsifier molecule

A = absorbance of a latex sample

A_2 = second virial coefficient

b = constant in Equation 45

c = concentration, gm/c.c.

d_i = diameter of a particle

d_m = density of monomer

d_p = density of latex particles

d_n = number average particle diameter

d_w = weight average particle diameter

D = diameter of a latex particle

D_1 = GPC calibration curve constant

D_2 = GPC calibration curve constant

D_o = the diameter of the smallest particle in the emulsion

D_N = the diameter of the largest particle in the system

D_p = self-diffusion coefficient of monomeric radicals in monomer swollen polymer particles

D_p^o = self-diffusion coefficient of monomeric radicals in vinyl acetate

D_w = self-diffusion coefficient of monomeric radicals in aqueous phase

$[E]$ = emulsifier concentration, gm./lit. H_2O

f = initiator efficiency factor

f_i = frequency of particles with diameter d_i

I = intensity of transmitted light

I_o = intensity of incident light

$[I]$ = initiator concentration

I_m = Bessel functions of the first kind

k = constant in Smith and Ewart's Equation for number of particles

k_d = desorption rate constant

k_i = initiation rate constant

k_{tc} = termination by combination rate constant

k_{td} = termination by disproportionation rate constant

k_{fp} = transfer to polymer rate constant

k_{fm} = transfer to monomer rate constant

k_{tr} = rate constant for transfer to monomer

k_o = desorption rate constant in Smith-Ewart Theory

k_p = propagation rate constant

k_{tp} = termination rate constant

k_p^* = terminal double bond polymerization rate constant

K^* = light scattering coefficient of the particles

ℓ = path length of the transmission cell, cm.

$m = k_o a_p / k_{tp}$

m_o = molecular weight of monomer

$\bar{M}$ = mean of the MWD

$[M_{aq}]$ = monomer concentration in water phase

$[M_p]$ = monomer concentration in monomer-swollen polymer particles

M_n = number average molecular weight

M_w = weight average molecular weight

MWD = molecular weight distribution

M_o = monomer concentration in monomer

$[M_o]$ = initial monomer concentration

n = number of radicals in a polymer particle

n_o = refractive index of the solvent

n_p = concentration of particles in the system

N = total number of polymer particles

N_A = Avogadro's number

N_n = number of particles containing n free radicals

P_r = concentration of molecules of chain length r

$P_r^\bullet$ = concentration of radicals of chain length r

μ_i = ith moment of polymer distribution, $\sum_{r=1}^{\infty} r^i P_r$

R_p = polymerization rate

R_{90^o} = Raleigh's ratio at angle 90^o

S = number of emulsifier molecules per unit volume of aqueous phase

SLS= sodium lauryl sulphate

t = reaction time

T = transmittance

v = average volume of a polymer particle

$\bar{v}_n$ = number average particle volume

$\bar{v}_w$ = weight average particle volume

V = retention volume count for GPC

V_p = total volume of monomer-swollen polymer particles

X = conversion

x_c = critical conversion

$\alpha = \pi D/\lambda_m$

$\zeta = (8\varepsilon)^{\frac{1}{2}}$

$\varepsilon = v\rho'/k_{tp}N$

λ_m = wavelength of light in the medium

λ = wavelength of light in vacuum

τ^* = turbidity

ρ = initiation rate

ρ' = total rate of entrance of radicals into all N particles

μ = rate of volume increase of a polymer particle

σ = standard deviation in MWD

8. REFERENCES

(1) Harkins W. D., J. Am. Chem. Soc., 69, 1428 (1947).

(2) Smith W. V., Ewart R.H., J. Chem. Phys., 16, 592 (1948).

(3) Stockmayer W. H., J. Polymer Sci., 24, 314 (1957).

(4) O'Toole J. T., J. Appl. Polymer Sci., 9, 1291 (1965).

(5) Sheinker A., Medvedev S. S., Dokl. Akad. Nauk SSSR, 97, 111 (1954).

(6) Brodnyan J. G., Cala J. A., Konen T., Kelley E. L., J. Colloid Sci., 18, 73 (1963).

(7) Ham G. E., Vinyl Polymerization, Vol. 1, Part 1, Marcel Dekker, New York (1967).

(8) French D. M., J. Polymer Sci., 32, 395 (1958).

(9) Stannett V., Litt M., Patsiga R., J. Phys. Chem., 64, 801 (1960).

(10) Litt M., Patsiga R., Stannett V., J. Polymer Sci., A-1, 8, 3607 (1970).

(11) O'Donnell J. T., Mesrobian R. B., Woodward A. R., J. Polymer Sci., 28, 171 (1958).

(12) Priest W. J., J. Phys. Chem., 56, 1077 (1952).

(13) Napper D. H., Parts A. G., J. Polymer Sci., 61, 113 (1962).

(14) Gulbekian E. V., J. Polymer Sci., A-1, 6, 2265(1968).

(15) Patsiga R. A., Ph. D. Thesis, State University College of Forestry at Syracuse Univ., Syracuse, New York 1962.

(16) Vanzo E., Ph. D. Thesis, State University College of Forestry at Syracuse University, Syracuse, New York, 1963.

(17) Okamura S., Motoyama T., J. Polymer Sci., 58, 221 (1962).

(18) Nomura M., Harada M., Nakagawara K., Eguchi W., Nagata S., J. Chem. Eng. (Japan), 4, 160 (1971).

(19) Gershberg D., Paper presented at Joint Meeting of AIChE and IChE (England), London, England, June 14, 1965.

(20) Dunn A. S., Taylor P. A., Die Makromol, Chem., 83, 207 (1965).

(21) Harriott P., J. Polymer Sci., A-1, 9, 1153 (1971).

(22) Friis N., Goosney D., Wright J. D., Hamielec A. E., J. Applied Polymer Sci., in press.

(23) Goosney D., M. Eng. Thesis, McMaster University, Hamilton, Ontario, Canada (1973).

(24) Friis N., Ph. D. Thesis, Danish Atomic Energy Commission Research Establishment, Riso, 4000, Roskilde, Denmark (1973).

(25) Friis N., Nyhagen L., J. Appl. Polymer Sci., 17, 2311(1973).

(26) Dunn A. S., Chong L. C. H., Br. Polymer J., 2, 49 (1970).

(27) Vanderhoff J. W., Bradford E. B., J. Colloid Sci., 17, 668 (1962).

(28) Vanderhoff J. W., Bradford E. B., J. Colloid Sci., 14, 543 (1959).

(29) Tabibian R. M., Heller W., Epel J. N., J. Colloid Sci.,

11, 195 (1956).

(30) Maron S. H., Pierce P. E., Ulevitch I. N., J. Colloid Sci., 18, 470 (1963).

(31) Pierce P. E., The Determination of Latex Particle Size by Transmission Measurements, Coatings and Resins Research Centre, 1964.

(32) Heller W., Pangonis W. J., Jacobson A., "Tables of Light Scattering Functions for Spherical Particles," Wayne State University Press, 1957.

(33) Poehlein G. W., Vanderhoff J. W., J. Polymer Sci., 11, 447 (1973).

(34) Brodnyan J. G., J. Colloid Sci., 15, 573 (1960).

(35) Brodnyan J. G., J. Colloid Sci., 15, 563 (1960).

(36) Ugelstad J., Mork P. C., Aasen J. O., J. Polymer Sci., A-1, 5, 2281 (1967).

(37) Graessley W. W., Hartung R. D., Uy W. C., J. Polymer Sci., A-2, 7, 1919 (1969).

(38) Stein D. J., Makromol. Chem., 76, 170 (1964).

(39) Instruction Manual, Beckman Model DU spectrophotometer, Beckman Instruments, Inc.

(40) Balke S. T., Hamielec A. E., LeClair B. P., Ind. Eng. Chem. Prod. Res. Development, 8, 54 (1969).

(41) Stacey K., Light Scattering In Physical Chemistry, Academic Press, New York (1956).

9. APPENDICES

9A. LIGHT TRANSMISSION TECHNIQUE FOR THE MEASUREMENT OF LATEX PARTICLE SIZE

9A.1. THEORETICAL BACKGROUND

Light transmission has been a standard method for the measurement of the size of colloidal spherical particles. The fundamental theory was developed by Mie. Heller et al.[29] proved its validity in the measurement of monodisperse polystyrene particles. Maron, Pierce and Ulevitch[30] applied the method to measure polydisperse polybutadiene-styrene particles.

The principle of light transmission is based on the relationship of the size of particles in a dispersion and the turbidity of the dispersion. Consider a sample irradiated by a light beam at a certain wavelength. Its transmittance, T, is defined as

$$T = I/I_o = \frac{\text{radiant energy transmitted by the sample}}{\text{radiant energy incident upon the sample}} \qquad (68)$$

The absorbance, A, is defined as:

$$A = \log_{10} (1/T) = \log_{10} (I_o/I) \qquad (69)$$

The turbidity, τ^*, of a dispersion is defined as:

$$\tau^* = (1/\ell) \ln (I_o/I) = 2.303\ A/\ell \qquad (70)$$

where ℓ = path length of the transmission cell.

Mie theory predicts that

$$\tau^* = K^* \pi r^2 n_p \qquad (71)$$

for a monodisperse spherical suspension,

where K^* = light scattering coefficient of the particles, and is a function of the ratio of the refractive index of particles to that of the dispersion medium, m and wavelength, λ_m,

r = radius of the particle,

n_p = concentration of particles in the system, number/c.c.

Let $\alpha = \pi D/\lambda_m$ where D = diameter of the particle. The concentration, c, of scattering particles in the dispersion in grams per c.c. is given by

$$c = \frac{4}{3}\pi r^3 d_p n_p \qquad (72)$$

where d_p = density of the particles.

$$\tau^* = \frac{3K^* c}{2 d_p D} \qquad (73)$$

Multiplying both sides by λ_m/π, we get

$$\frac{\lambda_m \tau^*}{\pi} = \frac{3K^* c}{2 d_p \alpha} \qquad (74)$$

or,

$$\left(\frac{\tau^*}{c}\right)_o = \left(\frac{3\pi}{2 d_p \lambda_m}\right)\frac{K^*}{\alpha} \qquad (75)$$

The zero subscript implies that (τ^*/c) must be extrapolated to c=0 to meet the Mie Theory requirements of no secondary scattering and no particle interactions.

Maron et al.[30] verified experimentally that the Mie theory is valid for systems containing polydisperse particles. The particle diameter determined from turbidity measurement should be the weight average particle diameter. Consider the turbidity due to any monodisperse species i. Equation 75 becomes

$$\tau_i^* = \left(\frac{3\pi}{2d_p\lambda_m}\right)\frac{K_i^* c_i}{\alpha_i} \qquad (76)$$

In the absence of secondary scattering or particle interactions, the total turbidity of the system, τ^*, must be the sum of the individual turbidities.

$$\therefore \quad \tau^* = \Sigma \tau_i^* = \left(\frac{3\pi}{2d_p\lambda_m}\right)\Sigma\frac{K_i^* c_i}{\alpha_i} \qquad (77)$$

Let F_i be the weight fraction of species i, i.e., $c_i = F_i c$

$$\therefore \left(\frac{\tau^*}{c}\right)_o = \left(\frac{3\pi}{2d_p\lambda_m}\right)\Sigma\frac{K_i^* F_i}{\alpha_i} \qquad (78)$$

Comparing Equations 75 and 78 yields

$$\frac{K^*}{\alpha} = \Sigma\frac{K_i^* F_i}{\alpha_i} \qquad (79)$$

Equation 79 indicates that it should be possible to obtain K^*/α from the weight fraction distribution of the system among the various particle diameters and α should correspond to a weight-average diameter. Since $\alpha = \pi D/\lambda_m$

$$\therefore \quad \frac{K^*}{d_w} = \sum \frac{K_i^* F_i}{D_i} \qquad (80)$$

Therefore for both monodisperse and polydisperse systems. A/c is related to turbidity by

$$\frac{A}{c} = \frac{\ell}{2.303}\left(\frac{\tau^*}{c}\right) = \left(\frac{3\pi\ell}{4.606 d_p \lambda_m}\right)\frac{K^*}{\alpha} \qquad (81)$$

For a system of fixed λ_m, ℓ and d_p, A/c is a function of K^* and α which in turn are functions of D only. Therefore a calibration curve can be established by measuring A/c versus D. Heller et al.[32] tabulated all the Mie functions and the right hand side of Equation 81 can be evaluated as a function of the particle diameter.

9A.2. APPARATUS AND PROCEDURE

A Beckman model DU spectrophotometer was used in the analysis. The operating procedures for this instrument are described in the Beckman Instruction Manual[39] and will not be repeated here.

The operating principle of the Beckman DU spectrophotometer is simple. Figure 39 shows the optical system of the instrument. Light from the tungsten lamp is focussed by the condensing mirror and directed in a beam to the diagonal slit entrance mirror. The entrance mirror deflects the light

through the entrance slit and into the monochromator to the collimating mirror. Light falling on the collimating mirror is rendered parallel and reflected to the quartz prism where it undergoes refraction. The back surface of the prism is aluminized so that light refracted at the first surface is reflected back through the prism, undergoing further refraction as it emerges from the prism. The desired wavelength of light is selected by rotating the Wavelength Selector which adjusts the position of the prism. The spectrum is directed back to the collimating mirror which centers the chosen wavelength on the exit slit and sample. Light passing through the sample strikes the phototube, causing a current gain. The current gain amplified and registered on the null meter. The Transmittance

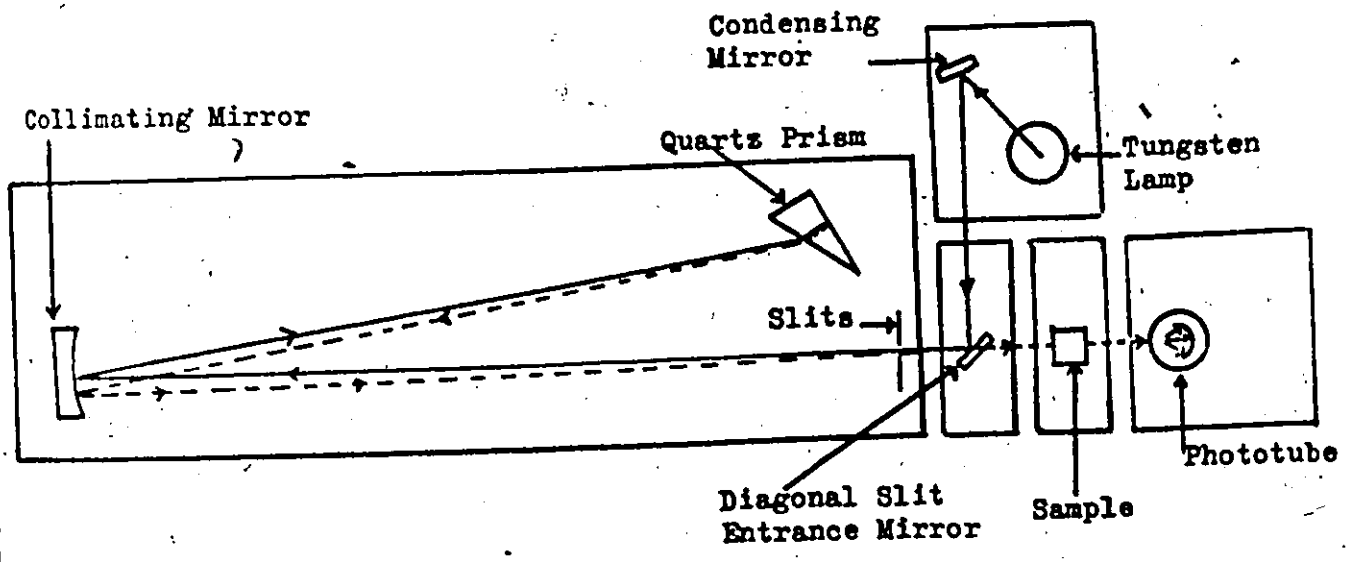

Fig. 39. Optical circuit of Beckman DU spectrophotometer.

Control is used to balance the null meter needle at zero before reading the absorbance of the sample.

Optical cells of spectrosil transmitting plates were used to hold the emulsion samples for measurements. They were cleaned with concentrated chromic acid. Before use, acetone was used to clean the inside and outside surfaces. A sample of known polymer concentration was diluted at least 100 times with distilled water and its absorbance, A, was measured with pure water as standard.

After determining the value of A/c, d_n and d_w at a certain wavelength can be found from the calibration curves (described in next paragraph).

9A.3. CALIBRATION CURVES

The calibration curves were established from samples whose d_n's and d_w's were measured by electron microscopy and their A/c values were calculated. They are shown in Figures 40 to 45.

By varying the recipe for emulsion polymerization seven experiments were performed to generate PVAc emulsions with different particle sizes. The samples were treated for electron microscopic measurements. d_n's and d_w's were calculated from their particle size distributions.

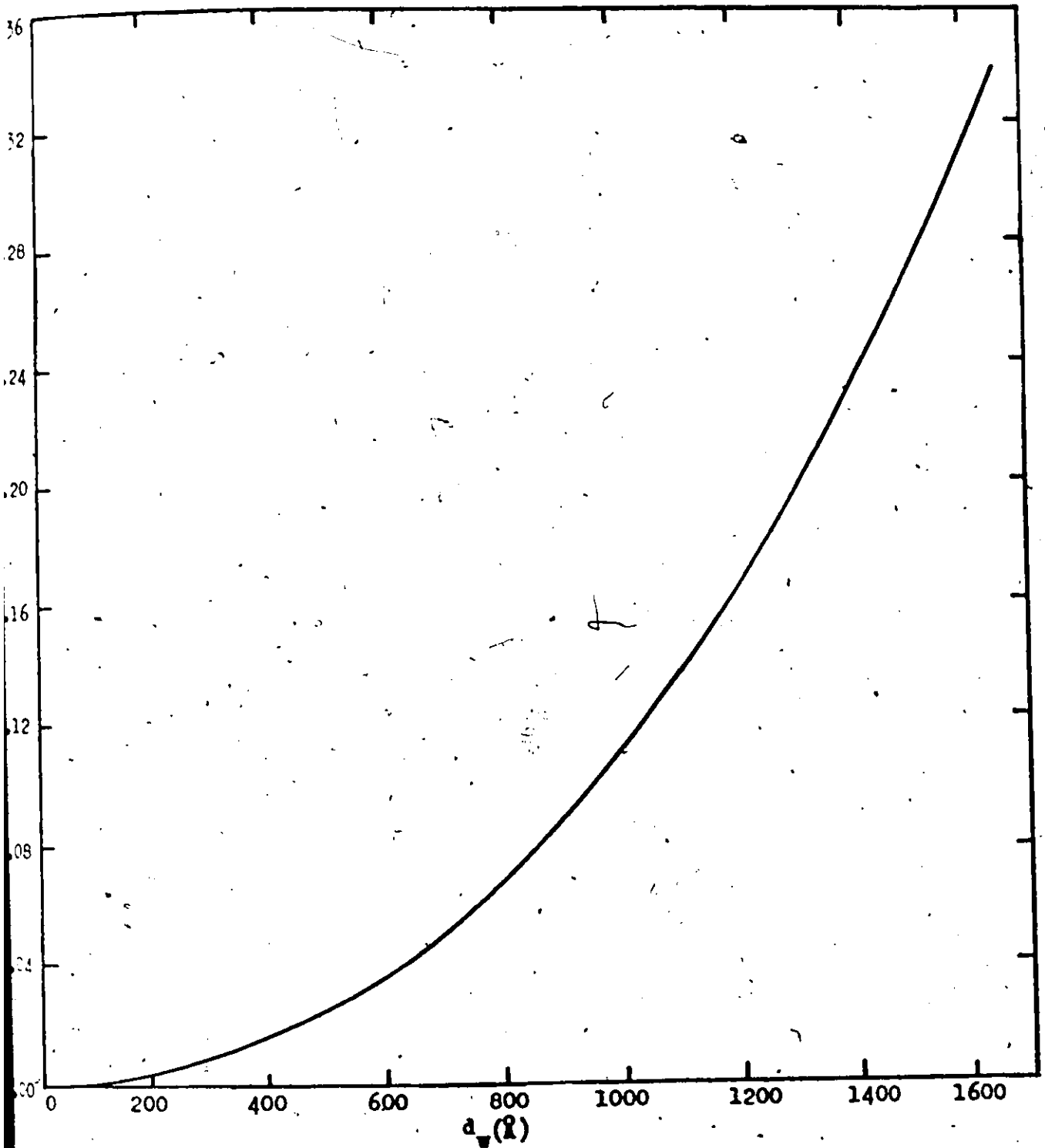

Fig. 40 Calibration curve, A/c versus d_w at λ = 5890Å.

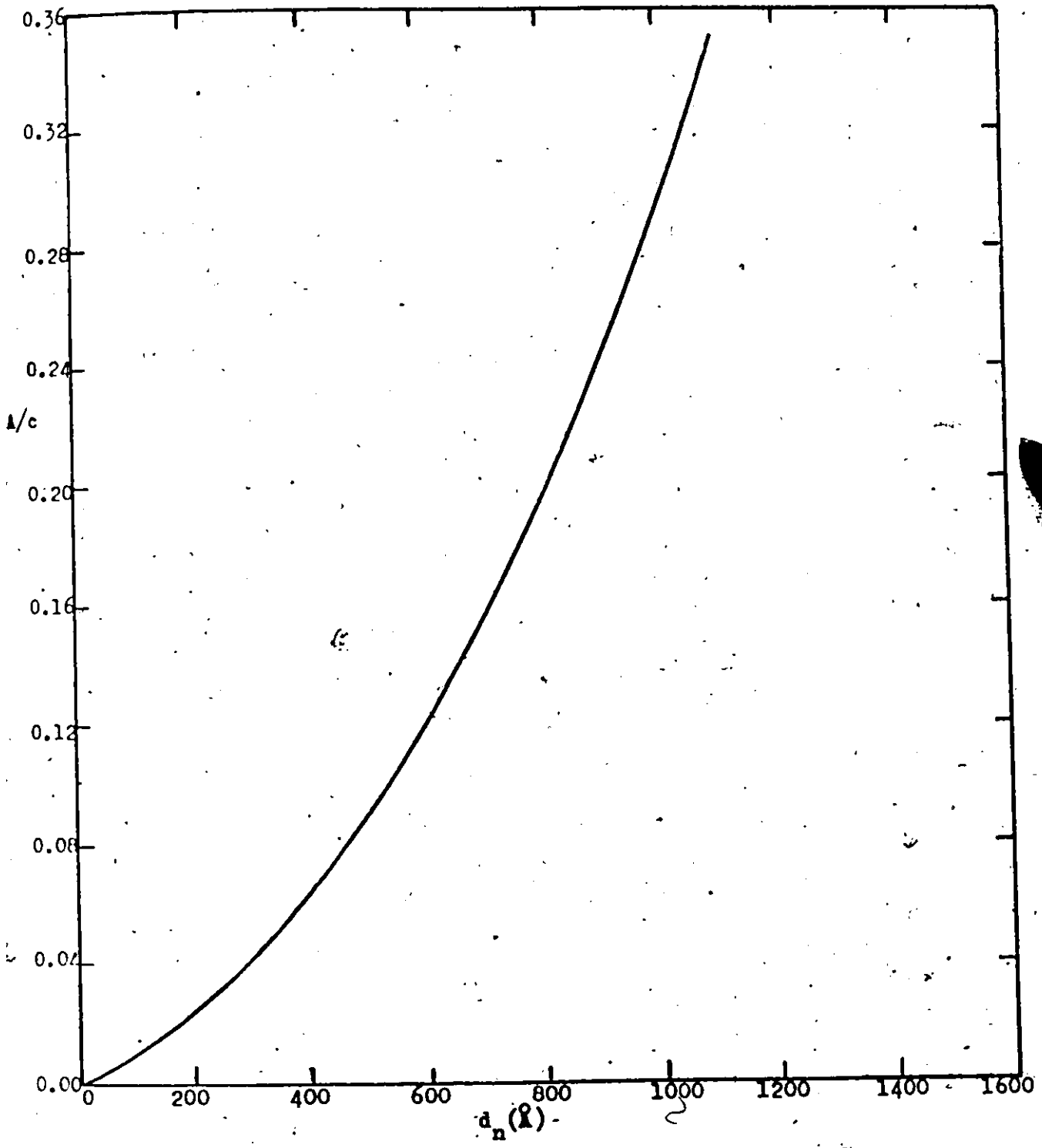

Fig. 41. Calibration curve, A/c versus d_n at λ = 5890Å

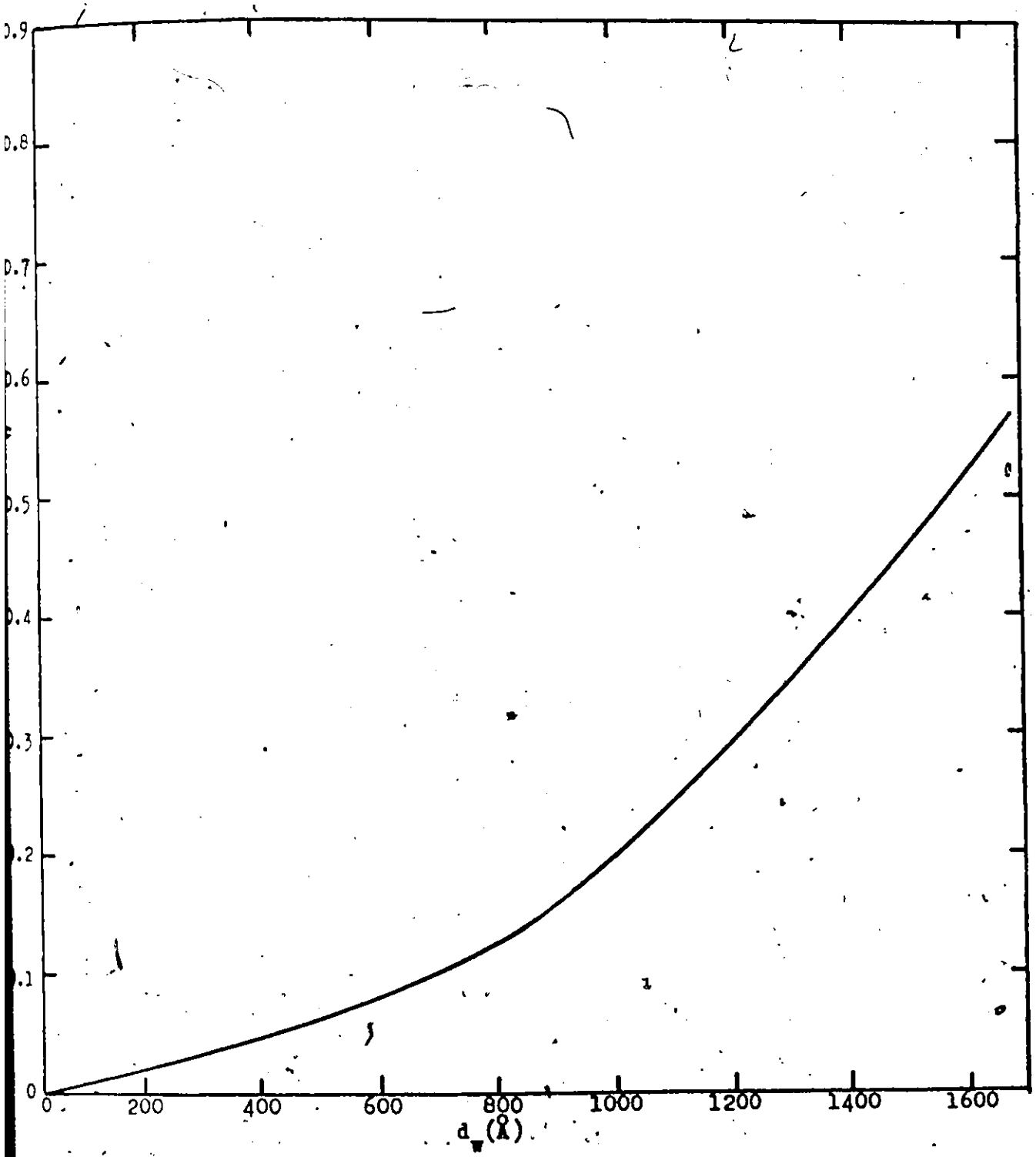

Fig. 42. Calibration curve, A/c versus d_w at λ = 5000Å.

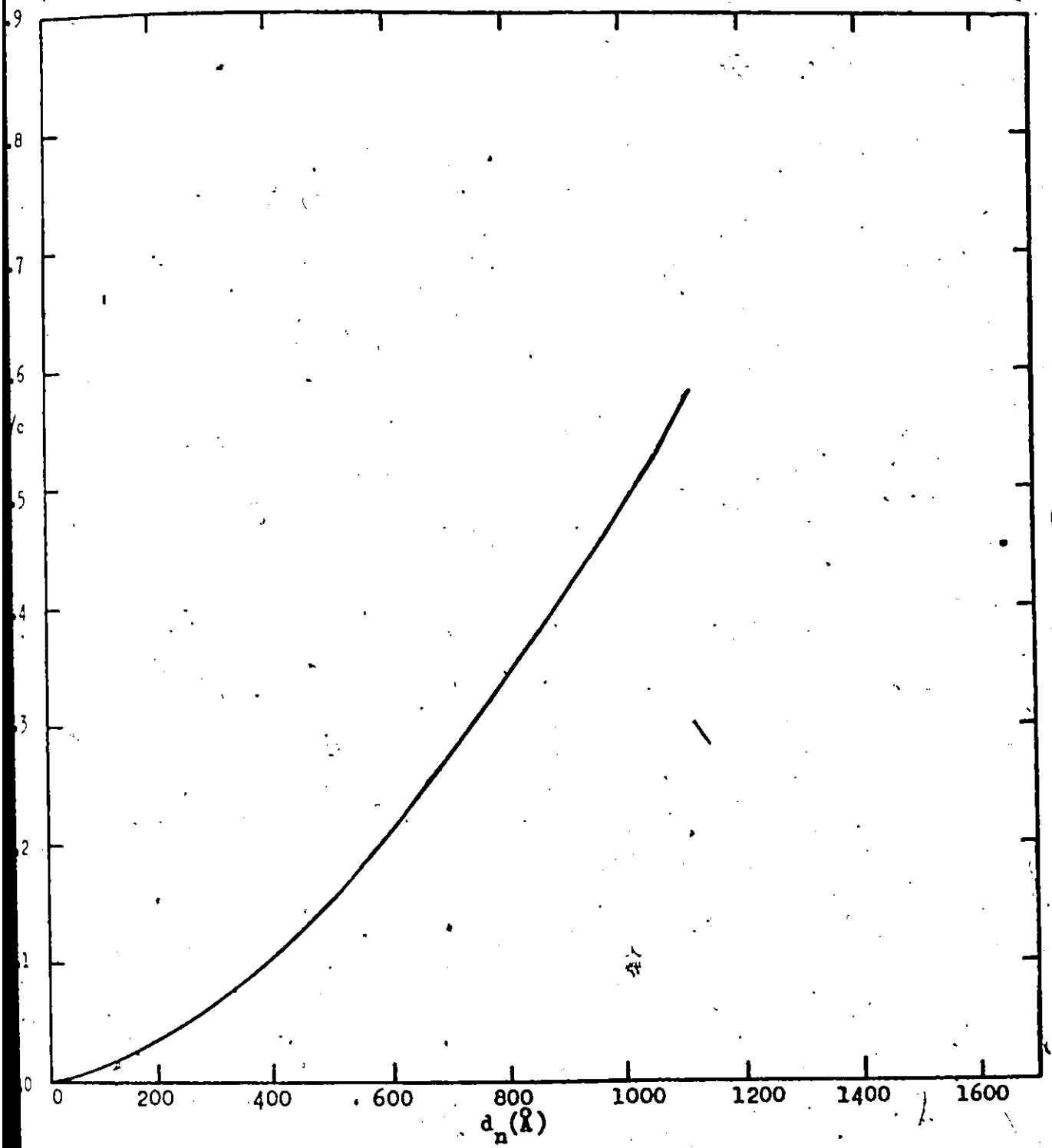

Fig. 43 Calibration curve, A/c versus d_n at λ = 5000Å.

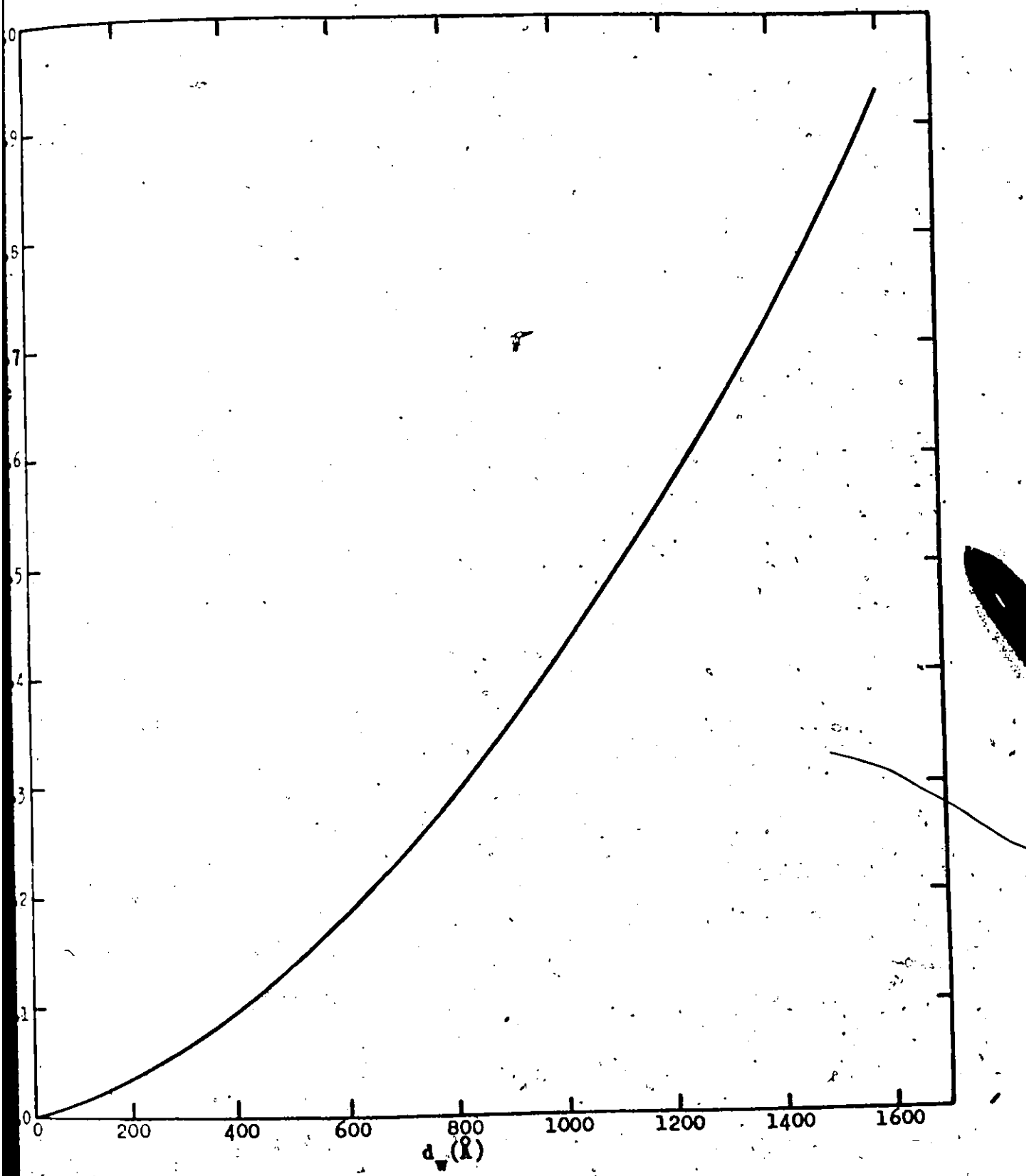

Fig. 44. Calibration curve, A/c versus d_w at λ = 4000Å.

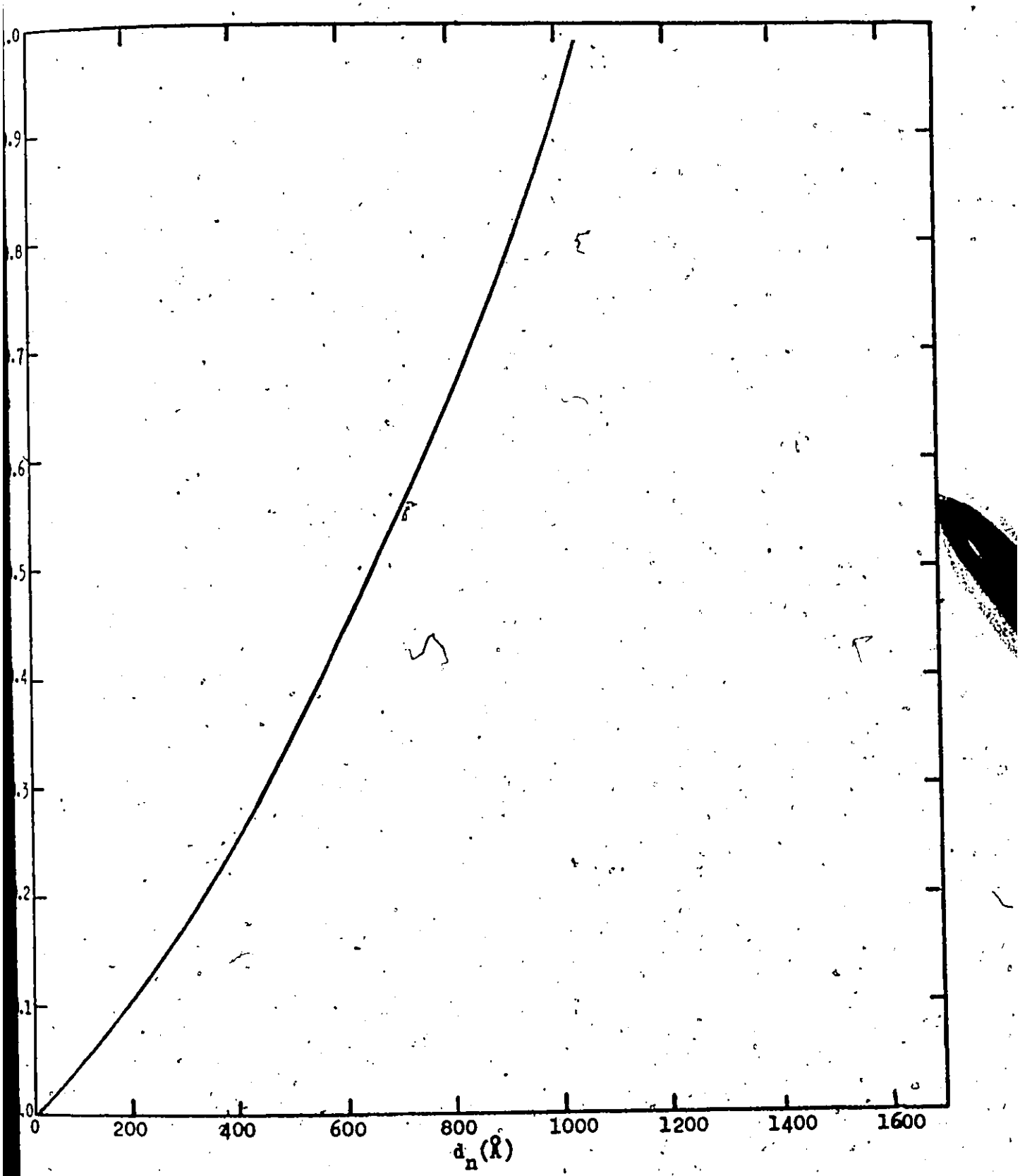

Fig. 45 Calibration curve, A/c versus d_n at λ = 4000Å.

9B. GEL PERMEATION CHROMATOGRAPHY

9B.1. INTRODUCTION

Gel Permeation Chromatography is an analytical technique for measuring the molecular weight distribution (MWD) of a polymer in solution. A gel permeation chromatograph (GPC) has one or several columns packed with porous material, such as, styragel, Bio-beads S, etc. which has a range of pore sizes. When a polymeric material with a distribution of molecular sizes is dissolved and injected into the chromatographic columns the large molecules will flow through

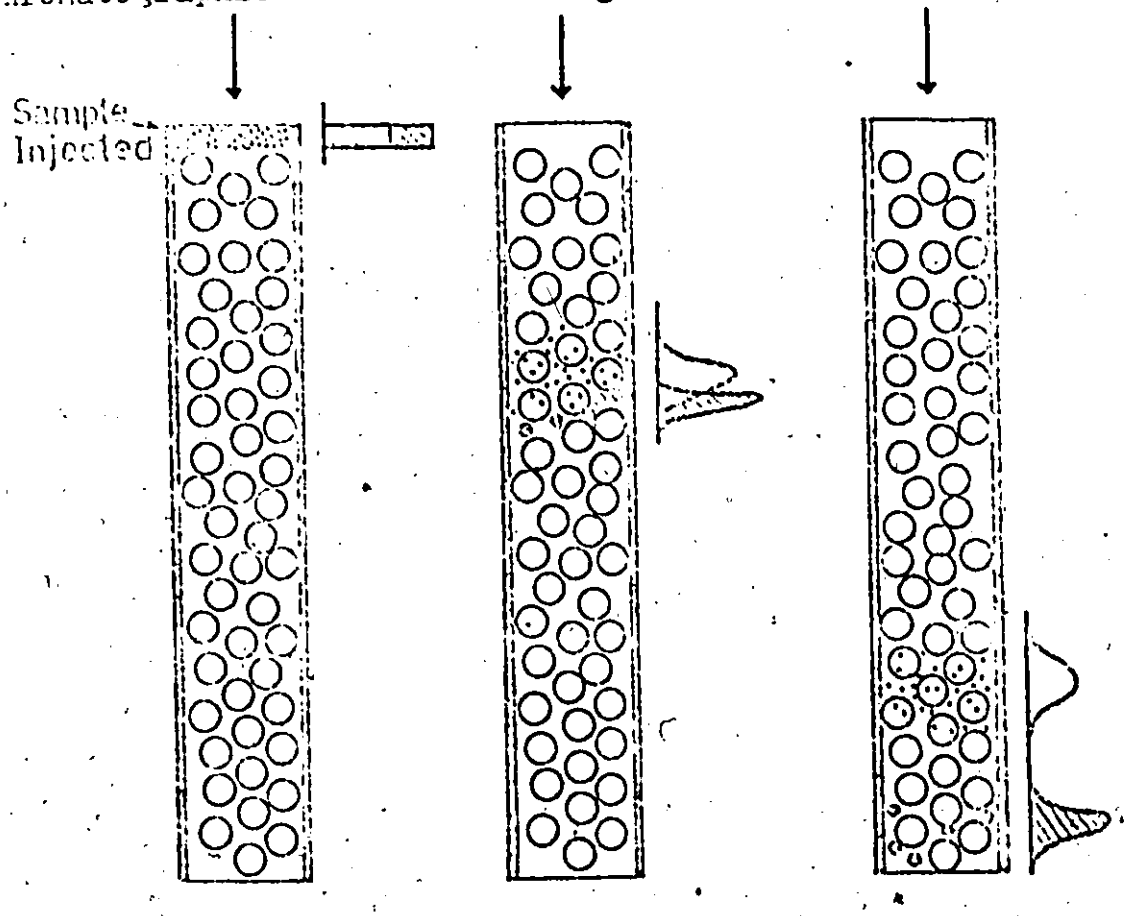

Fig. 46. GPC separation process.

in liquid phase since they are too large to diffuse into the pores of the packing material. The small molecules will diffuse into the pores temporarily and therefore, they flow through the column at a later stage. Figure 46 shows a GPC separation process for a mixture of two molecular sizes. Knowing the relationship between the elution volume and the molecular weight, the molecular weight distribution can be determined.

9B.2. EQUIPMENT

The gel permeation chromatograph, Model No. ALC-201, was supplied by Waters Associates. It consists of 9 3/8" diameter stainless steel columns packed with styragel (2 columns were 4 ft. long; 7 were 2 ft. long). Nominal exclusion limit of these columns ranged from 700 to 5×10^6 Å. The carrier solvent flow rate was 2.5 ml/min. at a temperature of 25°C. Sample concentrations of approximately 0.25% by weight PVAc in tetrahydrofuran (THF) were used.

The differential molecular weights were measured with a differential refractometer and recorded as chromatogram in a recorder chart.

9B.3. CALIBRATION AND CALCULATION

In order to interpret a chromatogram for molecular weight distribution the elution volumes have to be calibrated. When there are polymer standards available, such as, polystyrene,

a calibration curve of molecular weight versus retention volume can be constructed from a series of injections of these monodisperse standards. A typical calibration curve is shown in Figure 47. There is an upper and a lower limit of resolution. Molecules above and below these limits cannot be separated. In between these two limits, a linear curve of log M versus retention volume can be found and this is the range of molecular weights analysed by GPC.

For polyvinyl acetate, there are no known standards available. Goosney[23] established his calibration curve for PVAc/THF by a direct search technique after finding that the universal calibration curve was not effective. Standardized PVAc samples from Goosney's research were used in the present work to calibrate the GPC. This was made possible by a computer technique developed by Balke et al.[40]. This method utilizes two sets of information, for example, M_n and M_w of one broad sample and searches for an effective linear calibration curve that gives the best fit to these values when applied to the raw chromatograms.

Using the computer technique and 2 standardized PVAc samples, the calibration curve was established as follows;

$$M = 1.15 \times 10^{15} \exp(-0.572V) \qquad (82)$$

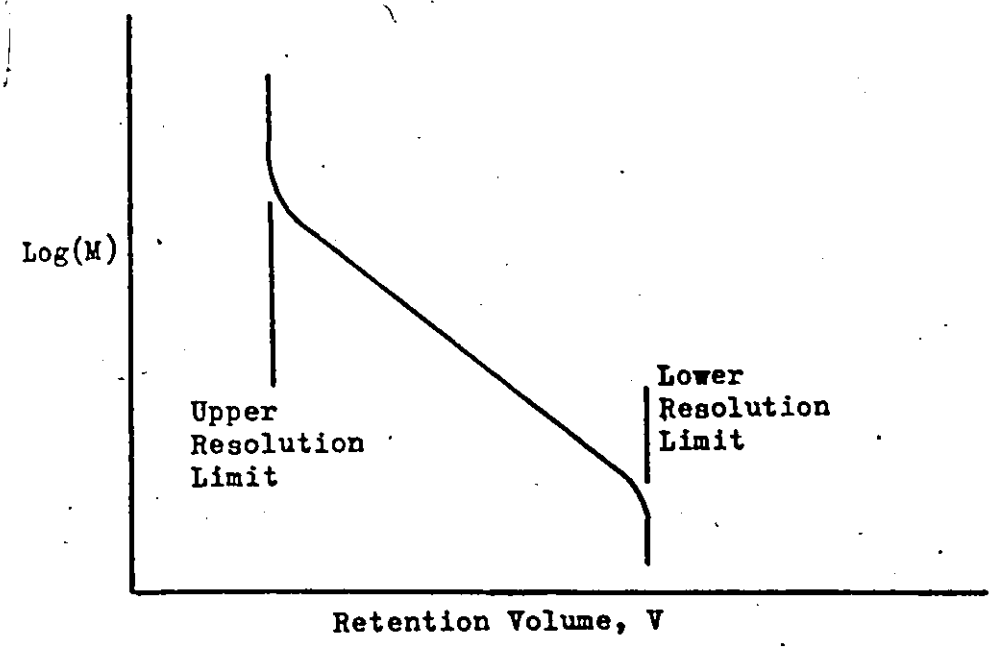

Fig. 47. General shape of calibration curve.

Number-average molecular weights, weight-average molecular weights and molecular weight distributions for all PVAc samples were evaluated by means of a digital computer program developed in this laboratory.

9C. ELECTRON MICROSCOPY

A Philips EM300 model electron microscope was used for particle size study. Micrographs were obtained at a magnification of x22,000. They were printed 5 times the size of the micrographs so that total magnification was x110,000. Magnification was also checked by the use of Dow Chemical monodisperse polystyrene latex with a particle diameter of

2640Å. Shadow lengths of the well-isolated particles were measured by a millimeter scale. The shadow lengths and diameters of the standard polystyrene particles were also measured for calibration purposes.

To obtain the particle diameter, D, of a particle with shadow length, L, we apply the following equations:-

$$D = 2L \tan(\frac{\theta}{2})(\frac{2640}{D_s}) \quad \text{Å} \tag{83}$$

where D_s = shadow diameter of the standard polystyrene latex,

θ = the shadowing angle which can be measured or can be related to the standard: $\text{Tan}(\theta/2) = D_s/2L_s$.

After obtaining the diameters of the particles, histograms of frequency versus d_i were drawn. Number-average and weight-average diameters were evaluated with the following definitions

$$d_w^3 = \frac{\Sigma f_i d_i^6}{\Sigma f_i d_i^3} \tag{84}$$

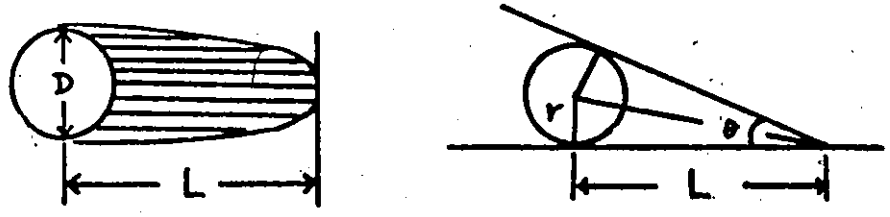

Fig. 48. Shadow length and particle dimension.

$$d_n^3 = \frac{\sum f_i d_i^3}{\sum f_i} \qquad (85)$$

The diameters had to be adjusted for in situ hardening.

9D. LIGHT SCATTERING

9D.1: THEORETICAL BACKGROUND

The measurement of weight-average particle diameters by light scattering was based on the method employed by Friis[24].

Debye's equation for light scattering is as follows:

$$\frac{K^{**}c}{R_{90^o}} = \frac{1}{M_w} + 2A_2c \qquad (86)$$

where K^{**} = light scattering constant,

A_2 = second virial coefficient,

M_w = weight average molecular weight,

R_{90^o} = Raleigh ratio measured at angle 90^o,

c = concentration (gm/c.c.)

The constant, K^{**}, is determined according to the relationship:

$$K^{**} = \frac{2\pi^2 \bar{n}_o^2 (d\bar{n}/dc)^2}{N_A \lambda^4} \qquad (87)$$

where $\bar{n}_o$ = refractive index of the solvent,

$d\bar{n}/dc$ = change in refractive index with concentration,

λ = wavelength of light in vacuum,

N_A = Avogadro's number.

All the factors in Equation 87 are known except $d\bar{n}/dc$ which can be determined by the use of a differential refractometer.

When $K^{**}c/R_{90}o$ is measured and plotted versus c, the intercept is a measure of $1/M_w$. $R_{90}o$ is a measure of the scattered intensity and may be obtained for dilute latex samples (10^{-5} - 10^{-3} gm/c.c.).

The light scattering instrument is calibrated with a glass standard supplied by the manufacturer and the measurements are performed with pure benzene as reference. The galvanometer deflection may be converted directly to an observed Raleigh ratio - R_{90o}^{obs} . The particle scattering factor is defined as

$$P_{90}o = R_{90}o / R_{90}^{obs}o \qquad (88)$$

Therefore Equation 87 becomes

$$\frac{K^{**}c}{R_{90}^{obs}o} = \frac{1}{M_w P_{90}o} + 2A_2c \qquad (89)$$

$P_{90}o$ can be determined from the dissymmetry ratio, Z, which is the ratio of the galvanometer reading at $45^{\circ}(G_{45}o)$ to that at $135^{\circ}(G_{135}o)$, i.e.,

$$Z = G_{45}o/G_{135}o \qquad (90)$$

When $K^{**}c/R_{90}^{obs}o$ is plotted as a function of concentration, the intercept gives the value of $1/M_w P_{90}o$. The tables in Stacey[41] is used to obtain the value of $1/P_{90}o$ from Z.

The weight average particle volume is obtained as

$$\bar{v}_w = M_w/N_A d_p \qquad (91)$$

The weight average particle diameter can then be calculated.

9D.2. EXPERIMENTAL PROCEDURE

The light scattering instrument used in this work was a SOFICA model 42000 with a 546.1 nm mercury lamp.

The latex was diluted with distilled water to a concentration of $3x10^{-5}$ to $3x10^{-4}$ gm PVAc/c.c. The galvanometer deflection was measured at angles 45°, 90° and 135°. The sample was diluted by a factor 2 and the measurements were repeated at the new concentration. The procedure was repeated four times. Then the weight average particle diameters were calculated from the procedure described in Section 9D.1.

9E. PARTICLE SIZE DISTRIBUTION FROM ELECTRON MICROSCOPY (EM), LIGHT TRANSMISSION AND LIGHT SCATTERING (LS)

Experiment A1.

Recipe: Sodium Persulphate = 1.2 gm.

Sodium Lauryl Sulphate = 5 gm.

Vinyl Acetate = 800 ml.

Water = 1750 ml.

Experimental Conditions: Temperature = 50°C

Stirring Rate = 150 r.p.m.

Results:

Particle Diamaters (Å)	Frequency (%)
0 - 165	8.610
165 - 330	16.960
330 - 495	12.160
495 - 660	9.510
660 - 825	8.940
825 - 990	7.120
990 -1155	7.530
1155 -1320	6.620
1320 -1485	6.540
1485 -1650	4.960
1650 -1815	4.640
1815 -1980	2.830
1980 -2145	3.060
2145 -2310	0.496
2310 -2475	0.414

d_w (EM) = 1650Å

d_n (EM) = 1090Å

d_w (LS) = 1565Å

λ, Wavelength (Å)	A/c
4000	0.9820
5000	0.5450
5890	0.3425

Experiment A2.

Recipe: Sodium Persulphate = 1.2 gm.

Sodium Lauryl Sulphate = 15 gm.

Vinyl Acetate = 800 ml.

Water = 1750 ml.

Experimental Conditions: Temperature = 50°C

Stirring Rate = 150 r.p.m.

Results:

Particle Diameters (Å)	Frequency (%)
100 - 200	7.990
200 - 300	20.260
300 - 400	17.040
400 - 500	11.320
500 - 600	9.893
600 - 700	8.104
700 - 800	7.865
800 - 900	4.410
900 -1000	3.456
1000 -1100	1.787
1100 -1200	2.863
1200 -1300	1.906
1300 -1400	0.834
1400 -1500	0.715
1500 -1600	0.358
1600 -1700	0.596
1700 -1800	0.119
1800 -1900	0.119
1900 -2000	0.238
2000 -2100	0.119

d_w (EM) = 1230Å

d_n (EM) = 685Å

d_w (LS) = 1120Å

λ, Wavelength (Å)	A/c
4000	0.6780
5000	0.3500
5890	0.2080

Experimental A3.

Recipe: Sodium Persulphate = 1.2 gm.

Sodium Lauryl Sulphate = 30 gm.

Vinyl Acetate = 400 ml.

Water = 1750 ml.

Experimental Conditions: Temperature = 50°C

Stirring Rate = 150 r.p.m.

Results:

Particle Diameters (Å)	Frequency (%)
100 - 200	25.540
200 - 300	33.010
300 - 400	14.730
400 - 500	9.824
500 - 600	6.680
600 - 700	3.144
700 - 800	3.734
800 - 900	1.375
900 -1000	0.982
1000 -1100	0.393
1100 -1200	0.196
1200 -1300	0.393

d_w (EM) = 770Å

d_n (EM) = 420Å

d_w (LS) = 700Å

λ, Wavelength (Å)	A/c
4000	0.1710
5000	0.0732
5890	0.0406

Experiment A4.

Recipe: Sodium Persulphate = 1.2 gm.

Sodium Lauryl Sulphate = 8 gm.

Vinyl Acetate = 400 ml.

Water = 1750 ml.

Experimental Conditions: Temperature = 50°C

Stirring Rate = 150 r.p.m.

Results:

Particle Diameters (Å)	Frequency (%)
100 - 200	21.650
200 - 300	26.770
300 - 400	14.620
400 - 500	11.720
500 - 600	8.140
600 - 700	5.935
700 - 800	3.585
800 - 900	3.310
900 -1000	1.930
1000 -1100	1.104
1100 -1200	0.828
1200 -1300	0.138
1300 -1400	0.000
1400 -1500	0.276

d_w (EM) = 910Å

d_n (EM) = 520Å

d_w (LS) =1100Å

λ, Wavelength (Å)	A/c
4000	0.4350
5000	0.2075
5890	0.1188

Experiment A5.

Recipe: Polyvinyl acetate latex from Experiment A4

Vinyl Acetate = 400 ml.

Experimental Conditions: Temperature = 50°C

Stirring Rate = 150 r.p.m.

Results:

Particle Diameters (Å)	Frequency (%)
100 - 200	22.100
200 - 300	25.050
300 - 400	13.200
400 - 500	12.250
500 - 600	8.070
600 - 700	5.700
700 - 800	2.460
800 - 900	2.660
900 -1000	1.614
1000 -1100	1.614
1100 -1200	1.140
1200 -1300	0.665
1300 -1400	0.855
1400 -1500	0.475
1500 -1600	1.045
1600 -1700	0.285
1700 -1800	0.190
1800 -1900	0.190
1900 -2000	0.095
2000 -2100	0.190
2100 -2200	0.095

d_w (EM) = 1360Å

d_n (EM) = 840Å

d_w (LS) = 1430Å

λ, Wavelength (Å)	A/c
4000	0.7040
5000	0.3630
5890	0.2160

Experiment A6.

Recipe: Sodium Persulphate = 1.2 gm.

Sodium Lauryl Sulphate = 12.5 gm.

Vinyl Acetate = 400 ml.

Water = 1750 ml.

Experimental Conditions: Temperature = 50°C

Stirring Rate = 150 r.p.m.

Results:

Particle Diameters (Å)	Frequency (%)
95 - 190	19.960
190 - 285	31.100
285 - 380	13.270
380 - 475	10.210
475 - 570	6.710
570 - 665	4.880
665 - 760	4.570
760 - 855	3.350
855 - 950	2.740
950 -1045	1.525
1045 -1140	1.067
1140 -1235	0.153
1235 -1330	0.305
1330 -1425	0.153

d_w (EM) = 850Å

d_n (EM) = 490Å

d_w (LS) = 936Å

λ, Wavelength (Å)	A/c
4000	0.3185
5000	0.1440
5890	0.0800

Experiment A7.

Recipe: Polyvinyl Acetate Latex from Experiment A6,

Vinyl Acetate = 400 ml.

Experimental Conditions: Temperature = 50°C

Stirring Rate = 150 r.p.m.

Results:

Particle Diameters (Å)	Frequency (%)
95 - 190	16.050
190 - 285	18.750
285 - 380	12.290
380 - 475	11.270
475 - 570	8.410
570 - 665	6.600
665 - 760	5.820
760 - 855	4.530
855 - 950	3.750
950 -1045	3.110
1045 -1140	1.810
1140 -1235	2.590
1235 -1330	1.550
1330 -1425	1.425
1425 -1520	0.906
1520 -1615	0.647
1615 -1710	0.259
1710 -1805	0.259

d_w (EM) = 1160Å

d_n (EM) = 650Å

d_w (LS) = 1250Å

λ, Wavelength (Å)	A/c
4000	0.5490
5000	0.2690
5890	0.1555